

A pedagogical review on *a posteriori* error estimation in Finite Element computations

Ludovic Chamoin^{1,2} and Frédéric Legoll^{3,4}

¹ Université Paris-Saclay, ENS Paris-Saclay, CNRS, LMT,
4 avenue des Sciences, 91190 Gif-sur-Yvette, France

² Institut Universitaire de France (IUF), 1 rue Descartes, 75231 Paris Cedex 5, France

³ Ecole Nationale des Ponts et Chaussées, Laboratoire Navier,
6-8 avenue Blaise Pascal, 77455 Marne-La-Vallée Cedex 2, France

⁴ Inria Paris, MATHERIALS project-team, 2 rue Simone Iff,
CS 42112, 75589 Paris Cedex 12, France

`ludovic.chamoin@ens-paris-saclay.fr`, `frederic.legoll@enpc.fr`

October 6, 2021

Abstract

This article is a review on basic concepts and tools devoted to *a posteriori* error estimation for problems solved with the Finite Element Method. For the sake of simplicity and clarity, we mostly focus on linear elliptic diffusion problems, approximated by a conforming numerical discretization. The review mainly aims at presenting in a unified manner a large set of powerful verification methods, around the concept of equilibrium. Methods based on that concept provide error bounds that are fully computable and mathematically certified. We discuss recovery methods, residual methods, and duality-based methods for the estimation of the whole solution error (i.e. the error in energy norm), as well as goal-oriented error estimation (to assess the error on specific quantities of interest). We briefly survey the possible extensions to non-conforming numerical methods, as well as more complex (e.g. nonlinear or time-dependent) problems. We also provide some illustrating numerical examples on a linear elasticity problem in 3D.

Keywords: Error estimation; Finite Element Method; Discretization error; Adaptivity; Goal-oriented strategy

Contents

1 Introduction

3

2	Reference problem and notations	4
2.1	Reference problem	4
2.2	Finite Element (FE) approximation	5
2.3	Notion of error estimate	6
2.4	<i>A priori</i> error estimation	7
3	Recovery methods	11
3.1	Richardson extrapolation	11
3.2	Basics on flux recovery methods	11
3.3	Recent advances in flux recovery methods	13
4	Residual methods	14
4.1	Explicit methods	15
4.2	Implicit methods	17
4.2.1	Hierarchical approach	17
4.2.2	Subdomain residual methods	18
4.2.3	Element residual methods	21
5	Duality-based methods	23
5.1	Dual approach	23
5.2	Constitutive relation error functional	25
5.3	Construction of a statically admissible flux field	27
5.3.1	Hybrid-flux approach	27
5.3.2	Flux-free approach	32
5.3.3	Full polynomial construction using a dual mesh	33
5.4	Numerical illustration	35
6	Unified point of view on <i>a posteriori</i> error estimation methods	36
7	Mesh adaptation	38
8	Goal-oriented error estimation	40
8.1	Adjoint problem and error indicator	41
8.2	Computation of upper error bounds	43
8.3	Numerical illustration	47
9	Extensions to other FE schemes	48
9.1	Splitting of the error	48
9.2	Estimation of the non-conforming part of the error	51
9.3	Estimation of the conforming part of the error	51
9.4	<i>A posteriori</i> bounds on the total error	54
10	Extensions to other mathematical problems	55
10.1	Advection-diffusion-reaction problems	55
10.1.1	<i>A priori</i> error estimation	56
10.1.2	<i>A posteriori</i> error estimation	57
10.1.3	Goal-oriented error estimation	58

10.2 Time-dependent and nonlinear problems	59
11 Conclusion	60
A Appendix: Proof of the lower bound for CRE error estimates	61

1 Introduction

A large number of physical phenomena are described by partial differential equations. Since it is usually not possible to obtain closed form expressions for the exact solution of these equations, numerical methods with mathematically-based algorithms and discretization techniques are often used as simulation tools. Such methods typically only deliver an approximate solution (somehow the best function within a predefined finite-dimensional space) that is different from the exact solution. Consequently, in order to certify the accuracy of numerical simulations, two important questions are

- (i) How large is the overall discretization error between the exact and the approximate solution?
- (ii) Where in the spatial domain (and time domain for time-dependent problems) is this error localized?

Answering in an appropriate manner to these two questions may be crucial in many engineering activities since a decision is often taken on the basis of numerical simulation results. Taking the argument one step further, a long-term goal in scientific computing is to design algorithms such that (i) a given precision is reached at the end of the simulation, and (ii) the computational work to achieve this accuracy is as small as possible.

In this article, we consider these questions for a particular numerical method, a conforming Finite Element Method (FEM), and mainly for a particular class of problems, namely linear elliptic diffusion problems. We already note that the approaches we discuss here can be extended to other mathematical problems and to other types of discretization. We review here the various *a posteriori* error estimation methods (and the associated adaptive strategies) which have been developed over the last years, enlightening specific properties and links between the methods. We particularly highlight that methods providing for fully computable and guaranteed error bounds can be unified around the tools of dual analysis and the concept of equilibrium.

This review article is organized as follows. The reference problem along with some elements of *a priori* error analysis is given in Section 2. The *a posteriori* error estimation methods are next presented in three groups: flux recovery methods in Section 3, residual methods in Section 4, and duality-based constitutive relation error methods in Section 5. Numerical illustrations of *a posteriori* error estimation on a three-dimensional elasticity problem are shown in Section 5.4. A unified perspective on these different methods is provided in Section 6. Mesh

adaptation is next discussed in Section 7. Goal-oriented error estimation, where the aim is to certify the error on a given quantity of interest rather than on the whole solution itself, is addressed in Section 8 (with, in particular, a numerical illustration in Section 8.3). Extensions to other Finite Element schemes (i.e. beyond classical conforming FEM) and to other mathematical problems are briefly discussed in Sections 9 and 10, respectively. Concluding remarks are collected in Section 11. We eventually provide in Appendix A a proof of the fact that the Constitutive Relation Error estimator presented in Section 5, and which is always an upper bound of the numerical error, is also, up to a multiplicative constant independent of the mesh size, a lower bound of the numerical error (see Theorem 35 and Corollary 36 there).

This review is written at an elementary level. It describes basic features of the approaches, presents them in a unified manner, and purposely skips some technicalities (for which we prefer to refer to the relevant bibliography). We hope it will be useful for researchers and engineers looking for an up-to-date overview of the field, both in terms of theoretical and implementation aspects.

2 Reference problem and notations

2.1 Reference problem

Throughout this article, except in Section 10, we consider the following problem:

$$-\operatorname{div}(\mathbb{A}\nabla u) = f \quad \text{in } \Omega, \quad u = 0 \quad \text{on } \Gamma_D, \quad (\mathbb{A}\nabla u) \cdot \mathbf{n} = g \quad \text{on } \Gamma_N, \quad (1)$$

where Ω is an open bounded subset of \mathbb{R}^d with Lipschitz boundary $\partial\Omega$, and Γ_D and Γ_N are parts of $\partial\Omega$ such that $\overline{\Gamma_D} \cup \overline{\Gamma_N} = \partial\Omega$, $\Gamma_D \cap \Gamma_N = \emptyset$ and $|\Gamma_D| \neq 0$. We assume that $f \in L^2(\Omega)$ and that $\mathbb{A} \in [L^\infty(\Omega)]^{d \times d}$ is a symmetric matrix (we refer to Section 10.1 for the study of some non-symmetric operators), which is uniformly bounded and positive in the sense that there exists $a_{\max} \geq a_{\min} > 0$ such that

$$\forall \boldsymbol{\xi} \in \mathbb{R}^d, \quad a_{\min} |\boldsymbol{\xi}|^2 \leq \mathbb{A}(x) \boldsymbol{\xi} \cdot \boldsymbol{\xi} \leq a_{\max} |\boldsymbol{\xi}|^2 \quad \text{a.e. in } \Omega. \quad (2)$$

The quantity $\mathbf{q} = \mathbb{A}\nabla u$ is the flux associated with u .

The norm and semi-norm of a function v in $H^k(\Omega)$ are denoted

$$\|v\|_k = \left(\int_{\Omega} \sum_{|\alpha| \leq k} |D^\alpha v|^2 \right)^{1/2}, \quad |v|_k = \left(\int_{\Omega} \sum_{|\alpha|=k} |D^\alpha v|^2 \right)^{1/2},$$

where $D^\alpha v$ is the α -th order derivative of v (with $\alpha \in \mathbb{N}^d$). Note that the norm of $v \in L^2(\Omega)$ is denoted $\|v\|_0$. When the norm is restricted over a subdomain $K \subset \Omega$, the subdomain is explicit in the notation. Hence, for instance, $\|v\|_{0,K}$ denotes the $L^2(K)$ norm of v .

Considering the Hilbert space $V = \{v \in H^1(\Omega), v = 0 \text{ on } \Gamma_D\}$ endowed with the H^1 norm $\|\cdot\|_1$, we recall that the weak formulation of (1) is:

$$\text{Find } u \in V \text{ such that, for any } v \in V, \quad B(u, v) = F(v), \quad (3)$$

where

$$B(u, v) = \int_{\Omega} \mathbb{A} \nabla u \cdot \nabla v, \quad F(v) = \int_{\Omega} f v + \int_{\Gamma_N} g v.$$

The well-posedness of (3) of course directly follows from the Lax-Milgram theorem. The bilinear form B is symmetric, continuous and coercive on V . It hence defines an inner product and induces the energy norm $\|v\| = \sqrt{B(v, v)}$ on V , which is equivalent to $\|v\|_1$ on V :

$$\forall v \in V, \quad \sqrt{\frac{a_{\min}}{1 + C_{\Omega}^2}} \|v\|_1 \leq \|v\| \leq \sqrt{a_{\max}} \|v\|_1, \quad (4)$$

where C_{Ω} is the Poincaré constant of Ω , which satisfies $\|v\|_0 \leq C_{\Omega} \|v\|_1$ for any $v \in V$. We see that

$$\forall v, w \in V, \quad |B(v, w)| \leq \|v\| \|w\|.$$

In the sequel, we also use the notation $\|\tilde{\mathbf{q}}\|_q = \sqrt{\int_{\Omega} \mathbb{A}^{-1} \tilde{\mathbf{q}} \cdot \tilde{\mathbf{q}}}$ for any vector-valued field $\tilde{\mathbf{q}} \in (L^2(\Omega))^d$.

2.2 Finite Element (FE) approximation

Before we proceed, we mention that we will assume throughout our text that the reader is reasonably familiar with finite element methods. We refer to the classical textbooks [29, 39, 49, 57, 98, 200] (see also introductory expositions in [45], and (in French) in [128, 161, 204, 205]).

Let \mathcal{T}_h be a partition of Ω . We denote by h_K the diameter of each element $K \in \mathcal{T}_h$ (i.e. the largest distance between any two points in K) and by ρ_K the diameter of the largest circle (or sphere) contained in K . We set $h = \max_{K \in \mathcal{T}_h} h_K$.

The mesh is assumed to be regular (non-degenerate), in the sense that there exists $\gamma_0 > 0$, independent of h , such that, for any $K \in \mathcal{T}_h$, we have $1 \leq h_K/\rho_K \leq \gamma_0$. Let $U(K)$ denote the neighborhood of the element K :

$$U(K) = \text{int} \left\{ \cup \bar{J}, \quad J \in \mathcal{T}_h, \quad \bar{J} \cap \bar{K} \neq \emptyset \right\}. \quad (5)$$

We introduce the space V_h^p of continuous and locally supported functions which are polynomials of degree up to p on each element K . Note that $V_h^p \subset V$. We are thus considering here a conforming Finite Element Method (FEM). Non-conforming FEM will be considered in Section 9. The FE approximation of (3) is

$$\text{Find } u_h \in V_h^p \text{ such that, for any } v \in V_h^p, \quad B(u_h, v) = F(v), \quad (6)$$

which is a well-posed problem, again in view of the Lax-Milgram theorem. Let

$$R(v) = F(v) - B(u_h, v)$$

be the so-called residual and

$$\|R\|_\star = \sup_{v \in V, v \neq 0} \frac{|R(v)|}{\|v\|}$$

be the dual norm of the residual. The discretization error of the approach is $e = u - u_h \in V$. It satisfies the following three properties:

$$\begin{aligned} \forall v \in V, \quad B(e, v) &= R(v) \quad (\text{residual equation}), \\ \forall v \in V_h^p, \quad B(e, v) &= 0 \quad (\text{Galerkin orthogonality}), \\ \|e\| &= \|R\|_\star. \end{aligned} \tag{7}$$

Remark 1. *In this article, we do not consider errors other than those arising from discretization. In particular, we do not consider any geometry error (the partition \mathcal{T}_h is assumed to exactly coincide with Ω) and any quadrature error (integrals over any element K are assumed to be exactly computed). In the same spirit, we note that the problem (6) may lead to a large linear system, which is then solved using iterative solvers. We ignore here the error coming from the use of such iterative solvers and refer to [119, 125, 166] for its assessment.*

A direct consequence of the Galerkin orthogonality is the best approximation property:

$$\forall v_h \in V_h^p, \quad \|e\| = \sqrt{\|u - v_h\|^2 - \|v_h - u_h\|^2} \leq \|u - v_h\|. \tag{8}$$

Using (4), this implies the Céa's lemma:

$$\forall v_h \in V_h^p, \quad \|e\|_1 \leq \sqrt{\frac{(1 + C_\Omega^2) a_{\max}}{a_{\min}}} \|u - v_h\|_1.$$

2.3 Notion of error estimate

The discretization error e has two components in a given subdomain of Ω : one that is locally generated and one that is transported from elsewhere (the so-called pollution error [19]). Its evaluation $\|e\|$ in the energy norm provides a global measure of the overall quality of the FE solution. The quantity $\|e\|$ may be evaluated using error estimation methods, which can be classified in two groups:

- (i) *a priori* error estimation, which can be performed before the approximate solution u_h is known;

- (ii) *a posteriori* error estimation, which is obtained after u_h is computed and therefore uses information from u_h to estimate $\|e\|$. The goal of *a posteriori* error estimates is not only to offer a criterion that indicates whether a prescribed accuracy is met (i.e. whether $\|e\|$ is smaller than some threshold), but also to give local error indicators which can be used to drive an adaptive mesh refinement strategy.

Focusing on the second group of methods, the global error estimate η usually satisfies $\eta^2 = \sum_{K \in \mathcal{T}_h} \eta_K^2$, where η_K is a local error estimate associated with each element K . A crucial property which is demanded to *a posteriori* error estimators is the equivalence between η and the energy norm of the exact error, i.e. that there exist positive constants C_1 and C_2 independent of h such that

$$C_1 \|e\| \leq \eta \leq C_2 \|e\|.$$

The quality of the estimator is assessed by the global effectivity index $i_{\text{eff}} = \eta / \|e\|$. The estimator is guaranteed (resp. relevant) if $i_{\text{eff}} \geq 1$ (resp. $i_{\text{eff}} \approx 1$). Local effectivity indices may also be defined.

One can then formulate properties describing an acceptable error estimate:

- **reliability**: ensure that $\|e\| \leq \eta$ holds, i.e. $i_{\text{eff}} \geq 1$, and that η is fully computable in order for η to serve as a stopping criterion;
- **accuracy**: ensure that the predicted error is close to the actual (unknown) error, i.e. $i_{\text{eff}} \approx 1$;
- **local effectivity**: ensure that $\eta_K \leq C \|e\|_{U(K)}$ for each element K , where we recall that $U(K)$ denotes the neighborhood of the element K (see (5)). This property is important for adaptive mesh refinement;
- **asymptotic exactness**: ensure that $\lim_{h \rightarrow 0} i_{\text{eff}} = 1$;
- **robustness**: guarantee the previous properties independently of the regularity of the solution and of the mesh, and independently of variations of the problem parameters;
- **practicality**: provide an estimate η and contributions η_K which can be evaluated locally, with a small computational cost. Indeed, if this evaluation turns out to require a global computation with large resources, it may be just cheaper to solve the reference problem on a uniformly refined mesh (even though an estimate of the error is not available).

2.4 *A priori* error estimation

A priori estimation of errors in numerical methods has long been an enterprise of numerical analysts [17, 224, 75, 40]. It allows to bound the error before any numerical solution is computed, and therefore gives rough information on the

asymptotic convergence and stability of the numerical method that is used. It is not designed to provide a computable error estimate for a given mesh. The general approach for *a priori* error estimation uses approximation theory or truncation error analysis [72]. It can be briefly presented as follows.

For any integers $l \in [1, p + 1]$ and $m \leq l$ (recall that p is the maximal polynomial degree in V_h^p), and for any $K \in \mathcal{T}_h$ and any $v \in H^l(U(K))$, the Clément interpolant $\Pi_h v \in V_h^p$ of v (see [78] and the textbook [98, Lemma 1.127 and Remark 1.129]) satisfies

$$\|v - \Pi_h v\|_{m,K} \leq C h_K^{l-m} \|v\|_{l,U(K)}, \quad (9)$$

where C is independent of h_K , $K \in \mathcal{T}_h$ and $v \in H^l(U(K))$, but depends on p and γ_0 (the regularity parameter of the mesh). We refer to [218] and the textbooks [234], [39, Sec. IX.3] and [49, Sec. 4.8] for related estimations. We deduce from (9) that, when $p \geq 1$, we have, for any $K \in \mathcal{T}_h$ and any $v \in H^1(U(K))$,

$$\|v - \Pi_h v\|_{0,K} \leq C h_K \|v\|_{1,U(K)}, \quad (10)$$

where C is independent of v and h_K . This property will be useful in the sequel, as well as the following edge estimate (see [98, Lemma 1.127 and Remark 1.129]). Let Γ_{int} denote the union of the internal edges (or, if $d \geq 3$, interfaces) of the mesh. For any edge $\Gamma \subset \Gamma_{\text{int}} \cup \Gamma_N$, let $U(\Gamma)$ denote the set of elements in \mathcal{T}_h sharing at least one vertex with Γ . Then, for any $v \in H^1(U(\Gamma))$, we have

$$\|v - \Pi_h v\|_{0,\Gamma} \leq C l_\Gamma^{1/2} \|v\|_{1,U(\Gamma)}, \quad (11)$$

where l_Γ is the diameter of Γ (when $d = 2$, l_Γ is simply the edge length) and where C is independent of v , l_Γ and Γ .

The *a priori* error estimation follows from (9). We assume that there exists an integer $\alpha \in [1, p]$ such that $\|u\|_{\alpha+1} < \infty$. When Ω is a (convex) domain without re-entrant corners, \mathbb{A} is sufficiently regular, $f \in L^2(\Omega)$ and when the Neumann boundary data g is sufficiently smooth on Γ_N and compatible with the homogeneous Dirichlet boundary condition on Γ_D , then the solution to (1) belongs to $H^2(\Omega)$ and we thus can take $\alpha = 1$ (see e.g. [98, Theorem 3.12]). We then infer from the best approximation property (8) (taking v_h equal to the Clément interpolant $\Pi_h u \in V_h^p$ of u) and from the bound (9) (with $m = 1$ and $l = \alpha + 1$) that

$$\|u - u_h\| = \|e\| \leq \|u - \Pi_h u\| \leq C h^\alpha \|u\|_{\alpha+1}, \quad (12)$$

where the constant C is independent of h and u (throughout the article, the constant C may change from one line to the next; when valid, the independence of that constant with respect to the mesh size and other quantities will always be underlined). When u is sufficiently smooth (that is when $\|u\|_{p+1} < \infty$), we have the optimal rate of convergence $\|e\| \leq C h^p \|u\|_{p+1}$.

The main drawback of this *a priori* bound is that the right-hand side of (12) is not computable in practice (since it is defined in terms of the unknown exact

solution u), and difficult to accurately estimate. In addition, when estimating this right-hand side is possible, it is usually observed that the above bound highly overestimates the exact error.

Remark 2. A direct consequence of (12) is that the L^2 -norm of the error satisfies $\|e\|_0 \leq C h^\alpha \|u\|_{\alpha+1}$, for some C independent of h and u . However, this bound is not sharp. Sharp bounds can be obtained using the Aubin-Nitsche lemma, which is based on the following adjoint problem:

$$\text{Find } \varphi \in V \text{ such that, for any } v \in V, \quad B^*(\varphi, v) = \int_{\Omega} (u - u_h)v, \quad (13)$$

where $B^*(w, v) = B(v, w)$ for any v and w in V . In our case, B is symmetric, hence $B^* = B$.

We follow [49, Sec. 5.4] or [39, Sec. X.1]. Assume that \mathbb{A} and Ω are such that the solution φ to (13) belongs to $H^2(\Omega)$ and satisfies

$$\|\varphi\|_2 \leq C \|u - u_h\|_0. \quad (14)$$

A sufficient condition is that \mathbb{A} is smooth and Ω is convex. Taking $v = u - u_h$ in (13), we have, for any $\varphi_h \in V_h^p$,

$$\|u - u_h\|_0^2 = B(u - u_h, \varphi) = B(u - u_h, \varphi - \varphi_h) \leq C \|u - u_h\|_1 \|\varphi - \varphi_h\|_1.$$

Using (9) to bound the last factor and next (14), we deduce that

$$\|u - u_h\|_0^2 \leq Ch \|u - u_h\|_1 \|\varphi\|_2 \leq Ch \|u - u_h\|_1 \|u - u_h\|_0$$

and hence

$$\|u - u_h\|_0 \leq Ch \|u - u_h\|_1. \quad (15)$$

In view of (12), we eventually obtain

$$\|u - u_h\|_0 \leq Ch^{\alpha+1} \|u\|_{\alpha+1},$$

where the constant C is independent of h and u . The convergence rate is now better than what we had at the beginning of the remark, simply using (12).

Remark 3. It is interesting at this point to draw a parallel between the properties of the Clément interpolant, or of finite element approximations that we mentioned above, and a classical result on the polynomial interpolation of some function $f \in C^{p+1}$. From the values of f at $p+1$ sampling points x_i ($i = 0, 1, \dots, p$), we define the Lagrange interpolant as the polynomial P of degree p such that $P(x_i) = f(x_i)$ for $i = 0, 1, \dots, p$. The interpolation error reads

$$R(x) = f(x) - P(x) = \frac{f^{(p+1)}(\nu_x)}{(p+1)!} \prod_{i=0}^p (x - x_i) \quad \text{with } \nu_x \in [x_0, x_p],$$

and it vanishes at sample points. For a uniform distribution of points, that is when $x_{i+1} - x_i = h$ for any $i = 0, 1, \dots, p-1$, the previous expression yields

$$|R(x)| \leq \frac{|f^{(p+1)}(\nu_x)|}{4(p+1)} h^{p+1}.$$

We thus again observe a convergence rate of the order h^{p+1} when using polynomials of degree p to approximate sufficiently smooth functions f .

To illustrate the *a priori* error estimate, we consider the simple problem shown on Figure 1, that is the Laplace equation $-\Delta u = 0$ in a square domain (of unit size) with prescribed boundary conditions: a Neumann condition $\nabla u \cdot \mathbf{n} = 1$ on the top side of the square, and homogeneous Dirichlet conditions $u = 0$ on the other sides. The expression of the exact solution of this problem (which is smooth) is available, so that the discretization error in the energy norm $\|e\|$ when computing a finite element approximation can be evaluated exactly. This error is shown in Figure 1 for several values of the uniform mesh size h , and when considering various finite element types. The asymptotic evolutions confirm the predictions given by *a priori* error estimation.

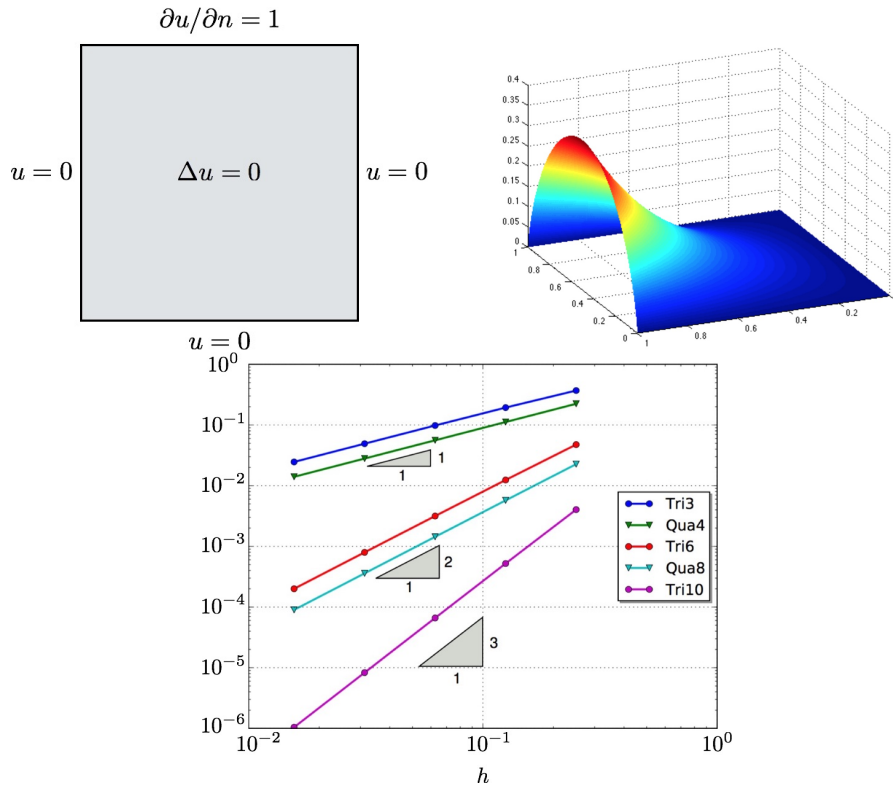


Figure 1: Considered problem (left) on a unit square with analytical solution u (center), and evolution of $\|e\|$ as a function of h (right) for various discretization spaces. The error when using P1 (resp. Q1) finite elements (Tri3, resp. Qua4) decays at the rate $O(h)$. When using P2 (resp. quadratic serendipity) finite elements (Tri6, resp. Qua8), it decays at the rate $O(h^2)$. When using P3 finite elements (Tri10), it decays at the rate $O(h^3)$.

In contrast to *a priori* error estimates, *a posteriori* error estimates use information from the numerical solution to estimate the error. Furthermore, these estimates allow to adapt the approximation spaces (and the related meshes) to efficiently approximate the solution to the problem. In the following sections, we review three families of *a posteriori* error estimation methods: flux recovery methods (in Section 3), residual methods (in Section 4) and duality-based methods (in Section 5). Such methods allow to get additional information on the discretization error, compared to the asymptotic convergence rate predicted by *a priori* error estimates. We then present in Section 6 a unified perspective that encompasses all these methods. We refer to [226] for a numerical comparison of some of these methods.

3 Recovery methods

This category of error estimators is based on using approximations of the exact solution which are more accurate than the numerical solution.

3.1 Richardson extrapolation

A well-known technique in this category is the Richardson extrapolation, in which approximate solutions are obtained on sequences of refined nested meshes (or with shape functions of increasing order) and compared one to each other to obtain an interpolated indication of the error. Consider a refined mesh \mathcal{T}_{h^*} obtained by subdivision of \mathcal{T}_h (we thus have $V_h \subset V_{h^*}$), and let $u_{h^*} \in V_{h^*}$ be the approximation of u computed on this refined mesh. Assuming that we are in the asymptotic range predicted by the *a priori* error estimate (12), we write $\|u - u_{h^*}\| \approx (h^*/h)^\alpha \|e\|$. Using the Galerkin orthogonality property (7), we obtain that

$$\|e\| = \left(\|u - u_{h^*}\|^2 + \|u_{h^*} - u_h\|^2 \right)^{1/2} \approx [1 - (h^*/h)^{2\alpha}]^{-1/2} \|u_{h^*} - u_h\|.$$

Having at our disposal u_h and u_{h^*} , we are thus in position to compute the value of the right-hand side, which provides an approximation of $\|e\|$.

3.2 Basics on flux recovery methods

Flux recovery methods, also referred to as flux-projection techniques, are alternative methods which are very popular in the engineering FE community. They were initially proposed in [250, 251, 252], and are known under the name of Zienkiewicz-Zhu (ZZ) estimators. The idea is to post-process the approximate flux $\mathbf{q}_h = \mathbb{A}\nabla u_h$ in order to get a smoother (continuous) representation \mathbf{q}_h^* of the exact flux $\mathbf{q} = \mathbb{A}\nabla u$, which is *expected* to be more accurate than \mathbf{q}_h . One next uses the estimate (obtained by substituting the unknown flux \mathbf{q} by the recovered flux \mathbf{q}_h^*)

$$\|e\| = \|\mathbf{q} - \mathbf{q}_h\|_q \approx \|\mathbf{q}_h^* - \mathbf{q}_h\|_q, \quad (16)$$

where the notation $\|\cdot\|_q$ is defined in Section 2.1. The quantity $\|\mathbf{q} - \mathbf{q}_h^*\|_q$ is hence thought to be much smaller than the error $\|\mathbf{q} - \mathbf{q}_h\|_q$.

The quality of the estimate $\eta = \|\mathbf{q}_h^* - \mathbf{q}_h\|_q$ depends on that of the smoothing, i.e. on how well \mathbf{q}_h^* approximates \mathbf{q} (see [11]). Assuming that there exists $c \in (0, 1)$ such that

$$\|\mathbf{q} - \mathbf{q}_h^*\|_q \leq c\|\mathbf{q} - \mathbf{q}_h\|_q,$$

we directly get, using the triangle inequality, that

$$\frac{\eta}{1+c} \leq \|e\| \leq \frac{\eta}{1-c}.$$

We thus see that, the smaller c is, the better the *a posteriori* estimate η is.

Several smoothing techniques may be used to build the field \mathbf{q}_h^* , which is usually chosen in $(V_h^p)^d$:

- Nodal averaging: the value of \mathbf{q}_h^* at each nodal point is defined as an average of the values of \mathbf{q}_h at the neighboring Gauss points (which is hence inexpensive to compute);
- Global L^2 projection of \mathbf{q}_h onto the FE space $(V_h^p)^d$;
- Local projection on element patches, which is the so-called Superconvergent Patch Recovery (SPR or ZZ2) technique developed in [249, 251, 252]. In this more advanced approach, superconvergence properties of the FEM (which occur in very specific cases, see e.g. [25, 243]) are taken into account with a local fitting procedure using polynomials of degree p . This technique, which is computationally efficient since it only requires to solve small systems, consists of two steps.

First, over each patch Ω_i of elements sharing the vertex node i , an intermediate recovered flux $\mathbf{g}_i(\mathbf{x}) = \sum_n \alpha_n^i \phi_n(\mathbf{x})$ (where ϕ_n are predefined polynomial functions of degree p) is constructed using values of \mathbf{q}_h at sampling points and performing a least squares fitting between \mathbf{g}_i and \mathbf{q}_h to determine the coefficients $\{\alpha_n^i\}_n$. In other words, a polynomial surface (of the same degree as the FE interpolation) is fitted to the FE flux values at sampling points. These points are (when they exist) superconvergence points \mathbf{x}_s where $|\mathbf{q}(\mathbf{x}_s) - \mathbf{q}_h(\mathbf{x}_s)| \leq C(u)h^{p+1}$. They are for instance element centroids for linear FE ($p = 1$), or Gauss-Legendre quadrature points.

Second, the recovered flux \mathbf{q}_h^* , which is chosen as a function in $(V_h^p)^d$, is defined at each node as the average of the values at this node of the different functions \mathbf{g}_i (note that a node may belong to various patches Ω_i , and thus several functions \mathbf{g}_i may be non-zero at that node). We next interpolate these nodal values using FE shape functions in order to get a continuous flux representation $\mathbf{q}_h^* \in (V_h^p)^d$. Under superconvergence properties, one can show that the estimate $\eta = \|\mathbf{q}_h^* - \mathbf{q}_h\|_q$ obtained in this way is asymptotically exact, i.e. $\lim_{h \rightarrow 0} \frac{\eta}{\|e\|} = 1$.

Remark 4. *Instead of fitting a polynomial of degree p to flux values at some sampling points as in the ZZ2 technique, the fitting of a polynomial of degree $p+1$ to solution values at nodal points was investigated in [248]. The approximation \mathbf{q}_h^* is next obtained after taking derivatives.*

3.3 Recent advances in flux recovery methods

A weakness of the general flux recovery approach (e.g. basic SPR technique) is that it does not use the fact that u_h solves (6). For instance, it does not use information from Neumann boundaries where imposed tractions are known *a priori*, which may lead to a lack of accuracy of the recovered flux field along such boundaries. Also, the strategy is hazardous in case of singularities (cracks, multi-materials, ...) or anisotropic meshes [54, 55], and may be not locally conservative, in the following sense. The estimated global error η can be written as a sum of local contributions, but these local contributions may highly under- or overestimate the true local error. In contrast, the approaches presented in Sections 4 and 5 below provide estimations of the local errors that have been observed, in practice, to be accurate even in difficult cases.

As a consequence of their weaknesses, several improvements to smoothing techniques have been introduced later on in order to insert more physical insight in the procedure, and improve the accuracy and robustness of the flux recovery. In particular, the idea of locally enforcing the equilibrium equation was introduced in [43, 46, 158, 211, 244, 245]. Equilibrium constraints are imposed on each patch by means of penalization (Recovery by Equilibrium in Patches (REP) method) or Lagrange multiplier fields (SPR-C method). They can also be directly inserted in the search space, which then consists of locally equilibrated fields, associated with the solution to some minimization problems over patches [136, 231]. They allow to enhance the quality of the flux field that is recovered over each patch and provide for a locally (but not globally) equilibrated flux field \mathbf{q}_h^* , i.e. a field that locally satisfies the equation $-\operatorname{div} \mathbf{q}_h^* = f$.

The SPR-C method is associated with a continuous fitting approach, and Lagrange multipliers are used to enforce internal and boundary equilibrium equations over each patch. To obtain a globally continuous flux field, a partition of unity is used to properly weight the flux polynomials constructed at the patch level.

An upper bound on the error can next be obtained, as we now show, using the enhanced recovered flux field \mathbf{q}_h^* and an additional correction term to account for the fact that this flux field does not *globally* satisfy the equilibrium equation (see also [91], where an alternative bound to the one given below is proposed). We first recall that

$$H(\operatorname{div}, \Omega) = \{\mathbf{p} \in [L^2(\Omega)]^d, \quad \operatorname{div} \mathbf{p} \in L^2(\Omega)\} \quad (17)$$

is an Hilbert space when endowed with the scalar product $\langle \mathbf{p}, \mathbf{q} \rangle_{H(\operatorname{div}, \Omega)} = \int_{\Omega} \mathbf{p} \cdot \mathbf{q} + (\operatorname{div} \mathbf{p})(\operatorname{div} \mathbf{q})$ and that, for any $\mathbf{p} \in H(\operatorname{div}, \Omega)$, the trace of $\mathbf{p} \cdot \mathbf{n}$ on $\partial\Omega$ is

well-defined. For any $v \in V$ and for any flux $\mathbf{p} \in H(\text{div}, \Omega)$, we then write

$$\begin{aligned} B(e, v) &= \int_{\Omega} \mathbb{A} \nabla(u - u_h) \cdot \nabla v = \int_{\Omega} (\mathbf{q} - \mathbf{q}_h) \cdot \nabla v \\ &= \int_{\Omega} (\mathbf{p} - \mathbf{q}_h) \cdot \nabla v + \int_{\Omega} (f + \text{div } \mathbf{p}) v + \int_{\Gamma_N} (g - \mathbf{p} \cdot \mathbf{n}) v. \end{aligned} \quad (18)$$

Taking $\mathbf{p} = \mathbf{q}_h^*$ and $v = e$, and assuming that the lack of equilibrium $g - \mathbf{q}_h^* \cdot \mathbf{n}$ along the Neumann boundary is negligible, we get

$$\begin{aligned} \|e\|^2 &= \int_{\Omega} (\mathbf{q}_h^* - \mathbf{q}_h) \cdot \nabla e + \int_{\Omega} (f + \text{div } \mathbf{q}_h^*) e \\ &\implies \|e\| \leq \| \mathbf{q}_h^* - \mathbf{q}_h \|_q + Ch \|f + \text{div } \mathbf{q}_h^*\|_0 \end{aligned} \quad (19)$$

where we used the Cauchy-Schwarz inequality and the Aubin-Nitsche lemma (see Remark 2) to bound $\|e\|_0$ by $Ch\|e\|$.

We observe that the upper bound involves two parts: the first one is the classical ZZ estimate (16), and the second one takes into account the lack of equilibrium of the recovered flux field \mathbf{q}_h^* . A numerical procedure based on the Richardson extrapolation (see Section 3.1) may be employed to evaluate the constant C . Indeed, considering $h^* \ll h$ and noticing that

$$\|e\|^2 \approx \frac{\|u_{h^*} - u_h\|^2}{1 - (h^*/h)^{2\alpha}} \quad \text{and} \quad \|e\|_0^2 \approx \frac{\|u_{h^*} - u_h\|_0^2}{1 - (h^*/h)^{2\alpha+2}},$$

$$\text{we get } C \approx \sqrt{\frac{\|u_{h^*} - u_h\|_0^2 (1 - (h^*/h)^{2\alpha})}{h^2 \|u_{h^*} - u_h\|^2 (1 - (h^*/h)^{2\alpha+2})}}.$$

Remark 5. *When a solution field u_h^* is also recovered from u_h , in addition to the locally equilibrated recovered flux \mathbf{q}_h^* , a lower bound on the error in the energy norm can be obtained. Starting again from (18) with $\mathbf{p} = \mathbf{q}_h^*$ and $v = u_h^* - u_h$, we get, using the Cauchy-Schwarz inequality, that*

$$\|e\| \geq \frac{\int_{\Omega} (\mathbf{q}_h^* - \mathbf{q}_h) \cdot \nabla (u_h^* - u_h) + \int_{\Omega} (f + \text{div } \mathbf{q}_h^*) (u_h^* - u_h)}{\|u_h^* - u_h\|}. \quad (20)$$

4 Residual methods

The idea of the residual methods is to use the residual equation (7) to indirectly bound the error $\|e\|$ or the dual norm $\|R\|_*$ of the residual (in the so-called explicit approaches, described in Section 4.1), or to approximate its solution e (in the so-called implicit approaches, described in Section 4.2). The residual actually contains three types of terms: (i) interior residuals that determine how well the approximate solution u_h satisfies the mathematical model in each element, (ii) boundary residuals associated to non-verification of the boundary conditions, and (iii) inter-element residuals related to discontinuities in normal fluxes along the edges of the mesh elements. Explicit residual methods differ from implicit residual methods in the way these three terms are handled.

4.1 Explicit methods

The explicit residual method introduced in [21, 130] employs information available from the FE solution u_h along with residuals to directly compute the error estimate. There is no need to solve any additional boundary value problem, in contrast to the implicit methods presented in Section 4.2 below. In the explicit methods, which share similarities with *a priori* error estimation [222], the three types of residual terms (exhibited after decomposing the weak residual functional) are post-processed separately and then lumped together.

We assume in the sequel that \mathbb{A} is sufficiently smooth in each element of the mesh (typically, $\mathbb{A} \in [H^1(K)]^{d \times d}$ for any $K \in \mathcal{T}_h$). Recalling that

$$\|e\| = \sup_{v \in V, v \neq 0} \frac{|R(v)|}{\|v\|} \quad \text{with} \quad R(v) = F(v) - B(u_h, v) = \langle R|_{u_h}, v \rangle_{V', V}, \quad (21)$$

where $R|_{u_h}$ is defined as an element of the dual space of V , the task is to find computable (local) estimates for the H^{-1} -norm of $R|_{u_h}$. We start from the residual equation (7) and write

$$\begin{aligned} \forall v \in V, \quad B(e, v) &= F(v) - B(u_h, v) \\ &= F(v - \Pi_h v) - B(u_h, v - \Pi_h v) \quad [\text{since } u_h \text{ solves (6)}] \\ &= \int_{\Omega} f(v - \Pi_h v) + \int_{\Gamma_N} g(v - \Pi_h v) - \int_{\Omega} \mathbb{A} \nabla u_h \cdot \nabla (v - \Pi_h v) \\ &= \sum_{K \in \mathcal{T}_h} \int_K r_K (v - \Pi_h v) - \sum_{\Gamma \subset \Gamma_{\text{int}} \cup \Gamma_N} \int_{\Gamma} t_{\Gamma} (v - \Pi_h v), \quad (22) \end{aligned}$$

where $\Pi_h v \in V_h^p$ is the Clément interpolant of v , and where Γ_{int} denotes the union of the internal edges. The quantities r_K and t_{Γ} , which are defined by

$$\begin{aligned} r_K &= f + \text{div} [(\mathbb{A} \nabla u_h)|_K], \\ t_{\Gamma} &= \begin{cases} \mathbb{A} \nabla u_h \cdot \mathbf{n} - g & \text{if } \Gamma \subset \Gamma_N, \\ \mathbb{A} \nabla u_h|_{K_1} \cdot \mathbf{n}_1 + \mathbb{A} \nabla u_h|_{K_2} \cdot \mathbf{n}_2 & \text{if } \Gamma = (\partial K_1 \cap \partial K_2) \subset \Gamma_{\text{int}}, \end{cases} \quad (23) \end{aligned}$$

are called the internal and boundary residuals, respectively (\mathbf{n}_1 and \mathbf{n}_2 are the outward normal vectors to ∂K_1 and ∂K_2 , respectively). They represent the two error sources and are computed from both the approximate solution u_h and input data. Using the Cauchy-Schwarz inequality as well as (10) and (11), we deduce from (22) that, for any $v \in V$,

$$\begin{aligned} &|B(e, v)| \\ &\leq \sum_{K \in \mathcal{T}_h} \|r_K\|_{0, K} \|v - \Pi_h v\|_{0, K} + \sum_{\Gamma \subset \Gamma_{\text{int}} \cup \Gamma_N} \|t_{\Gamma}\|_{0, \Gamma} \|v - \Pi_h v\|_{0, \Gamma} \\ &\leq C \left[\sum_{K \in \mathcal{T}_h} h_K^2 \|r_K\|_{0, K}^2 + \sum_{\Gamma \subset \Gamma_{\text{int}} \cup \Gamma_N} l_{\Gamma} \|t_{\Gamma}\|_{0, \Gamma}^2 \right]^{1/2} \left[\sum_{K \in \mathcal{T}_h} \|v\|_{1, U(K)}^2 + \sum_{\Gamma \subset \Gamma_{\text{int}} \cup \Gamma_N} \|v\|_{1, U(\Gamma)}^2 \right]^{1/2}. \end{aligned}$$

We notice that $\sum_{K \in \mathcal{T}_h} \|v\|_{1,U(K)}^2 + \sum_{\Gamma \subset \Gamma_{\text{int}} \cup \Gamma_N} \|v\|_{1,U(\Gamma)}^2 \leq \widehat{C} \|v\|^2$ where \widehat{C} is independent of h and $v \in V$. Taking $v = e$ in the above estimates, we deduce that

$$\|e\| = \frac{B(e, e)}{\|e\|} \leq C' \left[\sum_{K \in \mathcal{T}_h} h_K^2 \|r_K\|_{0,K}^2 + \sum_{\Gamma \subset \Gamma_{\text{int}} \cup \Gamma_N} l_\Gamma \|t_\Gamma\|_{0,\Gamma}^2 \right]^{1/2}. \quad (24)$$

Note that the constant C' , which only depends on the elements shapes and on a_{\min} and a_{\max} of (2), is usually unknown. It may be estimated but bounds are dictated by worst case scenarios and usually give very pessimistic estimators [127].

The bound (24) is the sum of both element-wise and edge-wise contributions. Element-wise indicators of the local contribution to the bound for $\|e\|$ may be defined under the form

$$\eta_K^2 = h_K^2 \|r_K\|_{0,K}^2 + \sum_{\Gamma \subset \partial K} \beta_\Gamma l_\Gamma \|t_\Gamma\|_{0,\Gamma}^2 \quad \text{with} \quad \beta_\Gamma = \begin{cases} 0 & \text{if } \Gamma \subset \Gamma_D \\ 1/2 & \text{if } \Gamma \subset \Gamma_{\text{int}} \\ 1 & \text{if } \Gamma \subset \Gamma_N \end{cases}. \quad (25)$$

Note that, for edges $\Gamma \subset \Gamma_{\text{int}}$, other splittings of the boundary residual $l_\Gamma \|t_\Gamma\|_{0,\Gamma}^2$ can be chosen. The local contributions (25), which are very cheap to compute, can serve to drive the mesh adaptivity, although they are not an estimate of the error in K (including local and transported components). Likewise, the upper bound (24) cannot be used as a global error estimate since it is not computable in practice due to constants that are, except in very specific cases [113, 130], unknown.

Remark 6. *Since the constants C in (10) and (11) are usually different, the weighting of internal and boundary residual contributions used in the definition (25) of η_K is not justified. However, the correct relative weighting to attach to each type of contribution is far from obvious. In [61], explicit estimates for Clément's interpolation operator (and therefore for the constants C in (10) and (11)) are given in specific cases. The bound (24) is written as*

$$\|e\| \leq c_1 \left(\sum_{K \in \mathcal{T}_h} h_K^2 \|r_K\|_{0,K}^2 \right)^{1/2} + c_2 \left(\sum_{\Gamma \subset \Gamma_{\text{int}} \cup \Gamma_N} l_\Gamma \|t_\Gamma\|_{0,\Gamma}^2 \right)^{1/2}$$

with explicit expressions of c_1 and c_2 . Nevertheless, the crude estimation usually leads to very pessimistic bounds even for regular meshes, particularly due to the fact that possible cancellations between residual types are lost when one deals with each type separately.

Remark 7. *The Aubin-Nitsche lemma (duality argument) can again be used to get a posteriori error bounds in the L^2 -norm. We recall (see (15)) that $\|u - u_h\|_0 \leq Ch \|u - u_h\|_1$. We are then in position to use the bound (24) on $\|u - u_h\|_1$ to obtain an a posteriori error bound on $\|u - u_h\|_0$.*

4.2 Implicit methods

Implicit residual methods, that we now describe, are more difficult and intrusive to implement in scientific computation softwares compared to explicit residual methods. They yet have the potential to provide more detailed and more robust information on the error and its sources. These methods avoid the difficult evaluation of some constants such as the one appearing in (24) by seeking an approximation of the solution e of the residual equation. By treating together the three contributions in the residual, implicit residual methods retain more of the structure of the residual equation than explicit methods do, and thus provide tighter error bounds.

4.2.1 Hierarchical approach

The residual equation (7) is a global equation which cannot be solved exactly (it is as complex as the reference problem). It requires a refined mesh in order to provide for a nontrivial FE approximate solution, a procedure which is usually not feasible. Defining the hierarchical complement space V^{comp} such that $V = V_h^p \oplus V^{\text{comp}}$ (where the decomposition is orthogonal in the sense of the symmetric bilinear form B), a first possibility (called *multilevel error estimation*) is to enlarge the Galerkin subspace V_h^p by $V_h^{\text{comp}} \subset V^{\text{comp}}$ leading to a new subspace $\widetilde{V}_h = V_h^p \oplus V_h^{\text{comp}}$ supposed to accurately approximate the solution e . By Galerkin orthogonality (see (7)), we know that $e \in V^{\text{comp}}$. For a simple implementation, V_h^{comp} may be chosen as the function space spanned by so-called *bubble functions* with disjoint supports [27].

We then search an approximation $\tilde{e}_h \in V_h^{\text{comp}}$ of e such that

$$\forall v \in V_h^{\text{comp}}, \quad B(\tilde{e}_h, v) = R(v)$$

and define $\eta = \|\|\tilde{e}_h\|\|$ as an error estimator. This estimator is reliable and effective if the saturation assumption is valid, namely if $e - \tilde{e}_h$ is much smaller than e . More precisely, letting \tilde{u}_h be the approximation of u in \widetilde{V}_h , it is easy to see that $\tilde{e}_h = \tilde{u}_h - u_h$, hence $e - \tilde{e}_h = u - \tilde{u}_h$. The saturation assumption hence holds whenever $u - \tilde{u}_h$ is much smaller than $u - u_h$. This can be quantified in a manner similar to that of Section 3, as follows: assuming that there exists $c \in (0, 1)$ such that

$$\|u - \tilde{u}_h\| = \|e - \tilde{e}_h\| \leq c \|u - u_h\| = c \|e\|,$$

we directly get, using the triangle inequality and the Galerkin orthogonality, that

$$\frac{\eta}{1+c} \leq \|e\| \leq \frac{\eta}{\sqrt{1-c^2}}.$$

As an alternative, the residual equation may be decomposed into a series of *decoupled local* boundary value problems, and local approximations of e are then searched. Such methods can be classified in different categories, depending on:

1. the small domain in which the local problem is posed: over each element in the mesh \mathcal{T}_h (element residual methods) or over patches of elements (subdomain residual methods);
2. the boundary conditions imposed on the local problems. When Dirichlet boundary conditions are used, one obtains continuous approximations of e and lower bounds on $\|e\|$. In contrast, using Neumann boundary conditions allows to derive equilibrated flux fields and upper bounds on $\|e\|$;
3. the numerical method used to approximate the solution of the local problems. In practice, a standard FE method on a finer mesh (or using higher-degree polynomial functions) is usually employed producing asymptotic estimates which have bounding properties only with respect to a reference numerical solution (more precisely, the quantities that can be computed in practice provide rigorous bounds on the error $u_h^* - u_h$ rather than on $u - u_h$, where u_h^* is the approximation of u obtained by using the finer mesh, resp. the higher-degree approximation space). Another option is to use a dual approach yielding a direct approximation of the local flux field and allowing for the computation of guaranteed upper bounds on the error. This approach will be further discussed in Section 5 below.

We first consider subdomain residual methods in Section 4.2.2 before turning to element residual methods in Section 4.2.3.

4.2.2 Subdomain residual methods

We describe here three subdomain implicit residual methods, the latter two being very close one to each other.

A first subdomain implicit residual method was proposed in [21], in which auxiliary local problems with homogeneous Dirichlet boundary conditions are solved on each patch Ω_i of elements connected to the vertex i . Denoting by $\{\varphi_j\}$ the basis functions of the approximation space V_h^p , and by $\{\phi_i\}$ the first-order Lagrange basis functions associated to the mesh vertices (the support of ϕ_i is Ω_i), we have, due to the partition of unity property $\sum_i \phi_i = 1$, that

$$\forall v \in V, \quad B(e, v) = R \left(v \sum_i \phi_i \right) = \sum_i R(v \phi_i). \quad (26)$$

The idea is to replace the above single global residual problem by a set of local, independent problems. Noticing that $v \phi_i \in V_0(\Omega_i)$, with $V_0(\Omega_i) = \{w \in H^1(\Omega_i), w = 0 \text{ on } \partial\Omega_i\}$, and inspired by (22), we introduce the following local problem on each patch Ω_i :

Find $e_i \in V_0(\Omega_i)$ such that, for any $v \in V_0(\Omega_i)$,

$$B_{\Omega_i}(e_i, v) = \sum_{K \subset \Omega_i} \int_K r_K v - \sum_{\Gamma \subset \Omega_i} \int_{\Gamma} t_{\Gamma} v, \quad (27)$$

where r_K and t_Γ are defined by (23) and where $B_{\Omega_i}(u, v) = \int_{\Omega_i} \mathbb{A} \nabla u \cdot \nabla v$ is the restriction of B on Ω_i . Defining the estimate $\eta^2 = \sum_i B_{\Omega_i}(e_i, e_i) = \sum_i \|e_i\|_{\Omega_i}^2$, it was shown in [21] that there exist C_1 and C_2 independent of h such that

$$C_1 \eta \leq \|e\| \leq C_2 \eta.$$

In view of (21), the quantity $\sum_i e_i \in V$ obviously satisfies the lower bound

$$\frac{|R(\sum_i e_i)|}{\|\sum_i e_i\|} \leq \|e\|. \quad (28)$$

However, this approach does not provide a guaranteed upper bound on e and η is often a poor approximation of the error.

A variation in the subdomain-residual method has been first proposed in [62, 163, 171, 196], using auxiliary local problems with Neumann boundary conditions. It explicitly employs the partition of unity property verified by piecewise affine FE shape functions $\{\phi_i\}$ in order to introduce well-posed (self-equilibrated) Neumann problems localized over patches Ω_i (which, we recall, are the support of the shape functions ϕ_i). Consider the space $W(\Omega_i) = \left\{ v \in L^1_{\text{loc}}(\Omega_i), \int_{\Omega_i} \phi_i \mathbb{A} \nabla v \cdot \nabla v < \infty, v = 0 \text{ on } \partial\Omega_i \cap \Gamma_D \right\}$, endowed with the inner product $B_{\phi_i, \Omega_i}(u, v) = \int_{\Omega_i} \phi_i \mathbb{A} \nabla u \cdot \nabla v$ and the associated semi-norm $\|v\|_{\phi_i, \Omega_i}$. Starting from (26), the idea is to introduce the following local problems:

$$\text{Find } \xi_i \in W(\Omega_i) \text{ such that, for any } v \in W(\Omega_i), \quad B_{\phi_i, \Omega_i}(\xi_i, v) = R(v \phi_i). \quad (29)$$

For patches Ω_i which are not connected to Γ_D , the local problems (29) are of Neumann type. The compatibility condition is satisfied since, for any constant test function $v = v_0$, we have $R(v_0 \phi_i) = v_0 R(\phi_i) = 0$, the last equality being a consequence of (7) and $\phi_i \in V_h^p$. The solution to (29) being defined up to an additive constant, it is in practice searched in the space $\left\{ v \in W(\Omega_i), \int_{\Omega_i} v \phi_i = 0 \right\}$. The well-posedness of (29) is established in [171] using a weighted Poincaré-Wirtinger inequality.

Using the above ξ_i , we now build an error estimator. For any $v \in V$, we see that $v|_{\Omega_i} \in W(\Omega_i)$ for any i . We thus infer from (26) and (29) that

$$\begin{aligned} B(e, v) &= \sum_i R(v \phi_i) = \sum_i B_{\phi_i, \Omega_i}(\xi_i, v) \leq \sum_i \sqrt{B_{\phi_i, \Omega_i}(\xi_i, \xi_i)} \sqrt{B_{\phi_i, \Omega_i}(v, v)} \\ &\leq \sqrt{\sum_i B_{\phi_i, \Omega_i}(\xi_i, \xi_i)} \sqrt{\sum_i B_{\phi_i, \Omega_i}(v, v)}. \end{aligned}$$

Choosing $v = e$, we obtain

$$\|e\|^2 = B(e, e) \leq \eta \sqrt{\sum_i B_{\phi_i, \Omega_i}(e, e)}$$

where $\eta = \sqrt{\sum_i B_{\phi_i, \Omega_i}(\xi_i, \xi_i)} = \sqrt{\sum_i \|\xi_i\|_{\phi_i, \Omega_i}^2}$. Noticing that $\sum_i B_{\phi_i, \Omega_i}(e, e) = \sum_i B_{\phi_i, \Omega}(e, e) = B(e, e)$, we then deduce that

$$\|e\| \leq \eta = \sqrt{\sum_i \|\xi_i\|_{\phi_i, \Omega_i}^2}. \quad (30)$$

Furthermore, a lower bound can be easily obtained as follows [196]: using (21) and the choice $\tilde{v} = \sum_i \xi_i \phi_i \in V$, we write

$$\|e\| = \sup_{v \in V, v \neq 0} \frac{|R(v)|}{\|v\|} \geq \frac{|R(\tilde{v})|}{\|\tilde{v}\|} = \frac{\eta^2}{\|\tilde{v}\|}. \quad (31)$$

Remark 8. *In practice, the local problems (29) are solved on the polynomial space $W^{p+k}(\Omega_i) = \mathcal{P}^{p+k}(\Omega_i) \cap W(\Omega_i)$ of polynomials with degree up to $p+k$, leading to the estimate η^* . It can be shown (see [196]) that $\|e\| \leq \eta^* + 2 \inf_{v \in V_h^{p+k}} \|u - v\|$ and that there exists a constant $C > 1$, independent of h and k , such that $\eta^* \leq C\|e\|$.*

In [184], yet another variation of the subdomain residual method (later named “flux free”) is considered, with another local problem (again complemented, as in [62, 171, 196], with Neumann boundary conditions). Defining $V(\Omega_i) = \{v \in H^1(\Omega_i), v = 0 \text{ on } \partial\Omega_i \cap \Gamma_D\}$, local problems on patches are introduced as:

$$\text{Find } z_i \in V(\Omega_i) \text{ such that, for any } v \in V(\Omega_i), \quad B_{\Omega_i}(z_i, v) = R(v \phi_i), \quad (32)$$

where B_{Ω_i} is defined as in (27), i.e. $B_{\Omega_i}(u, v) = \int_{\Omega_i} \mathbb{A} \nabla u \cdot \nabla v$ (note the difference between B_{Ω_i} and the bilinear form used in (29)). For patches Ω_i which are not connected to Γ_D , these local problems are again of Neumann type. The condition $\int_{\Omega_i} z_i = 0$ is imposed for these patches Ω_i . The problems (32) are then well-posed.

To build an error estimator, we proceed as follows. For any $v \in V$, we see that $v|_{\Omega_i} \in V(\Omega_i)$ for any i . We thus infer from (26) and (32) that

$$\begin{aligned} B(e, v) &= \sum_i R(v \phi_i) = \sum_i B_{\Omega_i}(z_i, v) = \sum_i B_{\text{brok}}(z_i, v) \\ &= B_{\text{brok}}\left(\sum_i z_i, v\right) \leq \sqrt{B_{\text{brok}}\left(\sum_i z_i, \sum_i z_i\right)} \sqrt{B(v, v)}, \end{aligned}$$

where $B_{\text{brok}}(u, v) = \sum_{K \in \mathcal{T}_h} B_K(u, v) = \sum_{K \in \mathcal{T}_h} \int_K \mathbb{A} \nabla u \cdot \nabla v$. Taking $v = e$, we deduce the upper bound

$$\|e\| \leq \eta = \sqrt{B_{\text{brok}} \left(\sum_i z_i, \sum_i z_i \right)}. \quad (33)$$

Numerical experiments show that the estimate (33) obtained by solving (32) is more accurate than the estimate (30) obtained by solving (29) (i.e. when weighting the operator) (see [184]). A lower bound on the error can be obtained as in the previous approach, using (21) and $\tilde{v} = \sum_i z_i \phi_i \in V$.

Remark 9. For linear elasticity problems, $B_{\Omega_i}(z_i, \mathbf{v})$ also vanishes when \mathbf{v} is a rigid body motion, that is when $\mathbf{v}(\mathbf{x}) = \mathbf{v}_0 + \mathbb{M}\mathbf{x}$ where \mathbf{v}_0 is constant and \mathbb{M} is a skew-symmetric matrix. It is necessary to change the right-hand side of (32) in $R((\mathbf{v} - \Pi_h^1 \mathbf{v}) \phi_i)$, where $\Pi_h^1 \mathbf{v}$ is the Clément interpolant of \mathbf{v} on piecewise affine FE functions, to ensure the solvability of (32) in this more complex setting (see [184]). In practice, $\Pi_h^1 \mathbf{v}$ is often replaced by the nodal interpolant of \mathbf{v} .

4.2.3 Element residual methods

Element implicit residual methods require solving auxiliary problems on each element K rather than on patches of elements as in Section 4.2.2 (see [28, 85, 226]). Defining $V(K) = \{v \in H^1(K), v = 0 \text{ on } \partial K \cap \Gamma_D\}$ and the broken space

$$V_{\text{brok}} = \oplus_K V(K),$$

the local problems typically read:

Find $e_K \in V(K)$ such that, for any $v \in V(K)$,

$$B_K(e_K, v) = \int_K r_K v + \sum_{\Gamma \subset \partial K \setminus \Gamma_D} \int_{\Gamma} R_{\Gamma} v, \quad (34)$$

with $R_{\Gamma} = -t_{\Gamma}/2$ (resp. $R_{\Gamma} = -t_{\Gamma}$) if $\Gamma \subset \Gamma_{\text{int}}$ (resp. $\Gamma \subset \Gamma_N$), where r_K and t_{Γ} are defined by (23).

For any $v \in V \subset V_{\text{brok}}$, we have

$$B(e, v) = R(v) = \sum_{K \in \mathcal{T}_h} B_K(e_K, v),$$

which implies, taking $v = e$, that the local estimates $\eta_K^2 = B_K(e_K, e_K)$ provide for a guaranteed upper bound on the error:

$$\|e\| \leq \eta = \sqrt{\sum_{K \in \mathcal{T}_h} \eta_K^2}. \quad (35)$$

In addition, a lower bound on $\|e\|$ can be derived from $e_{\text{est}} = \sum_K e_K$, see [90]. Note that $e_{\text{est}} \in V_{\text{brok}}$ but that, in general, $e_{\text{est}} \notin V$. In order to use (21), one has to introduce a correction $e_{\text{cor}} \in V_{\text{brok}}$ such that $e_{\text{est}} + e_{\text{cor}} \in V$.

However, the local problems (34) are not necessarily well-posed. For elements K which are not connected to Γ_D , the problem (34) is of Neumann type, and the compatibility relation is not satisfied (taking $v = 1$ in (34), the left-hand side vanishes but the right-hand side does not, in the general case). Keeping R_Γ defined from a trivial flux averaging as above, there are two possibilities to circumvent this issue:

- search e_K in a regularizing subspace of bubble functions $V^{\text{comp}}(K)$ (see [9, 28]) vanishing at vertex nodes, so that the bilinear form is coercive. The quality of the obtained estimates of course depends on the choice of the subspace. In addition, the upper bound is not guaranteed any more since e cannot usually be chosen as a test function in this variant of (34).
- search e_K in $V(K)$ but change the right-hand side of (34) in $\int_K r_K(v - \Pi_h^1 v) + \sum_{\Gamma \subset \partial K \setminus \Gamma_D} \int_\Gamma R_\Gamma(v - \Pi_h^1 v)$, where $\Pi_h^1 v$ is the Clément interpolant of v on piecewise affine FE functions (see [28]). The Neumann compatibility relation is now satisfied and this variant of (34) is well-posed, e_K being defined up to the addition of a constant. The upper bound (35) again holds [28].

An alternative and more effective possibility [8], which also provides for an upper bound on the error, is to consider a variant of (34) where R_Γ is replaced by some carefully chosen boundary data $\widehat{R}_{\Gamma,K}$ on ∂K . These data $\widehat{R}_{\Gamma,K}$ are constructed so that equilibrium over each element K is ensured, i.e. such that

$$\int_K r_K + \sum_{\Gamma \subset \partial K \setminus \Gamma_D} \int_\Gamma \widehat{R}_{\Gamma,K} = 0. \quad (36)$$

This is the basis of the so-called equilibrated element residual estimates.

The following variant of (34) is then considered:

Find $\widehat{e}_K \in V(K)$ such that, for any $v \in V(K)$,

$$B_K(\widehat{e}_K, v) = \int_K r_K v + \sum_{\Gamma \subset \partial K \setminus \Gamma_D} \int_\Gamma \widehat{R}_{\Gamma,K} v. \quad (37)$$

This again corresponds to a problem with Neumann boundary conditions. In view of (36), the compatibility condition holds and the solution \widehat{e}_K to (37) is therefore well-defined, up to the addition of a constant.

The tractions $\widehat{R}_{\Gamma,K}$ are often chosen of the following form: on each element K ,

$$\widehat{R}_{\Gamma,K}(\mathbf{x}) = \sigma_{\Gamma,K} \widehat{g}_\Gamma(\mathbf{x}) - \mathbb{A} \nabla u_{h|K} \cdot \mathbf{n}_K$$

where $\sigma_{\Gamma,K} = \pm 1$ (to ensure the continuity of the normal flux across the element edges) and where \widehat{g}_Γ is an approximation of the exact normal boundary flux $\mathbb{A}\nabla u|_\Gamma \cdot \mathbf{n}$ to be appropriately chosen (see Section 5.3 for technicalities when computing \widehat{g}_Γ). The fact that $\widehat{R}_{\Gamma,K}$ satisfies the equilibrium equation (36) provides for more realistic boundary conditions than the two approaches described at the beginning of this Section 4.2.3. The approach eventually provides a guaranteed error estimate that is observed to be more accurate.

Remark 10. *The change of the right-hand side of (34) performed in [28] can actually be seen as an implicit way of recovering equilibrated tractions.*

5 Duality-based methods

We now turn to a different class of methods. The *a posteriori* error estimation methods that we present in this section are built from a residual on the constitutive relation $\mathbf{q} = \mathbb{A}\nabla u$ rather than from a balance residual. More precisely, the estimation methods presented in Section 4 are based on the residuals $r_K = f + \operatorname{div}[(\mathbb{A}\nabla u_h)|_K]$ in each element K and on the flux jumps t_Γ , two quantities that enter in the right-hand side of (22) and of the auxiliary local problems (27), (34), (37), . . . The spirit of the approaches presented here is different. Recalling that $f \in L^2(\Omega)$, the problem (1) is written, somewhat as for mixed methods, in the form

$$-\operatorname{div} \mathbf{q} = f \text{ in } \Omega, \quad \mathbf{q} \cdot \mathbf{n} = g \text{ on } \Gamma_N, \quad \mathbf{q} \in H(\operatorname{div}, \Omega), \quad (38)$$

$$u = 0 \text{ on } \Gamma_D, \quad u \in H^1(\Omega), \quad (39)$$

$$\mathbb{A}\nabla u = \mathbf{q} \text{ in } \Omega, \quad (40)$$

where we recall that $H(\operatorname{div}, \Omega)$ is defined by (17) and that, for any $\mathbf{q} \in H(\operatorname{div}, \Omega)$, the trace of $\mathbf{q} \cdot \mathbf{n}$ on $\partial\Omega$ is well-defined.

The methods described in this Section 5 aim at

- building a function \widehat{u} that satisfies (39) (one usually chooses $\widehat{u} = u_h$);
- building a vector-valued function $\widehat{\mathbf{q}}$ that satisfies the equilibrium equation (38); this is often done by post-processing $\mathbb{A}\nabla u_h$;
- estimating the error $e = u - u_h$ in term of the error in (40), that is $\mathbb{A}\nabla \widehat{u} - \widehat{\mathbf{q}}$.

5.1 Dual approach

Starting from the residual equation (7) verified by $e \in V$, namely

$$\forall v \in V, \quad B(e, v) = F(v) - B(u_h, v),$$

we observe that e is equivalently the solution of the following (so-called primal) variational problem

$$J(e) = \inf \{J(w), \quad w \in V\},$$

where J is the quadratic functional

$$\begin{aligned} J(w) &= \frac{1}{2}B(w, w) - F(w) + B(u_h, w) \\ &= \frac{1}{2} \int_{\Omega} \mathbb{A} \nabla w \cdot \nabla w - \int_{\Omega} f w - \int_{\Gamma_N} g w + \int_{\Omega} \mathbb{A} \nabla u_h \cdot \nabla w. \end{aligned}$$

We also note that $J(e) = -\frac{1}{2} \int_{\Omega} \mathbb{A} \nabla e \cdot \nabla e$. We therefore have

$$\forall w \in V, \quad \|e\|^2 = -2J(e) \geq -2J(w).$$

An interesting consequence is that we can easily compute a lower bound on the error $\|e\|$, namely $\sqrt{-2J(w)}$ for any $w \in V$ such that $J(w) < 0$. However, this lower bound is usually poor unless w is a suitably chosen representation of e as in (20), (28) or (31).

Remark 11. *An alternative way to obtain that lower bound is as follows. Introduce the potential energy functional J_1 associated with the reference problem, which is defined by $J_1(w) = \frac{1}{2} \int_{\Omega} \mathbb{A} \nabla w \cdot \nabla w - \int_{\Omega} f w - \int_{\Gamma_N} g w$. We recall that the solution u to (1) satisfies $J_1(u) = \inf_{w \in V} J_1(w)$. We then have that $\|e\|^2 = 2(J_1(u_h) - J_1(u))$, and hence the lower bound*

$$\forall w \in V, \quad \|e\|^2 \geq -2(J_1(w) - J_1(u_h)) = -2J(w - u_h). \quad (41)$$

We note that, in view of (41), we would like to compute w such that $J_1(w)$ is as small as possible. In the space V_h^p , we know that u_h is the unique minimizer of J_1 . Using (41) with $w \in V_h^p$ is thus not informative. For (41) to be useful, w should be searched in a space larger than V_h^p , as performed in (20), (28) or (31).

A complementary variational principle can be associated to the primal variational principle and may be used to get an upper bound on $\|e\|$. To that aim, we introduce the space

$$W = \{\mathbf{p} \in H(\operatorname{div}, \Omega), \quad \operatorname{div} \mathbf{p} + f = 0 \text{ in } \Omega, \quad \mathbf{p} \cdot \mathbf{n} = g \text{ on } \Gamma_N\},$$

where we recall that the Hilbert space $H(\operatorname{div}, \Omega)$ is defined by (17).

Consider the quadratic functional

$$G(\mathbf{p}) = \frac{1}{2} \int_{\Omega} \mathbb{A}^{-1}(\mathbf{p} - \mathbb{A} \nabla u_h) \cdot (\mathbf{p} - \mathbb{A} \nabla u_h) = \frac{1}{2} \|\mathbf{p} - \mathbb{A} \nabla u_h\|_q^2$$

and the so-called complementary variational problem

$$\inf \{G(\mathbf{p}), \quad \mathbf{p} \in W\}. \quad (42)$$

The minimization problem (42) is well posed, and it is easy to see that the solution flux $\mathbf{q} = \mathbb{A} \nabla u$ (where u is the solution to the reference problem (1))

is the solution to (42). We obviously have $\|e\|^2 = 2G(\mathbf{q})$. We thus deduce the following upper bound:

$$\forall \mathbf{p} \in W, \quad \|e\|^2 \leq 2G(\mathbf{p}). \quad (43)$$

Remark 12. *An alternative way to obtain that upper bound is as follows. Introduce the complementary energy functional J_2 associated with the reference problem, which is defined by $J_2(\mathbf{p}) = \frac{1}{2} \int_{\Omega} \mathbb{A}^{-1} \mathbf{p} \cdot \mathbf{p}$. We recall that the exact flux $\mathbf{q} = \mathbb{A} \nabla u$ satisfies $J_2(\mathbf{q}) = \inf_{\mathbf{p} \in W} J_2(\mathbf{p})$. We then have that $\|e\|^2 = 2(J_2(\mathbf{q}) + J_1(u_h))$, from which we deduce the upper bound*

$$\forall \mathbf{p} \in W, \quad \|e\|^2 \leq 2(J_2(\mathbf{p}) + J_1(u_h)) = 2G(\mathbf{p}). \quad (44)$$

In view of (44), we would like to compute \mathbf{p} such that $J_2(\mathbf{p})$ is as small as possible.

5.2 Constitutive relation error functional

A flux field that belongs to W will be said to be statically admissible (in the sense that it verifies the equilibrium equations) and denoted $\hat{\mathbf{q}}$ in the following. For the pair $(u_h, \hat{\mathbf{q}}) \in V_h^p \times W$, we define the constitutive relation error (CRE) functional E_{CRE} by

$$E_{\text{CRE}}^2(u_h, \hat{\mathbf{q}}) = \frac{1}{2} \|\hat{\mathbf{q}} - \mathbb{A} \nabla u_h\|_q^2.$$

We of course note that $E_{\text{CRE}}^2(u_h, \hat{\mathbf{q}}) = G(\hat{\mathbf{q}}) = J_1(u_h) + J_2(\hat{\mathbf{q}})$. In view of (43), we then get that, for any $\hat{\mathbf{q}} \in W$, $\sqrt{2} E_{\text{CRE}}(u_h, \hat{\mathbf{q}})$ is an upper-bound on $\|e\|$ (without any generic multiplicative constant), and that $\|e\| = \inf_{\hat{\mathbf{q}} \in W} \sqrt{2} E_{\text{CRE}}(u_h, \hat{\mathbf{q}})$.

We show in what follows how to obtain more precise relations.

We first have the following result (the so-called Prager-Synge equality), which will be most useful in what follows.

Lemma 13. *For any $\hat{\mathbf{q}} \in W$, we have*

$$2 E_{\text{CRE}}^2(u_h, \hat{\mathbf{q}}) = \|e\|^2 + \|\mathbf{q} - \hat{\mathbf{q}}\|_q^2. \quad (45)$$

Proof. Let u be the solution to the reference problem (1). We write

$$\begin{aligned} 2 E_{\text{ERC}}^2(u_h, \hat{\mathbf{q}}) &= \|\hat{\mathbf{q}} - \mathbb{A} \nabla u_h\|_q^2 \\ &= \|(\hat{\mathbf{q}} - \mathbb{A} \nabla u) + (\mathbb{A} \nabla u - \mathbb{A} \nabla u_h)\|_q^2 \\ &= \|\hat{\mathbf{q}} - \mathbb{A} \nabla u\|_q^2 + \|u - u_h\|^2 + 2 \int_{\Omega} (\hat{\mathbf{q}} - \mathbb{A} \nabla u) \cdot \nabla (u - u_h). \end{aligned}$$

The last term in the above right-hand side vanishes by integration by part, using that both $\hat{\mathbf{q}}$ and $\mathbf{q} = \mathbb{A} \nabla u$ belong to W and that $u = u_h$ on Γ_D . We hence obtain (45). \square

We also have the following properties (see [150]):

$$(u_h, \hat{\mathbf{q}}) \in V_h^p \times W \text{ s.t. } E_{\text{CRE}}^2(u_h, \hat{\mathbf{q}}) = 0 \iff u_h = u \text{ and } \hat{\mathbf{q}} = \mathbf{q},$$

$$\text{Hypercircle property: } E_{\text{CRE}}^2(u_h, \hat{\mathbf{q}}) = 2 \|\mathbf{q} - \hat{\mathbf{q}}^m\|_q^2 \text{ where } \hat{\mathbf{q}}^m = \frac{1}{2}(\hat{\mathbf{q}} + \mathbb{A}\nabla u_h). \quad (46)$$

The hypercircle property can easily be shown as a consequence of the Prager-Synge equality (45), as illustrated on Figure 2. Introducing $\delta\mathbf{q} = (\hat{\mathbf{q}} - \mathbf{q}_h)/2$, we indeed infer from (45) that

$$\begin{aligned} 2 E_{\text{CRE}}^2(u_h, \hat{\mathbf{q}}) &= \|\mathbf{q} - \mathbf{q}_h\|_q^2 + \|\mathbf{q} - \hat{\mathbf{q}}\|_q^2 \\ &= \|\mathbf{q} - (\hat{\mathbf{q}}^m - \delta\mathbf{q})\|_q^2 + \|\mathbf{q} - (\hat{\mathbf{q}}^m + \delta\mathbf{q})\|_q^2 \\ &= 2 \|\mathbf{q} - \hat{\mathbf{q}}^m\|_q^2 + 2 \|\delta\mathbf{q}\|_q^2, \end{aligned}$$

and we observe that $2 \|\delta\mathbf{q}\|_q^2 = \|\hat{\mathbf{q}} - \mathbf{q}_h\|_q^2/2 = E_{\text{CRE}}^2(u_h, \hat{\mathbf{q}})$, which yields the hypercircle property.

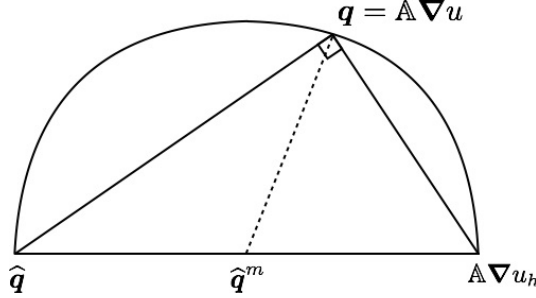


Figure 2: Geometrical illustration of the Prager-Synge equality and the hypercircle property.

A practical consequence of (45) is that the quantity $\sqrt{2} E_{\text{CRE}}(u_h, \hat{\mathbf{q}})$ is an upper bound on the error $\|e\|$ for any $\hat{\mathbf{q}} \in W$. The accuracy of this bound of course depends on the choice of $\hat{\mathbf{q}}$. As shown below, it is possible to efficiently build some $\hat{\mathbf{q}} \in W$ such that this upper bound is accurate in the sense that $\sqrt{2} E_{\text{CRE}}(u_h, \hat{\mathbf{q}})/\|e\|$ is close to 1.

In addition, depending on the precise way the flux $\hat{\mathbf{q}} \in W$ is constructed, a lower bound on $\|e\|$ can also be shown (see e.g. [145, 150]). This lower bound is usually of the form $E_{\text{CRE}}(u_h, \hat{\mathbf{q}}) \leq C \|e\|$, where C is a constant independent of the mesh size h , so that $E_{\text{CRE}}(u_h, \hat{\mathbf{q}})$ and $\|e\|$ have the same asymptotic convergence rate. The precise statement and the proof of such a bound for a 2D problem discretized by piecewise affine finite elements is given in Appendix A below.

5.3 Construction of a statically admissible flux field

In order to compute an upper bound on the error, one possibility is to use (43) and to approximate the complementary problem (42) using a FE discretization with equilibrium elements, namely functions in W (see [84, 107, 131, 168]). Even though this procedure usually provides for the sharpest error bounds, it is in practice very challenging for a twofold reason. First, the constraints in the space W make the practical construction of feasible functions $\hat{\mathbf{q}}$ not straightforward (and barely implementable in commercial finite element softwares since it refers to a non-conventional numerical architecture). Second, such an approach amounts to solve an additional global problem, and thus requires a large computational effort. In addition, it is unclear whether it is actually necessary to carry out any further global computations, since there is already some global information in the FE approximation u_h (and in the flux $\mathbf{q}_h = \mathbb{A}\nabla u_h$) that we have at our disposal.

In the following, we proceed differently. We detail various techniques that enable to recover a flux $\hat{\mathbf{q}}_h \in W$ from local independent computations and from postprocessing operations on u_h and \mathbf{q}_h . Note that we are able to build functions in W (a space that carries a *global* constraint) while only solving *local* problems because we are going to use the global information we already have, through the knowledge of $\mathbf{q}_h = \mathbb{A}\nabla u_h$.

5.3.1 Hybrid-flux approach

In this approach, also referred to as Element Equilibration Technique (EET), the computation of $\hat{\mathbf{q}}_h \in W$ is performed in two steps [8, 145, 146, 150, 193]:

- (i) construction of functions \hat{g}_K along element edges (with $\hat{g}_K = g$ on Γ_N) that should satisfy the so-called element equilibrium equation:

$$\forall K \in \mathcal{T}_h, \quad \int_K f + \int_{\partial K} \hat{g}_K = 0, \quad (47)$$

and should be continuous across adjacent element edges (equilibrium of edges). In analogy to mechanical problems, the functions \hat{g}_K are called equilibrated tractions. We will use the numerical solution (u_h, \mathbf{q}_h) to build these \hat{g}_K .

- (ii) local construction of $\hat{\mathbf{q}}_{h|K}$ over each element K , with prescribed tractions \hat{g}_K and source term f ; they should be a solution to the local Neumann problem

$$-\operatorname{div} \hat{\mathbf{q}}_{h|K} = f \quad \text{in } K, \quad \hat{\mathbf{q}}_{h|K} \cdot \mathbf{n}_K = \hat{g}_K \quad \text{on } \partial K. \quad (48)$$

We now successively detail these two steps.

Step 1: construction of equilibrated tractions \widehat{g}_K on the element edges. The compatibility (equilibrium) conditions on \widehat{g}_K are a global constraint, involving tractions on boundaries of all elements in the mesh \mathcal{T}_h . Nevertheless, we show below that the computation of the set of \widehat{g}_K can be performed locally, by solving small and independent linear systems of equations.

After ordering the elements, we define the function $\sigma_{\Gamma,K} : \partial K \rightarrow \{+1, -1\}$ by

$$\sigma_{\Gamma,K} = \begin{cases} +1 & \text{if } \Gamma = \overline{K} \cap \overline{J} \text{ for some element } J < K, \\ -1 & \text{if } \Gamma = \overline{K} \cap \overline{J} \text{ for some element } J > K, \\ +1 & \text{if } \Gamma \subset \Gamma_D. \end{cases} \quad (49)$$

We then construct the tractions \widehat{g}_K in the form $\widehat{g}_K = \sigma_{\Gamma,K} \widehat{g}_\Gamma$ where \widehat{g}_Γ is a smooth function defined on each element interface Γ . This ensures that the normal flux is continuous across the edges.

We request that $\widehat{\mathbf{q}}_h$ is a solution to (48) and satisfies the following energy condition (called *strong prolongation condition*): for each element K and each node i connected to K ,

$$\int_K (\widehat{\mathbf{q}}_h - \mathbf{q}_h) \cdot \nabla \varphi_i = 0, \quad (50)$$

where $\{\varphi_i\}$ are the basis functions of the approximation space V_h^p . This can be recast as

$$\sum_{\Gamma \subset \partial K} \int_\Gamma \sigma_{\Gamma,K} \widehat{g}_\Gamma \varphi_i = Q_i^K \quad \text{with} \quad Q_i^K = \int_K (\mathbf{q}_h \cdot \nabla \varphi_i - f \varphi_i). \quad (51)$$

Note that, if (51) is satisfied, then, by summing over i and by using the partition of unity property $\sum_i \varphi_i|_K = 1$, we check that (47) is satisfied.

We are now left with building \widehat{g}_Γ satisfying (51). For any adjacent elements K_α and K_β (sharing the interface $\Gamma_{\alpha,\beta}$), introduce the quantity

$$\widehat{b}_{\alpha,\beta}(i) = \int_{\Gamma_{\alpha,\beta}} \sigma_{\Gamma_{\alpha,\beta},K_\alpha} \widehat{g}_{\Gamma_{\alpha,\beta}} \varphi_i = \int_{\Gamma_{\alpha,\beta}} \widehat{g}_{K_\alpha} \varphi_i = - \int_{\Gamma_{\alpha,\beta}} \widehat{g}_{K_\beta} \varphi_i, \quad (52)$$

which is the projection of the traction $\widehat{g}_{\Gamma_{\alpha,\beta}}$ over the FE shape function φ_i . For each node i , the equation (51) can be recast as a linear system involving the quantities $\widehat{b}_{\alpha,\beta}(i)$ for the elements K_α and K_β that are connected to node i . The number of such elements is limited, and hence the dimension of this linear system is limited. As an illustration, in the 2D case and for a vertex node i which is not on the boundary $\partial\Omega$ (see Figure 3), the system is of the form

$$\begin{aligned} \widehat{b}_{1,2}(i) - \widehat{b}_{N_i,1}(i) &= Q_i^{K_1}, \\ \widehat{b}_{2,3}(i) - \widehat{b}_{1,2}(i) &= Q_i^{K_2}, \\ &\dots = \dots \\ \widehat{b}_{N_i,1}(i) - \widehat{b}_{N_i-1,N_i}(i) &= Q_i^{K_{N_i}}, \end{aligned} \quad (53)$$

where N_i is the number of elements connected to node i (for other nodes, the system is of a similar form).

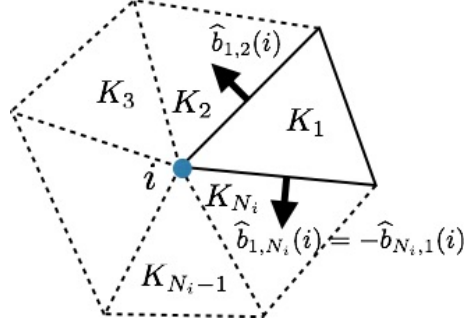


Figure 3: Illustration of the prolongation condition (50) applied to a 2D triangular mesh in the conforming case, yielding a local linear system on traction projections $\widehat{b}_{\alpha,\beta}(i)$ associated with vertex node i .

With obvious notations, the linear system (53) can be written in the compact form $\mathbb{M}\widehat{\mathbf{b}}(i) = \mathbf{Q}_i$, where $\widehat{\mathbf{b}}(i)$ and \mathbf{Q}_i are N_i -dimensional vectors and \mathbb{M} is a $N_i \times N_i$ matrix, the elements of which are 0, -1 or 1. It is easily checked that the kernel of \mathbb{M} is of dimension 1. The system (53) has solutions if and only if $\sum_{j=1}^{N_i} Q_i^{K_j} = 0$. This property indeed holds because it is exactly the weak formulation of the approximate solution u_h for the test function φ_i .

Once the projections $\widehat{b}_{\alpha,\beta}(i)$ are computed for all nodes i , the tractions \widehat{g}_Γ are next built as linear combinations of the basis functions φ_j . For instance, in a P1 setting, and letting K_α and K_β be the elements sharing the edge $\Gamma_{\alpha,\beta}$ that connects the nodes ℓ and m , we write

$$\widehat{g}_{\Gamma_{\alpha,\beta}} = c_\ell \varphi_\ell + c_m \varphi_m \quad (54)$$

and determine the coefficients c_ℓ and c_m such that

$$\begin{cases} \int_{\Gamma_{\alpha,\beta}} \sigma_{\Gamma_{\alpha,\beta},K_\alpha} [c_\ell \varphi_\ell + c_m \varphi_m] \varphi_\ell = \widehat{b}_{\alpha,\beta}(\ell), \\ \int_{\Gamma_{\alpha,\beta}} \sigma_{\Gamma_{\alpha,\beta},K_\alpha} [c_\ell \varphi_\ell + c_m \varphi_m] \varphi_m = \widehat{b}_{\alpha,\beta}(m). \end{cases}$$

Remark 14. When the node i is not connected to Γ_N , the associated local system, arising from (51), is underdetermined. In practice, the solution which is chosen is the one that minimizes a function of the form $\sum_{\alpha,\beta} \frac{(\widehat{b}_{\alpha,\beta}(i) - b_{\alpha,\beta}^m(i))^2}{l_{\alpha,\beta}^2}$,

where $l_{\alpha,\beta} = |\Gamma_{\alpha,\beta}|$ and where

$$b_{\alpha,\beta}^m(i) = \frac{1}{2} \int_{\Gamma_{\alpha,\beta}} \varphi_i (\mathbf{q}_{h|K_\alpha} + \mathbf{q}_{h|K_\beta}) \cdot \mathbf{n}_{K_\alpha} \quad (55)$$

is the average FE normal flux on $\Gamma_{\alpha,\beta}$. Consider for instance an internal node i , for which the system to solve is (53). We introduce the following N_i -dimensional vectors:

$$\begin{aligned} \widehat{\mathbf{X}} &= [\widehat{b}_{N_i,1}(i), \widehat{b}_{1,2}(i), \dots, \widehat{b}_{N_i-1,N_i}(i)]^T, \\ \mathbf{X}^m &= [b_{N_i,1}^m(i), b_{1,2}^m(i), \dots, b_{N_i-1,N_i}^m(i)]^T, \\ \mathbf{X}_0 &= \left[0, Q_i^{K_1}, Q_i^{K_2}, \dots, \sum_{j=1}^{N_i-1} Q_i^{K_j} \right] \quad \text{and} \quad \mathbf{A} = [1, 1, \dots, 1]^T. \end{aligned}$$

Then the set of solutions to (53) is the set $\{\widehat{\mathbf{X}} = s \mathbf{A} + \mathbf{X}_0, s \in \mathbb{R}\}$, s representing the unknown value $\widehat{b}_{N_i,1}(i)$. Introducing the matrix

$$\mathbb{D} = \text{diag} \left(l_{N_i,1}^{-2}, l_{1,2}^{-2}, \dots, l_{N_i-1,N_i}^{-2} \right),$$

the cost function mentioned above reads

$$\begin{aligned} f(s) &= (\widehat{\mathbf{X}} - \mathbf{X}^m)^T \mathbb{D} (\widehat{\mathbf{X}} - \mathbf{X}^m) \\ &= s^2 \mathbf{A}^T \mathbb{D} \mathbf{A} - 2s \mathbf{A}^T \mathbb{D} (\mathbf{X}^m - \mathbf{X}_0) + (\mathbf{X}^m - \mathbf{X}_0)^T \mathbb{D} (\mathbf{X}^m - \mathbf{X}_0). \end{aligned}$$

Its minimization among the solutions to (53) leads to the choice

$$s = (\mathbf{A}^T \mathbb{D} \mathbf{A})^{-1} \mathbf{A}^T \mathbb{D} (\mathbf{X}^m - \mathbf{X}_0).$$

We thus notice that $\widehat{\mathbf{X}}$ is obtained explicitly with very little computational effort.

Remark 15. Several variants of the above method, which is based on (50), have been proposed in the literature [105, 194]. For instance, a “weak” prolongation condition may be applied to shape functions associated with non-vertex nodes alone. Tractions are then constructed as $\widehat{g}_K = L + H$ where H (high-degree component) is fully computed from the weak prolongation condition whereas L (low-degree component) is obtained by minimizing a global complementary energy. This procedure is in practice applied in zones with large gradients or large element aspect ratio in order to optimize the estimate. In the other zones, the above method, based on (50), is used.

Another variant is to construct equilibrated tractions using the Partition of Unity Method (PUM) [143, 193]. This variant provides results similar to those obtained with the method based on (50), but is easier to implement in simulation softwares.

Step 2: local construction of the equilibrated flux $\widehat{\mathbf{q}}_{h|K}$. We first consider the specific case when the source term f is a polynomial function. In that case, it is possible to analytically identify a solution $\widehat{\mathbf{q}}_{h|K}$ to (48) in the form of a polynomial function with a degree consistent with those of f and $\widehat{\mathbf{g}}_K$ (recall that $\widehat{\mathbf{g}}_K$ is a linear combination of the basis functions in V_h^p , in view of (54)). We refer to [152] for details.

Remark 16. *A specific difficulty arises when the above analytical method is used for elasticity problems. Due to the symmetry of the stress tensor, tractions should be compatible at the element vertices (i.e. we should have $\sigma_{\Gamma_1, K} \widehat{\mathbf{g}}_{\Gamma_1} \cdot \mathbf{n}_2 = \sigma_{\Gamma_2, K} \widehat{\mathbf{g}}_{\Gamma_2} \cdot \mathbf{n}_1$). However, this compatibility condition is usually not satisfied when the tractions $\widehat{\mathbf{g}}$ are built as explained in Step 1 above. To circumvent this difficulty, a possibility is to split the element K in sub-elements and to search for an equilibrated stress field as a polynomial function in each sub-element [150].*

We next turn to the case of a general right hand side f , in which case (48) is going to be numerically solved. Once the tractions $\widehat{\mathbf{g}}_K$ have been computed, the best admissible flux $\widehat{\mathbf{q}}_{h|K}$ is the one that minimizes $\|\widehat{\mathbf{q}} - \mathbf{q}_h\|_{q, K}$ among all fluxes $\widehat{\mathbf{q}}$ satisfying (48), where $\mathbf{q}_h = \mathbb{A} \nabla u_h$ is the numerical flux. Recall indeed (see (43)) that $\|\widehat{\mathbf{q}} - \mathbf{q}_h\|_q$ is an upper bound on the error for any $\widehat{\mathbf{q}} \in W$.

For any $\widehat{\mathbf{q}}$ satisfying (48), we have

$$\|\widehat{\mathbf{q}} - \mathbf{q}_h\|_{q, K}^2 = \|\widehat{\mathbf{q}}\|_{q, K}^2 + \|\mathbf{q}_h\|_{q, K}^2 - 2 \left[\int_K f u_h + \int_{\partial K} \widehat{\mathbf{g}}_K u_h \right]$$

and it is thus equivalent to minimize $\|\widehat{\mathbf{q}}\|_{q, K}^2 = 2J_{2|K}(\widehat{\mathbf{q}})$ over fluxes $\widehat{\mathbf{q}}$ satisfying (48). This problem can be written as the minimization of $\int_K \mathbb{A}^{-1} \widehat{\mathbf{q}} \cdot \widehat{\mathbf{q}}$ under the constraint that $\int_K \nabla v \cdot \widehat{\mathbf{q}} - \int_K f v - \int_{\partial K} \widehat{\mathbf{g}}_K v = 0$ for any $v \in H^1(K)$. Introducing the Lagrangian functional

$$\mathcal{L}(\widehat{\mathbf{q}}, v) = \int_K \mathbb{A}^{-1} \widehat{\mathbf{q}} \cdot \widehat{\mathbf{q}} - \left[\int_K \nabla v \cdot \widehat{\mathbf{q}} - \int_K f v - \int_{\partial K} \widehat{\mathbf{g}}_K v \right],$$

we deduce from the saddle-point equation $\frac{\partial \mathcal{L}}{\partial \widehat{\mathbf{q}}} = 0$ that the minimizer $\widehat{\mathbf{q}}_{h|K}$ should satisfy $\mathbb{A}^{-1} \widehat{\mathbf{q}}_{h|K} = \nabla w_K$, where w_K is the Lagrange multiplier. We therefore obtain that $\widehat{\mathbf{q}}_{h|K} = \mathbb{A} \nabla w_K$. The above minimization problem is thus equivalent to finding a function $w_K \in H^1(K)$ such that

$$\forall v \in H^1(K), \quad B_K(w_K, v) = \int_K f v + \int_{\partial K} \widehat{\mathbf{g}}_K v, \quad (56)$$

and then taking $\widehat{\mathbf{q}}_{h|K} = \mathbb{A} \nabla w_K$.

In practice, a numerical approximation of $\widehat{\mathbf{q}}_{h|K}$ is obtained by solving (56) using an enriched FE method. The basis functions are polynomial functions over the whole element K , with a degree $p + k$ (recall that p is the order of the

polynomial functions used to discretize u_h). A Galerkin approximation of (56) in $V_h^{p+k}(K)$ is thus performed. Orthogonal hierarchical subspaces $\widetilde{V}_{h|K}^q$ (for $q = p + 1, p + 2, \dots, p + k$) can be introduced to solve (56) effectively [9]. The numerical comparisons performed in [26] show that the approach based on exactly solving (56) and the numerical approach we have just described (approximating (56) in $V_h^{p+k}(K)$) provide similar CRE values (i.e. error bounds) when choosing $k \geq 3$, even though the flux fields $\widehat{\mathbf{q}}_{h|K}$ obtained in the latter approach do not strictly satisfy the equation (48) in its strong form (and therefore do not provide for a mathematically guaranteed upper error bound). We also refer to [226] for similar investigations.

5.3.2 Flux-free approach

As an alternative to the hybrid-flux approach described in Section 5.3.1, an admissible flux $\widehat{\mathbf{q}}_h \in W$ can also be obtained using a flux-free technique [81, 110, 167, 187]. This approach is simpler to analyze and implement than the hybrid-flux approach since it circumvents the necessity of constructing equilibrated tractions on element edges (the quantities $\widehat{\mathbf{g}}_K$ in the above approach, which are boundary conditions for the local problems). Here the local boundary conditions appear naturally. However, the flux-free approach requires to solve local problems over patches of elements (in contrast to the problem (56), set over a single element) and is therefore more expensive. For instance, the local problem complexity is at least 3 times larger in 2D [73].

We recall that Ω_i is the patch of elements associated with the vertex i . Introduce the space

$$W_{\Omega_i} = \left\{ \begin{array}{l} \mathbf{p} \in H(\text{div}, K) \text{ and } \text{div } \mathbf{p} + r_K \phi_i = 0 \text{ on each } K \subset \Omega_i, \\ \mathbf{p} \cdot \mathbf{n} = 0 \text{ on } \partial\Omega_i \setminus (\Gamma_D \cup \Gamma_N), \quad \mathbf{p} \cdot \mathbf{n} = -t_\Gamma \phi_i \text{ on } \partial\Omega_i \cap \Gamma_N, \\ [[\mathbf{p} \cdot \mathbf{n}]] = -t_\Gamma \phi_i \text{ on } \Gamma_{\text{int}} \subset \Omega_i \end{array} \right\},$$

where r_K and t_Γ are defined by (23), $[[\cdot]]$ is the jump across an edge and where $\{\phi_i\}$ are the piecewise affine basis functions. Note that we do not impose any condition on $\mathbf{p} \cdot \mathbf{n}$ on $\partial\Omega_i \cap \Gamma_D$. For a vertex i inside Ω , the function ϕ_i vanishes on $\partial\Omega_i$, and thus the boundary condition on $\partial\Omega_i \cap \Gamma_N$ simply reads $\mathbf{p} \cdot \mathbf{n} = 0$. However, for a vertex i on the boundary of Ω , the function ϕ_i does not identically vanish on $\partial\Omega_i$.

A finite dimensional subspace $\widetilde{W}_{\Omega_i} \subset W_{\Omega_i}$ is next introduced and the following local problem is solved:

$$\widehat{\mathbf{p}}_i = \text{argmin} \left\{ J_{2|\Omega_i}(\mathbf{p}), \quad \mathbf{p} \in \widetilde{W}_{\Omega_i} \right\}. \quad (57)$$

We then set $\widehat{\mathbf{q}}_h = \mathbf{q}_h + \sum_i \widehat{\mathbf{p}}_i$ which is an element of W (in view of the definition of W_{Ω_i}). In practice, \widetilde{W}_{Ω_i} is defined using polynomial functions on each element, and constraints associated with this space are imposed using Lagrange multipliers.

Remark 17. To solve (57) in practice, it may be convenient to change variable and to work with $\widehat{\mathbf{p}}_i^* = \widehat{\mathbf{p}}_i + \phi_i \mathbb{A} \nabla u_h$ rather than $\widehat{\mathbf{p}}_i$. The field $\widehat{\mathbf{p}}_i^*$ should then satisfy

$$\begin{aligned} \operatorname{div} \widehat{\mathbf{p}}_i^* + f \phi_i - \mathbb{A} \nabla u_h \cdot \nabla \phi_i &= 0 \quad \text{on each } K \subset \Omega_i, \\ \widehat{\mathbf{p}}_i^* \cdot \mathbf{n} &= 0 \quad \text{on } \partial\Omega_i \setminus (\Gamma_D \cup \Gamma_N), \quad \widehat{\mathbf{p}}_i^* \cdot \mathbf{n} = g \phi_i \quad \text{on } \partial\Omega_i \cap \Gamma_N, \\ [[\widehat{\mathbf{p}}_i^* \cdot \mathbf{n}]] &= 0 \quad \text{on } \Gamma_{\text{int}} \subset \Omega_i. \end{aligned}$$

We eventually set $\widehat{\mathbf{q}}_h = \sum_i \widehat{\mathbf{p}}_i^*$, and we have $\widehat{\mathbf{q}}_h \in W$.

In [183], a variant of the original flux-free technique was investigated, with the goal of substantially reducing the computational cost while retaining a good quality of the bounds.

5.3.3 Full polynomial construction using a dual mesh

We now describe yet another method to build equilibrated flux fields $\widehat{\mathbf{q}}_h \in W$ (see [103] for an overview), based on a mixed formulation and the use of Raviart-Thomas-Nédélec (RTN) elements [44]. This method has been used in e.g. [88, 160, 99, 237, 238], where a simple construction of $\widehat{\mathbf{q}}_h$ is proposed using local computations (element by element construction) and low-order RTN elements.

Assume that u_h is a piecewise affine function and that $\operatorname{div} \mathbb{A} \nabla u_h = 0$ in each element K (this is for instance the case when \mathbb{A} is constant in each K). Changing of unknown function, consider $\widehat{\mathbf{p}}_K = \widehat{\mathbf{q}}_{h|K} - \mathbf{q}_{h|K}$ over each element K . We wish to build $\widehat{\mathbf{p}}_K$ such that

$$\operatorname{div} \widehat{\mathbf{p}}_K + f = 0 \quad \text{in } K. \quad (58)$$

We decompose f in K as

$$f = \bar{f}_K + \delta f \quad \text{with} \quad \bar{f}_K = \frac{1}{K} \int_K f \quad \text{and} \quad \int_K \delta f = 0.$$

Denoting by \mathbf{x}_K the geometric center of K , we observe that

$$\widehat{\mathbf{p}}_K = -\frac{\mathbf{x} - \mathbf{x}_K}{d} \bar{f}_K + \operatorname{curl} \boldsymbol{\psi}_K + \nabla \tau_K$$

is a solution to (58), where $\boldsymbol{\psi}_K$ is an arbitrary function in $(H^1(K))^d$ and $\tau_K \in H^1(K)$ is such that $-\Delta \tau_K = \delta f$. We complement the previous equation on τ_K by homogeneous Neumann boundary conditions $\nabla \tau_K \cdot \mathbf{n} = 0$ on ∂K as well as the condition $\int_K \tau_K = 0$. Since the integral over K of δf vanishes, the above problem is well-posed and τ_K is well-defined. An analytical solution can be found using the Green kernel.

Remark 18. Note that $\tau_K = 0$ when f is constant in K . Furthermore, if $f \in H^1(K)$, we have, using the Poincaré Wirtinger inequality on f and τ_K ,

that $\|\delta f\|_{0,K} \leq Ch\|f\|_{1,K}$, which implies that $\|\nabla\tau_K\|_{0,K} \leq Ch^2\|f\|_{1,K}$. We hence see that, for small h , the quantity $\nabla\tau_K$ is small in comparison to the error e (which is expected to be of the order of h since u_h is a piecewise affine function), so that the computation of τ_K may not be needed.

More generally, if $f \notin \oplus_K H^1(K)$, we see that the computation of τ_K is needed only in the elements K where f does not belong to $H^1(K)$.

The choice of ψ_K is guided by the fact that normal fluxes of the field $\widehat{\mathbf{q}}_{h|K} = \widehat{\mathbf{p}}_K + \mathbf{q}_{h|K}$ must be continuous. In view of the homogeneous Neumann boundary condition on τ_K , the set of functions $\psi_K \in (H^1(K))^d$ should satisfy, on all element edges,

$$[[\mathbf{curl} \psi_K]] \cdot \mathbf{n} + \left[\left[\mathbf{q}_{h|K} - \frac{\mathbf{x} - \mathbf{x}_K}{d} \bar{f}_K \right] \right] \cdot \mathbf{n} = 0. \quad (59)$$

Following [86] and restricting our presentation to the two-dimensional case, we observe that $\mathbf{curl} \psi_K \cdot \mathbf{n}_K = -\nabla_{s_K} \Psi_K$, where \mathbf{n}_K is the outgoing normal vector to ∂K , s_K is the curvilinear coordinate along ∂K (oriented in the trigonometric, counterclockwise sense) and $\Psi_K \in H^1(K)$ is such that $\mathbf{curl} \psi_K = \begin{pmatrix} \partial_2 \Psi_K \\ -\partial_1 \Psi_K \end{pmatrix}$. A possibility to ensure (59) is to choose $\Psi_K \in H^1(K)$ such that, along each edge in ∂K ,

$$\nabla_{s_K} \Psi_K = \mathbf{q}_{h|K} \cdot \mathbf{n}_K - \frac{(\mathbf{x} - \mathbf{x}_K) \cdot \mathbf{n}_K}{d} \bar{f}_K. \quad (60)$$

A necessary condition for the existence of such a function Ψ_K is of course that the integral over ∂K of $\mathbf{q}_{h|K} \cdot \mathbf{n}_K - (\mathbf{x} - \mathbf{x}_K) \cdot \mathbf{n}_K \bar{f}_K / d$ vanishes, because we need to ensure that $\int_{\partial K} \nabla_{s_K} \Psi_K = 0$. To that aim, the function u_h (and thus \mathbf{q}_h) may have to be locally modified (see [86, p. 207]). Under that assumption, and noticing that the right-hand side of (60) is constant on each edge, there exists a unique affine function Ψ_K with vanishing average over K and satisfying (60) (the expression of which can of course be given in closed form). We eventually observe that, up to the contribution $\nabla\tau_K$, the function $\widehat{\mathbf{p}}_K$ (and also $\widehat{\mathbf{q}}_h$ if \mathbb{A} is piecewise constant) belongs to the lowest-order RTN element.

Remark 19. *Higher-order RTN finite-dimensional subspaces of $H(\text{div}, \Omega)$ can also be constructed. They are useful to construct equilibrated fields for elasticity problems [15, 48, 173], where the situation is more difficult due to the symmetry of the stress tensor. They are denoted $RTN_k(\mathcal{T}_h)$ and defined as*

$$RTN_k(\mathcal{T}_h) = \{\mathbf{p}_h \in H(\text{div}, \Omega); \quad \mathbf{p}_{h|K} \in RTN_k(K) \text{ for any } K\},$$

where $RTN_k(K) = [P_k(K)]^d + \mathbf{x} P_k(K)$. In particular, any function $\mathbf{p}_h \in RTN_k(\mathcal{T}_h)$ is such that $\text{div} \mathbf{p}_h \in P_k(K)$ for all K and $\mathbf{p}_h \cdot \mathbf{n} \in P_k(\Gamma)$ for all edges Γ .

5.4 Numerical illustration

We report in this section on a numerical experiment borrowed from [193]. A linear elasticity problem is considered on a three-dimensional physical domain (which represents the hub of the main rotor of an helicopter). The mechanical structure is clamped on part of its boundary, and is subjected to a unit traction force density \mathbf{g} , normal to the boundary surface, on another part of its boundary. The loading plane is not exactly orthogonal to the main axis of the structure. The considered geometry and mesh, made of 1978 linear tetrahedral elements (17694 dofs), are shown in Figure 4.

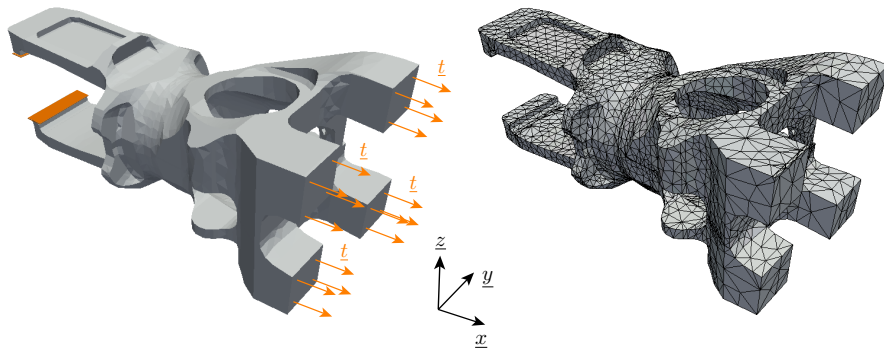


Figure 4: Model problem (left) and associated FE mesh (right). The colored planes represent clamped boundary parts.

A conforming FEM using a direct solver with Cholesky factorization is used to compute an approximate solution. In this example, a specific region of the structure plays an essential role for design purposes and engineering interest. The magnitude (in Frobenius norm) of the FE stress field in this region is shown on Figure 5.

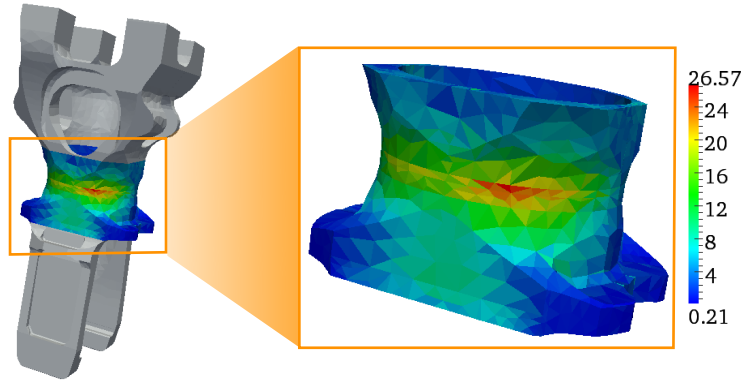


Figure 5: Magnitude of the FE stress field in the region of interest.

A posteriori error estimation is performed using the CRE concept presented in Section 5. The magnitude of the admissible stress field, obtained using hybrid-flux equilibration techniques, as well as the spatial distribution of the obtained CRE error estimate, are shown on Figure 6.

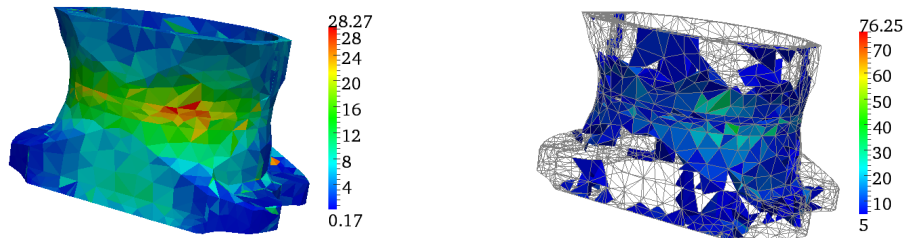


Figure 6: Magnitude of the admissible stress field (left) and spatial distribution of relevant local contributions to the error estimate (right).

6 Unified point of view on *a posteriori* error estimation methods

Among the error estimation methods presented in Sections 3, 4 and 5, and even though the philosophies behind these methods are pretty different, connections can be easily found around the concept of equilibrium (see [60] where such a unified perspective is also described). In the duality-based approach, this concept naturally appears to be fundamental to recover, from a statically admissible flux field \hat{q} , an upper bound on the global error $\|e\|$ measured in the energy norm (see Section 5.1).

This link between equilibrium and guaranteed upper error bounds is also exhibited in advanced recovery methods (see Section 3.3): choosing in (19) a field \mathbf{q}_h^* that is fully equilibrated leads to $\operatorname{div} \mathbf{q}_h^* + f = 0$ and yields an upper error bound $\|\mathbf{q}_h^* - \mathbf{q}_h\|_q$ which is equivalent to the one given by the constitutive relation error functional.

In addition, it is noticeable that the constitutive relation functional can also be understood from the residual functional. Indeed, for any flux $\mathbf{p} \in H(\operatorname{div}, \Omega)$ and any $v \in V$, we have

$$R(v) = B(e, v) = \int_{\Omega} (\mathbf{q} - \mathbf{q}_h) \cdot \nabla v = \int_{\Omega} (\mathbf{p} - \mathbf{q}_h) \cdot \nabla v + \int_{\Omega} (f + \operatorname{div} \mathbf{p}) v + \int_{\Gamma_N} (g - \mathbf{p} \cdot \mathbf{n}) v,$$

with $\mathbf{q} = \mathbb{A} \nabla u$ and $\mathbf{q}_h = \mathbb{A} \nabla u_h$. Writing the above equation for $\mathbf{p} = \hat{\mathbf{q}} \in W$ and $v = e$, we get

$$R(e) = \|e\|^2 = \int_{\Omega} (\hat{\mathbf{q}} - \mathbf{q}_h) \cdot \nabla e \leq \|\hat{\mathbf{q}} - \mathbf{q}_h\|_q \|e\|,$$

and thus $\|e\| \leq \|\hat{\mathbf{q}} - \mathbf{q}_h\|_q = \sqrt{2} E_{\text{CRE}}(u_h, \hat{\mathbf{q}})$. Consequently, strong similarities can be found between duality-based methods and some of the implicit residual methods (i.e. those providing upper error bounds) described in Section 4.2. We illustrate these similarities for hybrid-flux equilibration techniques first, and second for flux-free techniques.

First, the hybrid-flux equilibration technique presented in Section 5.3.1 is used to construct tractions \hat{g}_{Γ} in the equilibration procedure of the element residual method (see Section 4.2.3), in which the local problem to solve over each element K reads (see (37))

Find $\hat{e}_K \in V(K)$ such that, for any $v \in V(K)$,

$$B_K(\hat{e}_K, v) = \int_K r_K v + \sum_{\Gamma \subset \partial K \setminus \Gamma_D} \int_{\Gamma} \hat{R}_{\Gamma, K} v,$$

with $r_K = f + \operatorname{div}(\mathbb{A} \nabla u_h)|_K$ and $\hat{R}_{\Gamma, K} = \sigma_{\Gamma, K} \hat{g}_{\Gamma} - \mathbb{A} \nabla u_h|_K \cdot \mathbf{n}_K$. Consequently, and except for elements K connected to Γ_D , the problem (37) is similar to the one given in (56). In other words, from the solutions \hat{e}_K to (37), an equilibrated flux field \mathbf{q}_h^* such that $\mathbf{q}_h^*|_K = \mathbb{A} \nabla(\hat{e}_K + u_h|_K)$ is obtained. In practice, solving (37) or (56) with an enriched FE method (polynomial functions of degree $p+k$) leads to the same error bounds. Alternatively, introducing the local space

$$W_K = \{\mathbf{p} \in H(\operatorname{div}, K), \quad \operatorname{div} \mathbf{p} + r_K = 0 \text{ in } K, \quad \mathbf{p} \cdot \mathbf{n} = \hat{R}_{\Gamma, K} \text{ on } \Gamma \subset \partial K\},$$

an equilibrated flux field $\hat{\mathbf{q}}_h \in W$ can be constructed as $\hat{\mathbf{q}}_h|_K = \hat{\mathbf{p}} + \mathbb{A} \nabla u_h|_K$ with $\hat{\mathbf{p}} \in W_K$ [215]. This is the approach followed when solving (37) with a dual approach, or when solving (48) with polynomial flux functions.

Second, problems (57) stemming from the flux-free technique presented in Section 5.3.2 are the dual problems to the local problems (32), that are to

be solved over each patch in the subdomain residual method. Solving (32) with an enriched FE discretization (we denote \tilde{z}_i its solution) provides for a flux $\sum_i \mathbb{A} \nabla \tilde{z}_i + \mathbf{q}_h$ which is (up to the small numerical error introduced when solving (32)) statically admissible.

7 Mesh adaptation

Motivated by the fact that computational resources are limited, mesh-adaptive finite element algorithms have been developed. The adaptive procedures aim at automatically refining (or coarsening) a mesh and/or the FE basis (using polynomial functions of various degrees) to obtain a numerical solution having a specified accuracy while requiring the smallest possible computational cost [89, 93, 179, 233]. They may lead to non-conforming discretizations. They are usually based on local contributions η_K of *a posteriori* error estimates, even though other indicators providing guidance on where refinement should occur may be considered (the use of solution gradients is popular in fluid dynamics where error estimates are not readily available). Even though adaptive procedures have been applied for a long time, optimal strategies for deciding where and how to refine or change the basis are rare, and proofs of the optimality of enrichment in the vicinity of the largest error contributions have been investigated only recently [42, 63, 170, 221].

By far, *h*-adaptivity is the most popular strategy (see [109] for an overview and comparison between various *h*-adaptivity strategies). Conserving element type and interpolation, its interest comes from the fact that it can increase the asymptotic convergence rate, particularly when singularities are present. Indeed, *a priori* error analysis shows that a FE method based on polynomial functions of degree p used on a uniform mesh of size h converges as $\|e\| \leq C_1(u, p) h^{\min(p, q)} = C_2(u, p) N^{-\min(p, q)/d}$ where $q > 0$ depends on the solution smoothness (u should belong to $H^{q+1}(\Omega)$ for the estimate to hold) and N is the number of degrees of freedom. In contrast, the optimal adaptive *h*-refinement restores the optimal convergence $\|e\| \leq C_1(u, p) h^p = C_2(u, p) N^{-p/d}$.

The simplest *h*-adaptivity approach is *h*-refinement that consists in dividing some selected elements, keeping other elements unchanged (as performed for instance in quadtree/octree meshes). The adaptive process is based on the cycle

$$\boxed{\text{solve} \rightarrow \text{estimate} \rightarrow \text{mark} \rightarrow \text{refine}}$$

and refines a fixed percentage of elements having the largest error indicators. According to a marking threshold of the form $\theta = \lambda \max_j \eta_j$, where $\lambda \in [0, 1]$ is a parameter (a typical choice is $\lambda = 0.8$), elements K such that $\eta_K \geq \theta$ are marked. The refinement level (namely the number of small elements in which a selected element is divided) is then determined trying to equi-distribute discretization error contributions among the new elements. To that aim, the total number of elements in the refined mesh needs to be estimated. This is done from asymptotic convergence rate and prescribed error tolerance ϵ_0 . A

drawback of the h -refinement method is that it may lead to non-conforming meshes with hanging nodes.

Another more flexible approach, which also enables for mesh unrefinement, is h -remeshing. In this approach, the mesh is totally rebuilt following a remeshing map based on *a posteriori* error estimates. It thus requires a mesh generator able to respect a given remeshing map, which is the main drawback of this approach. To build this new mesh, one possibility is to set the problem as a constrained minimization, in order to define an optimal mesh minimizing the number of elements while ensuring a given accuracy tolerance ϵ_0 .

Denoting $r_K = h_K^*/h_K$ the local refinement ratio in the element K , where h_K^* is the size of the small elements $K^* \subset K$ after refinement, and noticing that $\eta_K^*/\eta_K \approx r_K^{\alpha_K}$ with $\eta_K^* = \sqrt{\sum_{K^* \subset K} (\eta_{K^*})^2}$ and α_K the local convergence rate predicted by *a priori* error estimation, the problem reads as

$$\min_{r_K} \sum_{K \in \mathcal{T}_h} \frac{1}{r_K^d} \quad \text{under the constraint} \quad \sum_{K \in \mathcal{T}_h} (\eta_K^*)^2 = \sum_{K \in \mathcal{T}_h} r_K^{2\alpha_K} \eta_K^2 = \epsilon_0^2. \quad (61)$$

When the exact solution is smooth, we have $\alpha_K = p$ for all elements K , and the constrained minimization problem can be solved analytically. It yields

$$r_K = \frac{\epsilon_0^{1/p}}{\eta_K^{2/(2p+d)} \left[\sum_{K \in \mathcal{T}_h} \eta_K^{2d/(2p+d)} \right]^{1/2p}}.$$

If the exact solution is not smooth enough, then $\alpha_K < p$ in some given zones. The standard strategies then consist in first empirically determining the rates α_K , and next numerically solving the constrained minimization problem (61) (e.g. by using an iterative algorithm). It can be shown that this h -remeshing procedure leads to an evenly-distributed accuracy of the approximate solution over the whole computational domain.

As an illustration, we show in Figure 7 some adaptivity results obtained on a two-dimensional mechanical structure when using h -remeshing. The obtained sequence of meshes enables one to progressively decrease the relative (global, i.e. in energy norm) discretization error, starting from 73% and reaching 5%.

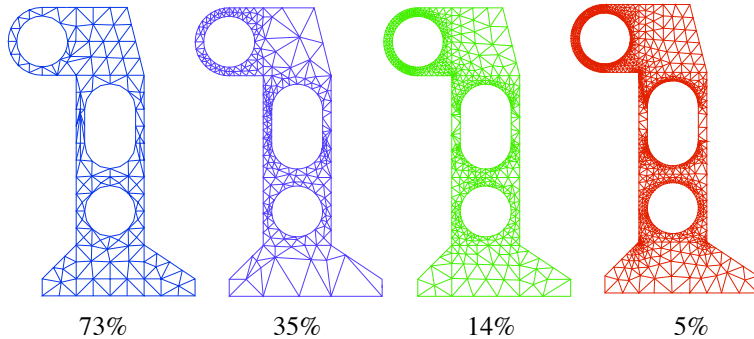


Figure 7: Sequence of meshes using a h -remeshing procedure, with values of the relative error estimate.

Another possibility for adaptivity, which is more powerful when the solution u is smooth, is to perform p -refinement. If the solution u is C^∞ , then it allows for an exponential convergence rate. Otherwise the convergence rate is limited by the solution smoothness. Again, this may yield a non-conforming discretization space.

Of course, hp -refinement strategies, combining h and p refinements, are also possible. They allow to recover an exponential convergence rate $\|e\| \leq C e^{-q_1 N^{q_2}}$, where q_1 and q_2 are positive constants that depend on the smoothness of u and on the FE mesh, even when singularities are present. This idea is (i) to increase the degree of polynomial basis functions in regions where the solution u is smooth and (ii) to decrease h near singularities of u .

Remark 20. *Though being well understood and available in various academic codes, adaptive methods with a posteriori error control have so far not become fully widespread in commercial softwares. One of the reasons for this shortcoming is probably the complex task of mesh generation, in particular for 3D domains where the practitioners have little trust in automatic refinement procedures.*

8 Goal-oriented error estimation

In practical applications, scientists and engineers are often interested in errors on some specific outputs of the computation, i.e. quantities of interest $Q(u)$ which are functionals of the solution u (typical examples include the average of the normal flux $q_n = \mathbf{q} \cdot \mathbf{n} = (\mathbb{A} \nabla u) \cdot \mathbf{n}$ over a part $\Gamma_Q \subset \partial\Omega$ of the boundary of the domain, or the average of the solution u in a local region of interest $\omega_Q \subset \Omega$). In such cases, energy-norm driven error estimation and mesh adaptation tools (presented in the above sections) fail to provide the required accuracy in the chosen quantity of interest using limited computational resources. We show in the following that, again using these tools but complementing them with

additional information, goal-oriented error estimation can be performed and adaptive techniques can be extended to that setting. We refer to [10, 18, 58, 76, 116, 153, 172, 175, 178, 181, 182, 190, 197, 202, 225] for more details on what we present below. Such strategies are highly beneficial compared to global error estimation and the associated mesh adaptivity, since complex features of the solution on some parts of the domain might not influence the quantity of interest (and thus do not need to be accurately captured by the numerical solution).

In this section, we consider a linear and continuous functional $Q : V \rightarrow \mathbb{R}$, and we define from this a quantity of interest $Q(u)$ (depending linearly on u). In practice, the functional Q is often defined in a global manner as

$$Q(v) = \int_{\Omega} (\tilde{f}_Q v + \tilde{\mathbf{q}}_Q \cdot \nabla v) + \int_{\Gamma_N} \tilde{g}_Q v + \int_{\Omega} \mathbb{A} \nabla \tilde{u}_Q \cdot \nabla v, \quad (62)$$

where $(\tilde{f}_Q, \tilde{\mathbf{q}}_Q, \tilde{g}_Q, \tilde{u}_Q)$ is a set of extraction functions which can be mechanically interpreted in an adjoint problem (see below) as body, pre-flux, traction, and pre-primal field loadings, respectively. These are defined explicitly or implicitly, depending on the quantity Q . The last extraction function \tilde{u}_Q , vanishing on Γ_N , is a regular field that enables one to extract components of the normal flux $\mathbf{q} \cdot \mathbf{n}$ on Γ_D (reaction forces) by imposing a non-homogeneous Dirichlet condition. More precisely, considering momentarily the case when \tilde{f}_Q , $\tilde{\mathbf{q}}_Q$ and \tilde{g}_Q vanish, evaluating the quantity of interest on the solution u to (1) and using that \tilde{u}_Q vanishes on Γ_N , we compute that $Q(u) = \int_{\Omega} \mathbb{A} \nabla \tilde{u}_Q \cdot \nabla u = \int_{\Gamma_D} \tilde{u}_Q \mathbf{q} \cdot \mathbf{n} + \int_{\Omega} \tilde{u}_Q f$. Up to the second term in $Q(u)$ (which is independent of the solution), we indeed see that \tilde{u}_Q allows to extract components of the normal flux $\mathbf{q} \cdot \mathbf{n}$ on Γ_D .

The quantity of interest $Q(u)$ can be written $\langle Q, u \rangle$ where Q belongs to the dual space V^* of V . Consequently, we have

$$|Q(u) - Q(u_h)| = |Q(e)| \leq \|Q\|_{\star} \|e\|,$$

where $\|Q\|_{\star} = \sup_{v \in V, \|v\|=1} |Q(v)|$ is the dual norm of Q . A target accuracy ϵ for the error on $Q(u)$ can thus be achieved by ensuring that $\|e\| \leq \epsilon / \|Q\|_{\star}$. However, such a method based on a mesh adaptation with respect to the error in the energy norm usually leads to an overestimation (and requires useless computational effort) since norm approximation does not take the locality of Q into account. We show in the following, using duality arguments, that a target accuracy ϵ for the error on $Q(u)$ can be achieved by only requesting that $\|e\|$ is of the order of $\sqrt{\epsilon}$.

8.1 Adjoint problem and error indicator

Considering in a general setting the problem written in its weak form (3), and in order to give an exact representation of the error $Q(u) - Q(u_h) = Q(e)$, the

following adjoint problem is introduced [34, 115]:

$$\text{Find } \tilde{u} \in V \text{ such that, for any } v \in V, \quad B^*(\tilde{u}, v) = Q(v), \quad (63)$$

where $B^*(u, v)$ is the formal adjoint of the primal form $B(u, v)$, defined by $B^*(u, v) = B(v, u)$. In the current symmetric case, the forms B and B^* are identical. We also define the adjoint flux $\tilde{\mathbf{q}} = \mathbb{A} \nabla \tilde{u}$.

The adjoint solution \tilde{u} yields the exact representation (primal-dual equivalence) of the error on $Q(u)$:

$$Q(e) = B^*(\tilde{u}, e) = B(e, \tilde{u}) = R(\tilde{u}) = \langle R|_{u_h}, \tilde{u} \rangle.$$

This shows that \tilde{u} provides for the sensitivity of the discretization error on $Q(u)$ to the local sources of discretization errors in the whole domain Ω . The adjoint solution, often termed generalized Green's function [104], conveys the locality of the targeted information. It indicates the influence of parts of the primal solution away from the spatial location of the target functional.

Remark 21. *In the case of a nonlinear quantity of interest, the general approach consists in performing a first order linearization $Q(u) - Q(u_h) \approx Q'|_{u_h}(e)$ and therefore considering $Q'|_{u_h}(v)$ as the right-hand side of the adjoint problem (63). Another approach that avoids linearization and thus keeps strict error bounds for nonlinear quantities of interest is presented in [141].*

A classical numerical approach then consists in computing an approximate solution \tilde{u}_h of \tilde{u} using the reference mesh \mathcal{T}_h . We thus get, using the Galerkin orthogonality, that

$$Q(e) = B(e, \tilde{u} - \tilde{u}_h) = B(e, \tilde{e}). \quad (64)$$

When a different mesh (e.g. with a local enrichment) is used to solve the adjoint problem, yielding an approximate adjoint solution \tilde{u}_+ , the relation (64) is changed in

$$Q(e) = B(e, \tilde{u} - \tilde{u}_+) + B(e, \tilde{u}_+), \quad (65)$$

where the second term $B(e, \tilde{u}_+) = R(\tilde{u}_+) = F(\tilde{u}_+) - B(u_h, \tilde{u}_+)$ is a fully computable correcting term.

Remark 22. *A local enrichment technique for the solution of the adjoint problem is proposed in [67, 117], using analytical or pre-computed numerical functions as an additive term to a classical FE solution computed on the mesh \mathcal{T}_h . This technique, referred to as non-intrusive in the sense that the global mesh is unchanged between the primal and the adjoint problems, is particularly interesting in the case of pointwise quantities of interest such as $u(\mathbf{x}_0)$ for some $\mathbf{x}_0 \in \Omega$ (assuming that the reference solution u is continuous at point \mathbf{x}_0). In such a case, analytical Green's functions can be introduced as an enrichment. This is an alternative to the method proposed in [197], based on using a regularized functional instead of the original pointwise functional. The regularized functional yields a modified quantity of interest that involves a smooth function*

k_{δ, \mathbf{x}_0} (characterized by the length-scale $\delta > 0$ and such that $\int_{\Omega} k_{\delta, \mathbf{x}_0} = 1$) which performs a weighted average over a small neighborhood of the point \mathbf{x}_0 .

An error indicator may be derived from (65) using the dual weighted residual (DWR) method proposed in [33] and based on hierarchical *a posteriori* error analysis. After computing an approximate adjoint solution \tilde{u}_+ from a hierarchically refined FE space $V_+ \supset V_h^p$ (higher-order basis functions and/or refined mesh), and assuming that the error between \tilde{u} and \tilde{u}_+ is small, the DWR method then consists in writing

$$Q(u) - Q(u_h) \approx R(\tilde{u}_+). \quad (66)$$

The quantity $R(\tilde{u}_+)$ is then taken as an error indicator on Q .

Remark 23. *Due to the Galerkin orthogonality, choosing $V_+ = V_h^p$ would of course lead to a meaningless indicator (in that case, we would have $R(\tilde{u}_+) = 0$). Consequently, a convenient approximation of the adjoint solution should involve a subspace in $(V_h^p)^\perp$.*

The above argument can be somewhat quantified. Let $u_+ \in V_+$ be the approximation (in the refined space) of the primal solution. We assume that the saturation assumption $|Q(u) - Q(u_+)| \leq \beta |Q(u) - Q(u_h)|$ is satisfied for some $0 \leq \beta < 1$. Using the fact that $u_+ - u_h \in V_+$ and next the fact that $\tilde{u}_+ \in V_+$, we obtain

$$Q(u_+) - Q(u_h) = B(u_+ - u_h, \tilde{u}_+) = B(u - u_h, \tilde{u}_+) = R(\tilde{u}_+).$$

From the triangle inequality, we eventually get

$$\frac{|R(\tilde{u}_+)|}{1 + \beta} \leq |Q(u) - Q(u_h)| \leq \frac{|R(\tilde{u}_+)|}{1 - \beta},$$

which quantifies the approximation (66). The indicator defined in (66) may be used to drive adaptive algorithms since it gives a clear and accurate distribution of error sources, but it does not provide for *guaranteed* error bounds on Q . Alternative techniques addressing this question are proposed in the next section.

8.2 Computation of upper error bounds

In the following, we bound the error on $Q(u)$ using (64). A first possibility [9] is to directly use the Cauchy-Schwarz inequality:

$$|Q(u) - Q(u_h)| = |B(e, \tilde{e})| \leq \|e\| \|\tilde{e}\| \leq \eta \tilde{\eta}, \quad (67)$$

where η and $\tilde{\eta}$ are upper error bounds (in the energy norm) for the primal and adjoint problems, respectively. This shows that any guaranteed global error estimate can be used to assess the error on $Q(u)$ and give a conservative bound. It also shows that the error on $Q(u)$ decreases with a rate which is twice larger

than that for the error on u in the energy norm (thus our above claim that an error of the order of $\sqrt{\epsilon}$ on $\|e\|$, and similarly on $\|\tilde{e}\|$, is enough to yield an error of the order of ϵ on $Q(u)$). However, the above estimate may be crude (and may not exploit the locality of $Q(u)$) due to the use of the Cauchy-Schwarz inequality, even though improvement techniques may be found in [151].

It is also possible, still starting from (64), to use a local Cauchy-Schwarz inequality, writing that

$$|Q(u) - Q(u_h)| = \left| \sum_{K \in \mathcal{T}_h} B_K(e, \tilde{e}) \right| \leq \sum_{K \in \mathcal{T}_h} \|e\|_K \|\tilde{e}\|_K, \quad (68)$$

but bounds on $\|e\|_K$ and $\|\tilde{e}\|_K$ (using for instance local error indicators η_K and $\tilde{\eta}_K$) are heuristic. In addition, a bound such as (68) is again very conservative, in the sense that it does not take into account possible cancellation of errors over the domain.

Remark 24. *A quantitative evaluation of $Q(e)$ involving the elementary components of e and \tilde{e} , but not providing for an upper error bound, can also be exhibited when using the DWR method and the approximate adjoint solution $\tilde{u}_+ \in V_+$ obtained with a fine mesh and/or a high-order method (see (66)). We can indeed write*

$$Q(u) - Q(u_h) \approx R(\tilde{u}_+) = R(\tilde{e}_+) = \sum_{K \in \mathcal{T}_h} \left[\int_K r_K \tilde{e}_+ + \int_{\partial K} R_{\partial K} \tilde{e}_+ \right],$$

where $\tilde{e}_+ = \tilde{u}_+ - \tilde{u}_h$ is an approximation of \tilde{e} , and where $R_{\partial K}$ is defined on ∂K by $R_{\partial K}(\mathbf{x}) = R_\Gamma(\mathbf{x})$ for any $\mathbf{x} \in \Gamma \subset \partial K \setminus \Gamma_D$ and $R_{\partial K}(\mathbf{x}) = 0$ for any $\mathbf{x} \in \partial K \cap \Gamma_D$ (we recall that r_K and R_Γ are defined in Section 4.2.3). Consequently, an error indicator can be defined as

$$|Q(u) - Q(u_h)| \approx \sum_{K \in \mathcal{T}_h} \rho_K \omega_K \quad \text{with} \quad \begin{cases} \rho_K = \|r_K\|_{0,K} + h_K^{-1/2} \|R_{\partial K}\|_{0,\partial K}, \\ \omega_K = \|\tilde{e}_+\|_{0,K} + h_K^{1/2} \|\tilde{e}_+\|_{0,\partial K}. \end{cases} \quad (69)$$

Note that ρ_K and ω_K are computable terms.

An alternative technique consists in using the parallelogram identity to get an upper bound on the error [175, 197]. Starting from the expression

$$B(e, \tilde{e}) = B\left(s e, \frac{1}{s} \tilde{e}\right) = \frac{1}{4} \left[\left\| s e + \frac{1}{s} \tilde{e} \right\|^2 - \left\| s e - \frac{1}{s} \tilde{e} \right\|^2 \right] = \frac{1}{4} [\chi_+ - \chi_-], \quad (70)$$

where $s \in \mathbb{R}$ is a scaling factor (to be optimized) and

$$\chi_+ = \left\| s e + \frac{1}{s} \tilde{e} \right\|^2, \quad \chi_- = \left\| s e - \frac{1}{s} \tilde{e} \right\|^2,$$

we directly get

$$\frac{1}{4} [\chi_+^{\text{low}} - \chi_-^{\text{upp}}] \leq Q(u) - Q(u_h) \leq \frac{1}{4} [\chi_+^{\text{upp}} - \chi_-^{\text{low}}], \quad (71)$$

where χ_-^{upp} and χ_-^{low} (resp. χ_+^{upp} and χ_+^{low}) are upper and lower bounds on χ_- (resp. χ_+). These can be derived from the various approaches detailed in the above sections.

Even though the error bounds defined in (71) are more accurate than those given by (67), error cancellations over the domain are still not captured by the approach. It appears that there is no method in the literature to conciliate the two requirements (i) take into account error cancellation (as done by the DWR method) and (ii) get guaranteed error bounds, even though recent works such as [151] have proposed first ideas in that direction.

Another alternative bounding technique (see [67, 139]) is based on the properties of the duality-based approaches presented in Section 5. Introduce the space of equilibrated fluxes (with respect to the adjoint problem)

$$\widetilde{W} = \left\{ \widetilde{\mathbf{p}} \in H(\text{div}, \Omega) \quad \text{such that, for any } v \in V, \quad \int_{\Omega} \widetilde{\mathbf{p}} \cdot \nabla v = Q(v) \right\}.$$

After constructing admissible flux fields $\widehat{\mathbf{q}}_h \in W$ and $\widetilde{\widehat{\mathbf{q}}}_h \in \widetilde{W}$ as a post-processing of \mathbf{q}_h and $\widetilde{\mathbf{q}}_h$ (as detailed in Section 5.3), a direct consequence of (67) and (43) is

$$|Q(u) - Q(u_h)| \leq 2 E_{\text{CRE}}(u_h, \widehat{\mathbf{q}}_h) E_{\text{CRE}}(\widetilde{u}_h, \widetilde{\widehat{\mathbf{q}}}_h). \quad (72)$$

An *a posteriori* error estimate on Q which is more accurate than (72) can be obtained using the hypercircle property (46) verified by $\widehat{\mathbf{q}}_h^m = \frac{1}{2}(\widehat{\mathbf{q}}_h + \mathbf{q}_h)$. Indeed, we infer from (64) and the fact that $\widetilde{\widehat{\mathbf{q}}}_h \in \widetilde{W}$ that

$$\begin{aligned} Q(u) - Q(u_h) &= B(u - u_h, \widetilde{u} - \widetilde{u}_h) = \int_{\Omega} \nabla(u - u_h) \cdot (\widetilde{\mathbf{q}} - \mathbb{A} \nabla \widetilde{u}_h) \\ &= \int_{\Omega} \nabla(u - u_h) \cdot (\widetilde{\widehat{\mathbf{q}}}_h - \mathbb{A} \nabla \widetilde{u}_h). \end{aligned}$$

We consequently obtain

$$\begin{aligned} Q(u) - Q(u_h) &= \int_{\Omega} \mathbb{A}^{-1}(\mathbf{q} - \mathbf{q}_h) \cdot (\widetilde{\widehat{\mathbf{q}}}_h - \mathbb{A} \nabla \widetilde{u}_h) \\ &= \int_{\Omega} \mathbb{A}^{-1}(\mathbf{q} - \widehat{\mathbf{q}}_h^m) \cdot (\widetilde{\widehat{\mathbf{q}}}_h - \mathbb{A} \nabla \widetilde{u}_h) + C_h, \end{aligned}$$

where $C_h = \frac{1}{2} \int_{\Omega} \mathbb{A}^{-1}(\widehat{\mathbf{q}}_h - \mathbf{q}_h) \cdot (\widetilde{\widehat{\mathbf{q}}}_h - \widetilde{\mathbf{q}}_h)$ is a computable term. From the Cauchy-Schwarz inequality and the use of (46), we eventually obtain the bound

$$|Q(u) - Q(u_h) - C_h| \leq E_{\text{CRE}}(u_h, \widehat{\mathbf{q}}_h) E_{\text{CRE}}(\widetilde{u}_h, \widetilde{\widehat{\mathbf{q}}}_h), \quad (73)$$

which is twice sharper than (72), and partially takes into account error cancellations (through the term C_h).

The quantity $Q(u_h) + C_h$ can be interpreted as a corrected approximation of the quantity of interest. Furthermore, the estimate (73) can also be written in the form of an error bound on Q as

$$|Q(u) - Q(u_h)| \leq \eta^Q := \max_{\theta=\pm 1} \left| C_h + \theta E_{\text{CRE}}(u_h, \widehat{\mathbf{q}}_h) E_{\text{CRE}}(\widetilde{u}_h, \widehat{\widetilde{\mathbf{q}}}_h) \right|. \quad (74)$$

Remark 25. *It can be shown that the bound (73) is equivalent to the one given by (71) when taking $\chi_-^{\text{low}} = \chi_+^{\text{low}} = 0$ and for the optimal value $s_{\text{opt}} = \sqrt{\frac{\|\widetilde{e}\|}{\|e\|}} \approx \sqrt{\frac{E_{\text{CRE}}(\widetilde{u}_h, \widehat{\widetilde{\mathbf{q}}}_h)}{E_{\text{CRE}}(u_h, \widehat{\mathbf{q}}_h)}}$, in the following sense. We infer from (64) and (70), with the lower bound $\chi_{\pm} \geq 0$, that, for any s ,*

$$-\frac{1}{4} \chi_-(s) \leq Q(u) - Q(u_h) \leq \frac{1}{4} \chi_+(s), \quad (75)$$

where $\chi_{\pm}(s) = \left\| \left\| s e \pm \frac{1}{s} \widetilde{e} \right\| \right\|^2 = s^2 \|e\|^2 + \frac{1}{s^2} \|\widetilde{e}\|^2 \pm 2 B(e, \widetilde{e})$. The interval given by (75) is the smallest for s such that $\chi_+(s) + \chi_-(s)$ is the smallest, thus the choice $s = s_{\text{opt}}$. The width of the interval in (75) is then $\|e\| \|\widetilde{e}\|$, which is bounded from above by $2 E_{\text{CRE}}(u_h, \widehat{\mathbf{q}}_h) E_{\text{CRE}}(\widetilde{u}_h, \widehat{\widetilde{\mathbf{q}}}_h)$. The center of the interval given by (75) is $(\chi_+(s) - \chi_-(s))/8 = B(e, \widetilde{e})/2$, which is exactly equal to C_h . For the choice $s = s_{\text{opt}}$, the bound (75) thus implies (73).

Remark 26. *A still sharper bound can be obtained from the previous approach when using an enriched adjoint solution \widetilde{u}_+ (see [67]). Starting from (65), we have (using an admissible flux field $\widehat{\widetilde{\mathbf{q}}}_+ \in \widetilde{W}$ obtained as a postprocessing of $\widetilde{\mathbf{q}}_+$) that*

$$\begin{aligned} Q(u) - Q(u_h) - R(\widetilde{u}_+) &= B(u - u_h, \widetilde{u} - \widetilde{u}_+) = \int_{\Omega} \nabla(u - u_h) \cdot (\widehat{\widetilde{\mathbf{q}}}_+ - \mathbb{A} \nabla \widetilde{u}_+) \\ &= \int_{\Omega} \mathbb{A}^{-1} (\mathbf{q} - \widehat{\mathbf{q}}_h^m) \cdot (\widehat{\widetilde{\mathbf{q}}}_+ - \mathbb{A} \nabla \widetilde{u}_+) + C_+, \end{aligned}$$

with $C_+ = \frac{1}{2} \int_{\Omega} \mathbb{A}^{-1} (\widehat{\mathbf{q}}_h - \mathbf{q}_h) \cdot (\widehat{\widetilde{\mathbf{q}}}_+ - \widetilde{\mathbf{q}}_+)$. This leads to the bound

$$|Q(u) - Q(u_h) - \overline{C}_+| \leq E_{\text{CRE}}(u_h, \widehat{\mathbf{q}}_h) E_{\text{CRE}}(\widetilde{u}_+, \widehat{\widetilde{\mathbf{q}}}_+), \quad (76)$$

where $\overline{C}_+ = R(\widetilde{u}_+) + C_+ = \frac{1}{2} \int_{\Omega} \mathbb{A}^{-1} (\widehat{\mathbf{q}}_h - \mathbf{q}_h) \cdot (\widehat{\widetilde{\mathbf{q}}}_+ + \widetilde{\mathbf{q}}_+)$ is a new computable correction term.

Once the error on $Q(u)$ has been estimated, an adaptive strategy similar to the one presented in Section 7 can be used to reach a given error tolerance. The adaptive algorithm, which should now be based on local error contributions given by (68), (69), (71) or (74), enables one to recover optimal convergence rates [169]. For instance, when using (74), and denoting θ_{\max} the maximizer there, we can proceed as follows. We first recast (74) as

$$\begin{aligned} |Q(u) - Q(u_h)| &\leq \left| C_h + \theta_{\max} E_{\text{CRE}}(u_h, \hat{\mathbf{q}}_h) E_{\text{CRE}}(\tilde{u}_h, \hat{\tilde{\mathbf{q}}}_h) \right| \\ &= \left| \sum_{K \in \mathcal{T}_h} C_h^K + \theta_{\max} \sqrt{\sum_{K \in \mathcal{T}_h} (\eta_K)^2} \right|, \end{aligned} \quad (77)$$

where $C_h^K = \frac{1}{2} \int_K \mathbb{A}^{-1} (\hat{\mathbf{q}}_h - \mathbf{q}_h) \cdot (\hat{\tilde{\mathbf{q}}}_h - \tilde{\mathbf{q}}_h)$ is the local contribution to C_h (by construction, C_h^K is an integral over K and $\sum_{K \in \mathcal{T}_h} C_h^K = C_h$) and where η_K is defined by

$$\begin{aligned} (\eta_K)^2 &= \frac{1}{2} \left(E_{\text{CRE}}(u_h, \hat{\mathbf{q}}_h) \right)^2 \left(E_{\text{CRE},K}(\tilde{u}_h, \hat{\tilde{\mathbf{q}}}_h) \right)^2 \\ &\quad + \frac{1}{2} \left(E_{\text{CRE}}(\tilde{u}_h, \hat{\tilde{\mathbf{q}}}_h) \right)^2 \left(E_{\text{CRE},K}(u_h, \hat{\mathbf{q}}_h) \right)^2, \end{aligned}$$

where $E_{\text{CRE},K}(u_h, \hat{\mathbf{q}}_h) = \|\hat{\mathbf{q}}_h - \mathbb{A} \nabla u_h\|_{q,K} / \sqrt{2}$ is the local contribution to $E_{\text{CRE}}(u_h, \hat{\mathbf{q}}_h)$, in the sense that $(E_{\text{CRE}}(u_h, \hat{\mathbf{q}}_h))^2 = \sum_{K \in \mathcal{T}_h} (E_{\text{CRE},K}(u_h, \hat{\mathbf{q}}_h))^2$

(and likewise for $E_{\text{CRE},K}(\tilde{u}_h, \hat{\tilde{\mathbf{q}}}_h)$). We thus observe that

$$\sum_{K \in \mathcal{T}_h} (\eta_K)^2 = (E_{\text{CRE}}(u_h, \hat{\mathbf{q}}_h) E_{\text{CRE}}(\tilde{u}_h, \hat{\tilde{\mathbf{q}}}_h))^2.$$

In view of (77), we then take $C_h^K + \theta_{\max} \eta_K$ as a local indicator of the error in the element K , and proceed with an adaptive algorithm based on these local contributions.

8.3 Numerical illustration

To illustrate the performance of the approach, we again consider the numerical example described in Section 5.4, now focusing on a specific quantity of interest, which we choose as the average (over a critical three-dimensional subdomain ω of the structure) of the zz component of the stress tensor σ (where z is the axial direction of the structure): $Q(u) = \frac{1}{|\omega|} \int_{\omega} \sigma_{zz}(u)$. The subdomain ω is shown on Figure 8 and includes around 15 finite elements.

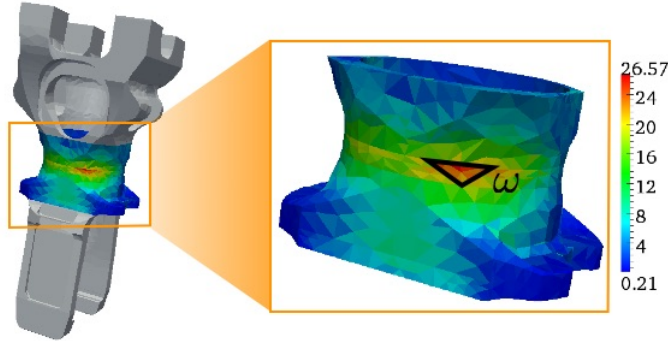


Figure 8: Representation of the subdomain of interest ω . Our quantity of interest is the average of σ_{zz} over ω . The value of the stress field (in Frobenius norm) in the neighborhood of ω is indicated on the figure.

The reference value of the quantity of interest (computed using a very fine mesh) is $Q(u) = 33.24$. Using the mesh presented in Section 5.4, we obtain the approximate value $Q(u_h) = 28.18$. To obtain a bound on $Q(u) - Q(u_h)$, we follow the procedure explained in Remark 26. The bound (76) yields that the exact value $Q(u)$ satisfies $31.17 \leq Q(u) \leq 34.29$ (the correction term \bar{C}_+ is such that $Q(u_h) + \bar{C}_+ = 32.73$). We observe that the actual exact value indeed satisfies these bounds, and that the lower (resp. upper) bound underestimates (resp. overestimates) the exact value of Q by only 6% (resp. 3%). The bound (76) thus yields a very accurate estimate.

9 Extensions to other FE schemes

Pioneering works on model verification for non-conforming FE schemes were developed in [32, 59, 83, 129, 209] (recent contributions include e.g. [7]). It was then shown that *a posteriori* error estimation for conforming and non-conforming FE schemes could be phrased in a united framework [4, 5, 6, 31, 101, 103, 166]. In both cases, one can get computable upper bounds on the error measured in the energy norm. In this section, we restrict our presentation to the reference problem presented in Section 2.1, discretized using piecewise affine, but not necessarily conforming, FE approximations. We recall that

$$V = \{v \in H^1(\Omega), \quad v = 0 \text{ on } \Gamma_D\}.$$

9.1 Splitting of the error

A conforming Galerkin discretization consists in introducing the finite dimensional subspace $V_h^1 \subset V$. However, there may be advantages in using non-conforming discretization spaces that are not a subspace of V . These spaces are

still constructed on families of regular partitions \mathcal{T}_h of Ω . In the following, as in Section 4.2.3, we refer to a broken Sobolev space

$$X_{\text{brok}} = \oplus_K H^1(K)$$

and we introduce, for each element K , the function $\sigma_{\Gamma,K} : \partial K \mapsto \{-1, +1\}$ defined by (49). For any $v \in X_{\text{brok}}$, we denote by $[[v]]$ (resp. $\langle v \rangle$) its jump across (resp. its average on) the internal element edges. We also introduce $\mathbf{n} = \sigma_{\Gamma,K} \mathbf{n}_K$ (which is a well-defined vector on each edge) and the normal flux $q_n(v) = \mathbf{n} \cdot \mathbf{q}(v) = \mathbf{n} \cdot \mathbb{A} \nabla v$.

For any given parameter $\kappa > 0$, we introduce the forms

$$B_{\text{brok}}(w, v) = \sum_{K \in \mathcal{T}_h} \int_K \mathbb{A} \nabla w \cdot \nabla v - \sum_{\Gamma \subset \Gamma_{\text{int}} \cup \Gamma_D} \int_{\Gamma} \left([[w]] \langle q_n(v) \rangle + \langle q_n(w) \rangle [[v]] \right) + \sum_{\Gamma \subset \Gamma_{\text{int}} \cup \Gamma_D} \frac{\kappa}{h_{\Gamma}} \int_{\Gamma} [[w]] [[v]]$$

and

$$F_{\text{brok}}(v) = \sum_{K \in \mathcal{T}_h} \int_K f v + \sum_{\Gamma \subset \Gamma_N} \int_{\Gamma} g v.$$

Note that, for any v and w in X_{brok} , an integral over an edge of the product $\langle q_n(v) \rangle [[w]]$ is interpreted as a duality pairing. Furthermore, on edges $\Gamma \subset \Gamma_D$, $[[v]]$ and $\langle v \rangle$ simply denote the function v itself: $[[v]] = \langle v \rangle = v$ on $\Gamma \subset \Gamma_D$. Note also that functions in X_{brok} do not necessarily vanish on Γ_D .

We consider the following problem:

$$\text{Find } U \in X_{\text{brok}} \text{ such that, for any } v \in X_{\text{brok}}, \quad B_{\text{brok}}(U, v) = F_{\text{brok}}(v). \quad (78)$$

By choosing appropriate test functions $v \in X_{\text{brok}}$ (e.g. supported on a single element K , or non-zero on a single edge Γ), it can be easily shown [14] that the unique solution U to (78) corresponds to the solution u to (1). We have thus recast the problem of interest as (78).

We then introduce a finite dimensional subspace $X_h \subset X_{\text{brok}}$, based on the partition \mathcal{T}_h of Ω , and construct an approximation $U_h \in X_h$ by considering the finite-dimensional problem

$$\forall v \in X_h, \quad B_{\text{brok}}(U_h, v) = F_{\text{brok}}(v). \quad (79)$$

If κ sufficiently large, then the above problem has a unique solution (see [4]). In the following, we consider two choices of X_h , which differ by the conditions which are applied on $\Gamma_{\text{int}} \cup \Gamma_D$:

- Discontinuous Galerkin FEM:

$$X_h^{\text{DG}} = \{v \in X_{\text{brok}}, \quad v|_K \in P_1(K) \text{ for any } K \in \mathcal{T}_h\};$$

- Crouzeix-Raviart FEM:

$$X_h^{\text{CR}} = \{v \in X_h^{\text{DG}}, \int_{\Gamma} [[v]] = 0 \text{ for any } \Gamma \subset \Gamma_{\text{int}} \cup \Gamma_D\}.$$

We recall that the conforming FEM corresponds to the choice

$$X_h^{\text{CG}} = V_h^1 = \{v \in X_h^{\text{DG}}, [[v]] = 0 \text{ on any } \Gamma \subset \Gamma_{\text{int}} \cup \Gamma_D\}.$$

We of course have $X_h^{\text{CG}} \subset X_h^{\text{CR}} \subset X_h^{\text{DG}} \subset X_{\text{brok}}$. Note that functions in X_h^{CR} are continuous at the midpoints of the interior edges, and vanish at the midpoints of edges on Γ_D .

Since the error $e = u - U_h$ is in general not in V , a natural idea is to split it into a part that belongs to V and a remainder. We thus consider the projection $\phi \in V$ of e (which is the so-called conforming error), defined by

$$\forall v \in V, \quad B(\phi, v) = \int_{\Omega} \mathbb{A} \nabla_h e \cdot \nabla v = \int_{\Omega} f v + \int_{\Gamma_N} g v - \int_{\Omega} \mathbb{A} \nabla_h U_h \cdot \nabla v, \quad (80)$$

where, for any $w \in X_{\text{brok}}$, $\nabla_h w$ is equal, on each element K , to ∇w . The remaining part $\rho = e - \phi$ is orthogonal to V , in the sense that

$$\forall v \in V, \quad \int_{\Omega} \mathbb{A} \nabla_h \rho \cdot \nabla v = 0. \quad (81)$$

Denoting $\mathbf{q}(\rho) = \mathbb{A} \nabla_h \rho$, we thus see that $\mathbf{q}(\rho)$ is divergence free in Ω (at least in the sense of distributions), and that $\mathbf{q}(\rho) \in (L^2(\Omega))^d$. There thus exists $\boldsymbol{\psi} \in (H^1(\Omega))^d$ such that $\mathbf{q}(\rho) = \mathbf{curl} \boldsymbol{\psi}$. We next infer from (81), using an integration by parts, that $\mathbf{n} \cdot \mathbf{curl} \boldsymbol{\psi} = 0$ on Γ_N . Summarizing, $\mathbf{q}(\rho)$ can be expressed as the curl of a function $\boldsymbol{\psi}$ belonging to

$$H = \{\mathbf{w} \in (H^1(\Omega))^d, \quad \mathbf{n} \cdot \mathbf{curl} \mathbf{w} = 0 \text{ on } \Gamma_N\},$$

and we have the splitting

$$\mathbf{q}(e) = \mathbb{A} \nabla_h e = \mathbf{q}(\phi) + \mathbf{curl} \boldsymbol{\psi}, \quad (82)$$

which is an orthogonal decomposition in the sense that

$$\int_{\Omega} \mathbb{A}^{-1} \mathbf{q}(e) \cdot \mathbf{q}(e) = \int_{\Omega} \mathbb{A}^{-1} \mathbf{q}(\phi) \cdot \mathbf{q}(\phi) + \int_{\Omega} \mathbb{A}^{-1} (\mathbf{curl} \boldsymbol{\psi}) \cdot (\mathbf{curl} \boldsymbol{\psi}), \quad (83)$$

since $\int_{\Omega} \mathbb{A}^{-1} \mathbf{q}(\phi) \cdot \mathbf{curl} \boldsymbol{\psi} = 0$ in view of (81). The above equation can equivalently be written $\|e\|_h^2 = \|\mathbf{q}(\phi)\|_q^2 + \|\mathbf{q}(\rho)\|_{q,h}^2 = \|\phi\|^2 + \|\rho\|_h^2$, with the notation $\|e\|_h^2 = \int_{\Omega} \mathbb{A} \nabla_h e \cdot \nabla_h e$.

Remark 27. If \mathbb{A} is the identity matrix, the splitting (82) is the classical Helmholtz decomposition of the vector $\nabla_h e$.

9.2 Estimation of the non-conforming part of the error

The non-conforming part ρ of the error may be estimated using the identity

$$\|\rho\|_h = \|\mathbf{q}(\rho)\|_{q,h} = \min_{v \in V} \|v - U_h\|_h, \quad (84)$$

which can be established as follows. We first observe that, for any $v \in V$, we have, in view of (81),

$$\|v - U_h\|_h^2 = \|v - u + \phi + \rho\|_h^2 = \|v - u + \phi\|_h^2 + \|\rho\|_h^2.$$

This implies that $\|v - U_h\|_h \geq \|\rho\|_h$ for any $v \in V$. Furthermore, $\|v - U_h\|_h = \|\rho\|_h$ for the specific choice $v = u - \phi \in V$, which shows (84).

In order to use (84) to estimate $\|\rho\|_h$, we need to find a suitable choice for $\hat{u}_h \in V$. This function can be constructed by smoothing the approximation U_h with an averaging operator, i.e. defining \hat{u}_h as a continuous and piecewise affine function over \mathcal{T}_h with value at node i taken as the average of the values of U_h at this node (except for nodes on Γ_D , where the value of \hat{u}_h is taken to be zero). This gives a computable upper bound on the non-conforming part of the error:

$$\|\rho\|_h^2 \leq \sum_{K \in \mathcal{T}_h} \eta_{\text{NC},K}^2 \quad \text{with} \quad \eta_{\text{NC},K}^2 = \int_K \mathbb{A} \nabla(\hat{u}_h - U_h) \cdot \nabla(\hat{u}_h - U_h).$$

It can be shown [5, 6] that this estimator is efficient in the sense that there exists C , independent of the mesh size, such that

$$\eta_{\text{NC},K}^2 \leq C \int_{U(K)} \mathbb{A} \nabla_h \rho \cdot \nabla_h \rho,$$

where $U(K)$ is the patch of elements (defined in (5)) composed of K and its neighbors.

Remark 28. *The estimate on the non-conforming part of the error is consistent with a conforming Galerkin discretization. Indeed, in this case, our above construction yields $\hat{u}_h = U_h \in V$ and thus $\eta_{\text{NC},K} = 0$.*

9.3 Estimation of the conforming part of the error

To estimate the conforming part ϕ of the error, the classical *a posteriori* error estimation tools developed in the above sections for conforming Galerkin discretization can be reused. We here follow the strategy of the equilibrated element residual method (see Section 4.2.3). Introduce a set of tractions $\hat{g}_{\Gamma,K}$ defined on element boundaries, such that

- they are equilibrated at the element level, that is,

$$\forall K \in \mathcal{T}_h, \quad \int_K f + \sum_{\Gamma \subset \partial K} \int_{\Gamma} \hat{g}_{\Gamma,K} = 0; \quad (85)$$

- they satisfy

$$\widehat{g}_{\Gamma, K_1} + \widehat{g}_{\Gamma, K_2} = 0 \quad \text{on } \partial K_1 \cap \partial K_2, \quad \widehat{g}_{\Gamma, K} = g \quad \text{on } \partial K \cap \Gamma_N. \quad (86)$$

Simply using (86), we obtain from (80) that

$$\forall v \in V, \quad B(\phi, v) = \sum_{K \in \mathcal{T}_h} \left(\int_K f v + \sum_{\Gamma \subset \partial K} \int_{\Gamma} \widehat{g}_{\Gamma, K} v - \int_K \mathbb{A} \nabla U_h \cdot \nabla v \right), \quad (87)$$

a relation that will be useful below.

The technique for the construction of the flux functions $\widehat{g}_{\Gamma, K}$ is again based on a post-processing of the numerical solution U_h to (79), and it differs depending on the non-conforming FE scheme. However, it is in any case less complex than the technique introduced in Section 5.3 for a conforming FE scheme. We detail the procedure in the two cases that we consider, the Discontinuous Galerkin FEM and the Crouzeix-Raviart FEM:

- For Discontinuous Galerkin (DG) FEM, the absence of any continuity requirement on the test functions $v \in X_h^{\text{DG}}$ involved in (79) makes the construction of $\widehat{g}_{\Gamma, K}$ easy. On any edge $\Gamma \subset \Gamma_{\text{int}} \cup \Gamma_D$ and for any element K such that $\Gamma \subset \partial K$, we define $\widehat{g}_{\Gamma, K}$ by the simple closed form expression

$$\widehat{g}_{\Gamma, K} = \sigma_{\Gamma, K} \left(\langle q_n(U_h) \rangle - \frac{\kappa}{h_{\Gamma}} [[U_h]] \right).$$

The key point to check that (85) indeed holds is that the characteristic function $\chi_K \in X_h^{\text{DG}}$ of any element K is an admissible test function for the DG FEM. Taking $v = \chi_K$ in (79), we easily obtain that the tractions defined above indeed satisfy (85). In addition, the property (86) obviously holds.

- In contrast to DG, the Crouzeix-Raviart scheme imposes a weak continuity condition on the test functions $v \in X_h^{\text{CR}}$ between neighboring elements. We can thus not choose a test function supported on a single element. For a given edge Γ , let $\theta_{\Gamma} \in X_h^{\text{CR}}$ be the function whose value is unity at the midpoint of Γ and which vanishes at the midpoint of all the other edges. The support of θ_{Γ} is the set of elements of which Γ is an edge. In the two-dimensional case, the support of θ_{Γ} is $K_1 \cup K_2$, where K_1 and K_2 are the two triangles sharing the edge Γ , and θ_{Γ} is actually the unique piecewise affine function which vanishes everywhere in $\Omega \setminus (K_1 \cup K_2)$, and which is equal to 1 at both endpoints of the edge Γ and equal to -1 at the third vertex of K_1 and of K_2 . We then get $\theta_{\Gamma} = 1$ on Γ (and thus $[[\theta_{\Gamma}]] = 0$ on Γ). This property also holds in dimension $d \geq 3$. In addition, for any element K , we have $\sum_{\Gamma \subset \partial K} \theta_{\Gamma} = 1$ on K since $\sum_{\Gamma \subset \partial K} \theta_{\Gamma}$ is an affine function equal to 1 at the midpoint of each edge of K .

On any edge $\Gamma \subset \Gamma_{\text{int}} \cup \Gamma_D$ and for any element K such that $\Gamma \subset \partial K$, we now define $\widehat{g}_{\Gamma,K}$ as a constant function with value given by

$$h_\Gamma \widehat{g}_{\Gamma,K} = \int_K \mathbb{A} \nabla U_h \cdot \nabla \theta_\Gamma - \int_K f \theta_\Gamma + \sum_{\Gamma' \subset \partial K} \frac{\kappa}{h_{\Gamma'}} \int_{\Gamma'} [[U_h]] [[\theta_\Gamma]].$$

We now check that these tractions indeed satisfy (86), under the additional assumption that \mathbb{A} is piecewise constant on the mesh. Let K_1 and K_2 be the two elements sharing the edge Γ (for brevity, we only consider the case when $\partial K_1 \cup \partial K_2$ does not contain any edge of $\partial\Omega$). We then have, using (79) with $v = \theta_\Gamma$, that

$$\begin{aligned} & h_\Gamma (\widehat{g}_{\Gamma,K_1} + \widehat{g}_{\Gamma,K_2}) \\ &= \int_\Omega \mathbb{A} \nabla_h U_h \cdot \nabla_h \theta_\Gamma - \int_\Omega f \theta_\Gamma + \sum_{\Gamma' \subset \partial K_1 \cup \partial K_2} \frac{\kappa}{h_{\Gamma'}} \int_{\Gamma'} [[U_h]] [[\theta_\Gamma]] \\ &= \sum_{\Gamma' \subset \Gamma_{\text{int}}} \int_{\Gamma'} \left([[U_h]] \langle q_n(\theta_\Gamma) \rangle + \langle q_n(U_h) \rangle [[\theta_\Gamma]] \right), \end{aligned} \quad (88)$$

where we have used, in the first line, that θ_Γ is supported in $K_1 \cup K_2$. Since θ_Γ and U_h are piecewise affine functions and since \mathbb{A} is piecewise constant, we have that $\mathbf{q}(\theta_\Gamma)$ and $\mathbf{q}(U_h)$ are piecewise constant. We therefore have that, on each edge, $\langle q_n(\theta_\Gamma) \rangle$ and $\langle q_n(U_h) \rangle$ are constant. We thus compute that $\int_{\Gamma'} [[U_h]] \langle q_n(\theta_\Gamma) \rangle = \langle q_n(\theta_\Gamma) \rangle_{|\Gamma'} \int_{\Gamma'} [[U_h]] = 0$, where the last equality stems from the fact that $U_h \in X_h^{\text{CR}}$. The second term in the right-hand side of (88) vanishes for the same reasons. We hence deduce (86).

We next check that the local equilibrium property (85) holds. For any K , we compute that

$$\begin{aligned} & \int_K f + \sum_{\Gamma \subset \partial K} \int_\Gamma \widehat{g}_{\Gamma,K} \\ &= \int_K f + \sum_{\Gamma \subset \partial K} \left(\int_K \mathbb{A} \nabla U_h \cdot \nabla \theta_\Gamma - \int_K f \theta_\Gamma + \sum_{\Gamma' \subset \partial K} \frac{\kappa}{h_{\Gamma'}} \int_{\Gamma'} [[U_h]] [[\theta_\Gamma]] \right) \\ &= \sum_{\Gamma \subset \partial K} \left(\sum_{\Gamma' \subset \partial K} \frac{\kappa}{h_{\Gamma'}} \int_{\Gamma'} [[U_h]] [[\theta_\Gamma]] \right) \quad \left[\text{since } \sum_{\Gamma \subset \partial K} \theta_\Gamma = 1 \text{ on } K \right] \\ &= \sum_{\Gamma' \subset \partial K} \frac{\kappa}{h_{\Gamma'}} \int_{\Gamma'} [[U_h]] \left[\sum_{\Gamma \subset \partial K} \theta_\Gamma \right]. \end{aligned} \quad (89)$$

For any edge $\Gamma' \subset \partial K$, let us denote K and K' the two elements sharing that edge. We know that $\sum_{\Gamma \subset \partial K} \theta_\Gamma = 1$ in K . In K' , we have $\theta_\Gamma = 0$ for all $\Gamma \subset \partial K \setminus \Gamma'$, hence $\sum_{\Gamma \subset \partial K} \theta_\Gamma = \theta_{\Gamma'}$, which is continuous across Γ' and

equal to 1 there. We hence get that $\sum_{\Gamma \subset \partial K} \theta_\Gamma$ is equal to 1 on both sides of the edge Γ' , and we thus infer (85) from (89).

Once we have defined equilibrated tractions $\widehat{g}_{\Gamma,K}$, we proceed similarly to (37) and introduce local residual problems. Here, they consist in finding $w_K \in H^1(K)$ such that

$$\forall v \in H^1(K), \quad \int_K \mathbb{A} \nabla w_K \cdot \nabla v = \int_K f v + \sum_{\Gamma \subset \partial K} \int_\Gamma \widehat{g}_{\Gamma,K} v - \int_K \mathbb{A} \nabla U_h \cdot \nabla v.$$

Since (85) is satisfied, the above Neumann problem is well-posed and uniquely defines w_K , up to an additive constant. In view of (87), we deduce that

$$\forall v \in V, \quad B(\phi, v) = \sum_{K \in \mathcal{T}_h} \int_K \mathbb{A} \nabla w_K \cdot \nabla v,$$

and we get, applying the Cauchy-Schwarz inequality, an upper bound on the conforming part of the error:

$$\|\phi\|^2 \leq \sum_{K \in \mathcal{T}_h} \eta_{\text{CF},K}^2 \quad \text{with} \quad \eta_{\text{CF},K}^2 = \int_K \mathbb{A} \nabla w_K \cdot \nabla w_K.$$

It can be shown [4] that this estimator is efficient in the sense that there exists C , independent of the mesh size, such that

$$\eta_{\text{CF},K}^2 \leq C \int_{U(K)} \mathbb{A} \nabla \phi \cdot \nabla \phi,$$

where $U(K)$ is again the patch of elements composed of K and its neighbors.

Remark 29. *A similar bound can be obtained using duality arguments and the CRE concept [87, 103], constructing an equilibrated flux field $\widehat{\mathbf{q}}_h \in W$ and defining $\eta_{\text{CF},K} = \|\widehat{\mathbf{q}}_h - \mathbb{A} \nabla U_h\|_{q,K}$. As highlighted previously, the procedure to recover $\widehat{\mathbf{q}}_h$ (e.g. using the hybrid-flux approach or RTN elements) is here less technical than in the classical conforming FEM.*

9.4 A posteriori bounds on the total error

In view of (83), and collecting the bounds from above and below established on the two error components, we eventually get

$$\frac{1}{C} \sum_{K \in \mathcal{T}_h} (\eta_{\text{CF},K}^2 + \eta_{\text{NC},K}^2) \leq \|e\|_h^2 \leq \sum_{K \in \mathcal{T}_h} (\eta_{\text{CF},K}^2 + \eta_{\text{NC},K}^2),$$

for some C independent of h , where we recall that $\|\cdot\|_h$ is the broken energy norm.

10 Extensions to other mathematical problems

In all the above sections, we have considered the problem (1), namely a time-independent, linear elliptic problem in divergence form, with a symmetric matrix \mathbb{A} . In order to show the versatility of the approaches we have presented, we turn in this section to more general problems. We consider a non-symmetric problem in Section 10.1. Time-dependent and nonlinear problems are next briefly discussed in Section 10.2.

10.1 Advection-diffusion-reaction problems

We consider a scalar advection-diffusion-reaction problem of the form

$$-\operatorname{div}(\mathbb{A}\nabla u) + \mathbf{c} \cdot \nabla u + r u = f \text{ in } \Omega, \quad u = 0 \text{ on } \Gamma_D, \quad (\mathbb{A}\nabla u) \cdot \mathbf{n} = g \text{ on } \Gamma_N. \quad (90)$$

We introduce

$$B(u, v) = \int_{\Omega} \mathbb{A}\nabla u \cdot \nabla v + (\mathbf{c} \cdot \nabla u)v + r u v, \quad F(v) = \int_{\Omega} f v + \int_{\Gamma_N} g v,$$

and assume that the matrix \mathbb{A} satisfies (2), that $r - \frac{1}{2} \operatorname{div} \mathbf{c} \geq 0$ in Ω and that $\mathbf{c} \cdot \mathbf{n} \geq 0$ on Γ_N . The bilinear form B is hence coercive on V . For the sake of simplicity, we again assume that \mathbb{A} is symmetric. Note however that B is not symmetric, due to the presence of the advection term.

The weak formulation of (90) is

$$\text{Find } u \in V \text{ such that, for any } v \in V, \quad B(u, v) = F(v).$$

It has a unique solution in view of the above assumptions. This solution may show boundary layers, namely subregions of Ω where the derivatives of u are very large [126, 222]. We define the numerical problem as:

$$\text{Find } u_h \in V_h^p \text{ such that, for any } v \in V_h^p, \quad B(u_h, v) = F(v). \quad (91)$$

Remark 30. *Even though the bilinear form B is coercive, the problem (91) may be ill-conditioned, typically in the case of advection-dominated problems (i.e. when the Péclet number P_e is large; considering for instance the simple case $r = 0$, we recall that the Péclet number is $P_e = h \|\mathbf{c}\|_{L^\infty(\Omega)} / a_{\min}$, where a_{\min} is the coercivity constant in (2)). Stabilization techniques (see e.g. [50, 108, 123, 200, 228]) are then required. The streamline diffusion FE method (SDFEM, or SUPG) is one of them. It consists in adding to the standard Galerkin FEM some weighted residuals that can be interpreted as artificial diffusion along streamlines. This leads to the new forms*

$$B_{\text{stab}}(u, v) = B(u, v) + \sum_{K \in \mathcal{T}_h} \delta_K \int_K (\mathcal{L}u) (\mathcal{L}_{ss}v),$$

$$F_{\text{stab}}(v) = F(v) + \sum_{K \in \mathcal{T}_h} \delta_K \int_K f (\mathcal{L}_{ss}v),$$

where δ_K is a local stabilization parameter, $\mathcal{L}u = -\operatorname{div}(\mathbb{A}\nabla u) + \mathbf{c}\cdot\nabla u + ru$ is the operator of the problem and \mathcal{L}_{ss} is the skew-symmetric part of \mathcal{L} . The stabilized problem then consists in finding $u_h^{\text{stab}} \in V_h^p$ such that $B_{\text{stab}}(u_h^{\text{stab}}, v) = F_{\text{stab}}(v)$ for any $v \in V_h^p$. As is well-known, this approach is strongly consistent, in the sense that the exact solution u satisfies $B_{\text{stab}}(u, v) = F_{\text{stab}}(v)$ for any $v \in V_h^p$.

10.1.1 A priori error estimation

We introduce the Clément interpolant $\Pi_h u$ of the exact solution u , as defined in Section 2.4, and decompose the overall error as $e = (u - \Pi_h u) + (\Pi_h u - u_h) = \mu + e_h$. The term μ corresponds to the interpolation error, while e_h belongs to V_h^p .

When $\mathbf{c} = 0$, the bilinear form B is symmetric and Galerkin orthogonality yields

$$\|e\|^2 = B(e, \mu + e_h) = B(e, \mu) \leq \|e\| \|\mu\|, \quad (92)$$

and thus $\|e\| \leq \|\mu\|$, which corresponds to the best approximation property. The error (in the energy norm) can thus be bounded as in Section 2.4, from a standard interpolation estimate [75, 224]. In particular, when $u \in H^q(\Omega)$ for some $q \geq p + 1$, we get

$$\|e\| \leq C h^p \|u\|_{p+1}, \quad (93)$$

where C depends on p and the geometry of the mesh (but is independent of h and u).

In the general case (i.e. for a non-symmetric bilinear form B), the estimate $|B(e, \mu)| \leq \|e\| \|\mu\|$ used in (92) does not hold. We follow here the procedure introduced in [222] to estimate the error. The form B is split in its symmetric and skew symmetric parts:

$$\begin{aligned} B(w, v) &= \frac{1}{2}(B(w, v) + B(v, w)) + \frac{1}{2}(B(w, v) - B(v, w)) \\ &= B_{\text{symm}}(w, v) + B_{\text{skew}}(w, v), \end{aligned}$$

with

$$\begin{aligned} B_{\text{symm}}(w, v) &= \int_{\Omega} \left[\mathbb{A}\nabla w \cdot \nabla v + \left(r - \frac{1}{2} \operatorname{div} \mathbf{c}\right) w v \right] + \frac{1}{2} \int_{\Gamma_N} \mathbf{c} \cdot \mathbf{n} w v, \\ B_{\text{skew}}(w, v) &= \frac{1}{2} \int_{\Omega} \mathbf{c} \cdot (v \nabla w - w \nabla v). \end{aligned}$$

Remark 31. From this decomposition of B , it is straightforward to understand why the inequality in (92) does not hold. The skew symmetric part B_{skew} does not contribute to the “energy” norms $\|e\|$ and $\|\mu\|$, but it contributes to $B(e, \mu)$.

We next define a dual norm (the so-called skew norm) to accommodate for the skew symmetric part of B :

$$\|w\|_{\text{skew}} := \sup_{v \in V} \frac{|B_{\text{skew}}(w, v)|}{\|v\|}.$$

For any w and v in V , we thus have $|B_{\text{skew}}(w, v)| \leq \|w\|_{\text{skew}} \|v\|$. Using that $B_{\text{skew}}(w, v) = -B_{\text{skew}}(v, w)$, we also have $|B_{\text{skew}}(v, w)| \leq \|w\|_{\text{skew}} \|v\|$. We thus obtain

$$\begin{aligned} \|e\|^2 &= |B(e, \mu)| = |B_{\text{symm}}(e, \mu) + B_{\text{skew}}(e, \mu)| \\ &\leq |B_{\text{symm}}(e, \mu)| + |B_{\text{skew}}(\mu, e)| \leq \|\mu\| \|e\| + \|\mu\|_{\text{skew}} \|e\|, \end{aligned}$$

hence

$$\|e\| \leq \|\mu\| + \|\mu\|_{\text{skew}}. \quad (94)$$

Focusing on $\|\mu\|_{\text{skew}}$, we get, using the Poincaré inequality in V , that

$$\|\mu\|_{\text{skew}} = \sup_{v \in V} \frac{|B_{\text{skew}}(v, \mu)|}{\|v\|} \leq C \|\mu\|_1,$$

where the constant C is large for advection-diffusion problems with large Péclet number P_e . Inserting the above bound in (94) and using an interpolation estimate, we recover (93) when $u \in H^q(\Omega)$ for some $q \geq p + 1$.

Remark 32. *An alternative approach to estimate the error consists in using the coercivity of B in V : there exists some $c > 0$ such that $B(v, v) \geq c \|v\|_1^2$ for any $v \in V$. Writing this coercivity estimate for $e \in V$ and using next the variational formulations that u and u_h satisfy, we obtain that, for any $v_h \in V_h^p$,*

$$c \|e\|_1^2 \leq B(e, e) = B(u - u_h, u - u_h) = B(u - u_h, u - v_h).$$

Using next that B is continuous in V , we deduce that

$$c \|e\|_1^2 \leq C \|u - u_h\|_1 \|u - v_h\|_1,$$

and therefore $\|e\|_1 \leq C \|u - v_h\|_1$ for any $v_h \in V_h^p$. Using classical approximation results, we hence infer that $\|e\|_1 \leq C h^p \|u\|_{p+1}$. We eventually write that $\|e\| = \sqrt{B(e, e)} \leq C \|e\|_1$ and deduce (93).

Remark 33. *Suppose that $u \in H^2(\Omega)$, that $P_e > 1$ and that we use piecewise affine finite elements. We can then show that $\|u - u_h\|_1 \leq Ch(1 + P_e)\|u\|_2$ when using the (original, non-stabilized) bilinear form B , whereas $\|u - u_h^{\text{stab}}\|_1 \leq Ch(1 + \sqrt{P_e})\|u\|_2$ when using the stabilized formulation described in Remark 30.*

10.1.2 *A posteriori* error estimation

Several *a posteriori* error estimates have been developed for advection-diffusion-reaction problems in the literature. We detail some of them below. They basically follow similar methodologies as for pure diffusion problems (i.e. with a symmetric operator), since the Cauchy-Schwarz inequality (in the sense of (92)) is not needed when establishing *a posteriori* estimates.

In [126], the use of the explicit residual method (in the vein of Section 4.1) leads to the general form $\eta = \sqrt{\sum_{K \in \mathcal{T}_h} \eta_K^2}$ for the estimate of the error in the energy norm, with

$$\begin{aligned} \eta_K^2 &= \alpha_K \|f + \operatorname{div}(\mathbb{A} \nabla u_h) - \mathbf{c} \cdot \nabla u_h - r u_h\|_{0,K}^2 \\ &\quad + \sum_{\Gamma \subset \partial K \setminus \Gamma_N} \frac{\beta_\Gamma}{2} \left\| [[\mathbb{A} \nabla u_h \cdot \mathbf{n}]]_\Gamma \right\|_{0,\Gamma}^2 + \sum_{\Gamma \subset \partial K \cap \Gamma_N} \beta_\Gamma \|\mathbb{A} \nabla u_h \cdot \mathbf{n} - g\|_{0,\Gamma}^2, \end{aligned}$$

where $\alpha_K = \min(h_K^2 a_{\max}^{-1}, 1)$ and $\beta_\Gamma = \min(h_\Gamma a_{\max}^{-1}, a_{\max}^{-1/2})$. It is shown that η provides for a global upper estimate, and η_K provides for a local lower estimate, up to unknown multiplicative constants. These estimates are robust in the advection-dominated regime. We refer to [126] for more details.

Implicit methods such as the element residual method (in the vein of Section 4.2.3) may also be used. They involve the resolution of local problems of the following form (compare with (34)): find $e_K \in V(K)$ such that, for any $v \in V(K)$,

$$\begin{aligned} B_K(e_K, v) &= \int_K (f + \operatorname{div} \mathbb{A} \nabla u_h - \mathbf{c} \cdot \nabla u_h - r u_h) v \\ &\quad - \frac{1}{2} \sum_{\Gamma \subset \partial K \setminus \partial \Omega} \int_\Gamma [[\mathbb{A} \nabla u_h \cdot \mathbf{n}]] v - \sum_{\Gamma \subset \partial K \cap \Gamma_N} \int_\Gamma (\mathbb{A} \nabla u_h \cdot \mathbf{n} - g) v, \end{aligned}$$

where we recall that $V(K) = \{v \in H^1(K), v = 0 \text{ on } \partial K \cap \Gamma_D\}$. Local estimates η_K are next computed using e_K . The above problem may be in practice solved with higher-order elements (bubble functions). A difficulty comes from the fact that the solution e_K may have oscillations in convection-dominated problems. This can again be addressed using stabilization techniques.

Duality-based approaches (in the spirit of the approaches presented in Section 5) can also be employed for advection-diffusion-reaction problems [100, 103]. Defining the flux as $\mathbf{q} = \mathbb{A} \nabla u - \mathbf{c} u$, the CRE framework provides for a guaranteed estimate of the global error measured using the norm $\|v\|_\oplus := \|v\| + \|v\|_{\text{skew}}$. It can be shown that this norm, which is an augmented energy norm, is equivalent to the dual norm of the residual $R(v) = F(v) - B(u_h, v)$.

Remark 34. *When the hybrid-flux technique of Section 5.3.1 is considered to compute an admissible flux field, the associated prolongation condition should be consistent with the discretization of the problem (in particular when stabilization is used) in order to recover required properties, and in particular the solvability condition on the linear system (53). We refer to [186] for details.*

10.1.3 Goal-oriented error estimation

The splitting between the symmetric and the skew symmetric parts of B can also be used for goal-oriented error estimation [185, 186, 216]. Introducing the

adjoint problem $B(v, \tilde{u}) = Q(v)$ for any $v \in V$ (possibly solved in practice using a stabilization technique), that is

$$\begin{aligned} -\operatorname{div}(\mathbb{A}\nabla\tilde{u}) - \mathbf{c} \cdot \nabla\tilde{u} + (r - \operatorname{div} \mathbf{c})\tilde{u} &= \tilde{f}_Q - \operatorname{div}(\tilde{\mathbf{q}}_Q + \mathbb{A}\nabla\tilde{u}_Q) \quad \text{in } \Omega, \\ \tilde{u} &= 0 \quad \text{on } \Gamma_D, \\ \mathbb{A}\nabla\tilde{u} \cdot \mathbf{n} + \mathbf{c} \cdot \mathbf{n}\tilde{u} &= \tilde{g}_Q + (\tilde{\mathbf{q}}_Q + \mathbb{A}\nabla\tilde{u}_Q) \cdot \mathbf{n} \quad \text{on } \Gamma_N, \end{aligned}$$

where $\tilde{\mathbf{q}}_Q$, \tilde{f}_Q and \tilde{g}_Q are the extraction functions used in the definition (62) of the quantity of interest Q , we get

$$Q(e) = B(e, \tilde{u}) = B(e, \tilde{e}) + R(\tilde{u}_h),$$

with $R(\tilde{u}_h) = F(\tilde{u}_h) - B(u_h, \tilde{u}_h) \neq 0$ if different discretizations are used for u_h and \tilde{u}_h , or if a stabilized discretization is used for one of the two problems.

Denoting by e^s and \tilde{e}^s the solutions in V to the symmetrized residual equations,

$$\begin{aligned} \forall v \in V, \quad B_{\text{symm}}(e^s, v) &= F(v) - B(u_h, v), \\ \forall v \in V, \quad B_{\text{symm}}(\tilde{e}^s, v) &= Q(v) - B(v, \tilde{u}_h), \end{aligned}$$

we get that

$$|Q(u) - Q(u_h) - R(\tilde{u}_h)| = |B_{\text{symm}}(e^s, \tilde{e}^s)| \leq \|e^s\| \|\tilde{e}^s\|.$$

Classical estimates in energy norm (induced by the symmetric part of the operator) can next be used to bound $\|e^s\|$ and $\|\tilde{e}^s\|$.

10.2 Time-dependent and nonlinear problems

For linear time-dependent problems, effective *a posteriori* error estimation tools (both for the global error and for errors on quantities of interest) have been proposed. We refer to [37] for parabolic problems, to [16, 79, 232, 240, 246] for transient elastodynamics, and to [149, 165, 177, 241] for vibratory dynamics with error estimates on the eigenfrequencies. A large set of applications of *a posteriori* error estimates for both parabolic and hyperbolic problems is also described in [97].

For nonlinear problems, there are much fewer contributions than for linear problems. It is important to distinguish between nonlinear *time-dependent* and nonlinear *time-independent* problems:

- For the latter case, we mention [22, 155] for the design of estimates for nonlinear elasticity problems (where ∇u is considered small, as in linear elasticity, but where the constitutive relation between stress and strain is nonlinear), [51] for large strain elasticity (where ∇u is not considered to be small), [127] for Hencky-type plasticity problems, [77, 111, 114, 191, 203] for elastoplasticity, and [36, 80, 96, 159, 242] for contact-friction problems.

- For the former case, viscoplasticity problems have been considered in [106, 156, 189, 192], Navier-Stokes equations have been addressed in [9, 219, 234] with residual methods, and nonlinear dynamics has been studied in [201]. Other nonlinear contexts have also been investigated in [122]. In most cases, techniques devised for linear problems or time-independent nonlinear problems are used at each time step, and the estimation is thus limited to spatial error. For such nonlinear time-dependent problems, error estimators based on the constitutive law residual have been introduced and take all error sources into account [137, 138, 147, 148]. They refer to the concept of dissipation error which is constructed from dual convex potentials (in the Legendre-Fenchel sense) that describe the material behavior [207]. This concept also enables to get upper bounds for quantities of interest in complex nonlinear cases [139, 140].

Let us also add that specific indicators for various error sources (space/time discretizations, linearization procedure and stopping criteria for iterative algorithms introduced to solve the nonlinear problems, ...) have also been established, see [82, 95, 102, 189, 239].

11 Conclusion

We have presented a review on *a posteriori* error estimation tools applied to linear elliptic problems solved with FEM. On the one hand, we have shown that inexpensive methods (such as explicit residual methods) may be sufficient to obtain an indication on the discretization error or to drive mesh adaptation. On the other hand, we have emphasized that more advanced error estimators, which require more expensive computations, are able to provide accurate information on the error value. We have also highlighted that dual analysis and equilibrium concepts are at the heart of all robust estimates that provide guaranteed error bounds, and that can be extended to general engineering problems. For the sake of brevity, we have often limited ourselves in terms of technical details. We refer the interested reader to reference textbooks on this topic, such as [9, 24, 150, 220, 234, 235].

In addition to FEM, verification has now become a challenging issue in various innovating numerical strategies that have emerged during the last decades. In this context, some first tools have been developed to assess discretization errors in association with errors coming from other sources. These tools use concepts similar to those presented in this article. Among all *a posteriori* error estimates that have appeared in these new contexts, we wish to cite those related to

- mixed FE discretizations [47, 236];
- domain decomposition techniques [38, 188, 208];
- virtual element methods [35, 41, 56];

- solution to stochastic problems [20, 53, 66, 144, 162, 174, 217];
- fracture mechanics, possibly with enrichment techniques such as XFEM [112, 180, 210, 214, 223, 225, 247];
- isogeometric analysis [30, 52, 92, 133, 134, 135, 229];
- the use of surrogate mathematical models, leading to modeling errors when compared to a reference model [23, 176, 230];
- the use of reduced order modeling by means of Reduced Basis methods [118, 121, 164, 195, 198, 199, 212, 213], Proper Generalized Decomposition [12, 13, 64, 70, 71, 142, 206] or alternative methods [3, 65, 94, 132];
- multiscale modeling as in the Heterogeneous Multiscale Method (HMM) [1, 2, 124], the Variational Multiscale Method (VMM) [154], the Generalized Finite Element Method (GFEM) [227] or the Multiscale Finite Element Method (MsFEM) [68, 69, 74, 120].

A Appendix: Proof of the lower bound for CRE error estimates

We have seen in Section 5.2 that the Constitutive Relation Error (CRE) estimate is an upper bound on the numerical error. More precisely, we have seen (see (43) or (45)) that

$$\| \|u - u_h\| \|^2 \leq E_{\text{CRE}}^2(u_h, \mathbf{p})$$

for any statically admissible $\mathbf{p} \in W$. We show here a converse inequality. In contrast to some other methods (see e.g. (31) for the subdomain residual methods described in Section 4.2.2), obtaining such a lower bound is not straightforward. Establishing this lower bound is also enlightning because the proof below uses the specificities of the construction of the equilibrated flux field (in contrast to the above upper bound).

For the sake of simplicity, we consider the problem (1) in dimension $d = 2$, although our arguments carry over to the three-dimensional case. We assume that we use a mesh made of triangles, and that the mesh is regular in the sense that

- the number of triangles in Ω_i (the set of elements having i as a vertex) is bounded independently of the mesh size h ;
- in the union $\cup_{K \in \mathcal{T}_h} \cup_{i \in K} \Omega_i$, each triangle is accounted for a number of times which is bounded from above independently of h .

We also assume that we use P1 finite elements, and denote $\{\phi_i\}$ the basis functions. Our arguments presumably carry over to more general cases, at the possible price of additional work.

Theorem 35. *Under the above assumptions, let u be the solution to (3) and $\widehat{\mathbf{q}}_h \in [L^2(\Omega)]^2$ be the equilibrated flux field constructed with the hybrid-flux technique (see Section 5.3.1). We assume that the numerical solution $u_h \in H^1(\Omega)$ to (6) is such that*

$$\text{on any triangle } K, \quad \operatorname{div}(\mathbb{A}\nabla u_h) = 0. \quad (\text{H1})$$

Denoting $\mathbf{q}_h = \mathbb{A}\nabla u_h$, we also assume that

$$\begin{aligned} &\text{on any edge } \Gamma_{\alpha,\beta} \text{ separating the elements } K_\alpha \text{ and } K_\beta, \\ &(\mathbf{q}_h|_{K_\alpha} + \mathbf{q}_h|_{K_\beta}) \cdot \mathbf{n} \text{ is constant} \end{aligned} \quad (\text{H2})$$

and that

$$\begin{aligned} &\text{on any edge } \Gamma_{\alpha,\beta} \text{ separating the elements } K_\alpha \text{ and } K_\beta, \\ &(\mathbf{q}_h|_{K_\alpha} - \mathbf{q}_h|_{K_\beta}) \cdot \mathbf{n} \text{ is constant.} \end{aligned} \quad (\text{H3})$$

We furthermore assume that

$$\text{on any triangle } K, \quad f \text{ is constant.} \quad (\text{H4})$$

Then, there is a constant C independent of h such that

$$E_{\text{CRE}}^2(u_h, \widehat{\mathbf{q}}_h) \leq C \| \|u - u_h\| \|^2. \quad (95)$$

Of course, Assumptions (H2) and (H3) are equivalent to the fact that, on each edge $\Gamma_{\alpha,\beta}$ separating K_α and K_β , the normal fluxes $\mathbf{q}_h|_{K_\alpha} \cdot \mathbf{n}$ and $\mathbf{q}_h|_{K_\beta} \cdot \mathbf{n}$ are constant. We note that assumptions (H1), (H2) and (H3) are satisfied as soon as \mathbb{A} is constant on each triangle K (recall that we use P1 elements). Our proof of Theorem 35 essentially follows the arguments of [145]. In Corollary 36 below, we relax Assumption (H4).

Proof. The proof of Theorem 35 falls in 6 steps.

Step 1. We follow the notations introduced in Section 5.3.1. Consider the local linear system (53) associated with an interior node i and define the quantity

$$\widehat{d}_{\alpha,\beta}(i) = \widehat{b}_{\alpha,\beta}(i) - b_{\alpha,\beta}^m(i)$$

where α and β are two adjacent triangles in Ω_i and $\widehat{b}_{\alpha,\beta}(i)$ (resp. $b_{\alpha,\beta}^m(i)$) is defined by (52) (resp. (55)).

Let N_i denote the number of triangles in Ω_i . We infer from (53) (recall that

ϕ_i are the piecewise affine basis functions) and (H1) that

$$\begin{aligned}
& \widehat{d}_{1,2}(i) - \widehat{d}_{N_i,1}(i) \\
&= \left(\widehat{b}_{1,2}(i) - b_{1,2}^m(i) \right) - \left(\widehat{b}_{N_i,1}(i) - b_{N_i,1}^m(i) \right) \\
&= Q_i^{K_1} - (b_{1,2}^m(i) - b_{N_i,1}^m(i)) \\
&= \int_{K_1} (\mathbf{q}_h \cdot \nabla \phi_i - f \phi_i) \\
&\quad - \frac{1}{2} \left(\int_{\Gamma_{1,2}} \phi_i (\mathbf{q}_h|_{K_1} + \mathbf{q}_h|_{K_2}) \cdot \mathbf{n}_{K_1} - \int_{\Gamma_{N_i,1}} \phi_i (\mathbf{q}_h|_{K_{N_i}} + \mathbf{q}_h|_{K_1}) \cdot \mathbf{n}_{K_{N_i}} \right) \\
&= \int_{\Gamma_{1,2}} \phi_i \mathbf{q}_h|_{K_1} \cdot \mathbf{n}_{K_1} + \int_{\Gamma_{N_i,1}} \phi_i \mathbf{q}_h|_{K_1} \cdot \mathbf{n}_{K_1} - \int_{K_1} f \phi_i \\
&\quad - \frac{1}{2} \left(\int_{\Gamma_{1,2}} \phi_i (\mathbf{q}_h|_{K_1} + \mathbf{q}_h|_{K_2}) \cdot \mathbf{n}_{K_1} - \int_{\Gamma_{N_i,1}} \phi_i (\mathbf{q}_h|_{K_{N_i}} + \mathbf{q}_h|_{K_1}) \cdot \mathbf{n}_{K_{N_i}} \right) \\
&= - \int_{K_1} f \phi_i \\
&\quad + \frac{1}{2} \int_{\Gamma_{1,2}} \phi_i (\mathbf{q}_h|_{K_1} - \mathbf{q}_h|_{K_2}) \cdot \mathbf{n}_{K_1} + \frac{1}{2} \int_{\Gamma_{N_i,1}} \phi_i (\mathbf{q}_h|_{K_{N_i}} - \mathbf{q}_h|_{K_1}) \cdot \mathbf{n}_{K_{N_i}}.
\end{aligned}$$

Similarly, we compute that

$$\begin{aligned}
& \widehat{d}_{2,3}(i) - \widehat{d}_{1,2}(i) = - \int_{K_2} f \phi_i \\
&\quad + \frac{1}{2} \int_{\Gamma_{2,3}} \phi_i (\mathbf{q}_h|_{K_2} - \mathbf{q}_h|_{K_3}) \cdot \mathbf{n}_{K_2} + \frac{1}{2} \int_{\Gamma_{1,2}} \phi_i (\mathbf{q}_h|_{K_1} - \mathbf{q}_h|_{K_2}) \cdot \mathbf{n}_{K_1},
\end{aligned}$$

and likewise for any $\widehat{d}_{\alpha,\alpha+1}(i) - \widehat{d}_{\alpha-1,\alpha}(i)$ (with $3 \leq \alpha \leq N_i - 1$), until

$$\begin{aligned}
& \widehat{d}_{N_i,1}(i) - \widehat{d}_{N_i-1,N_i}(i) = - \int_{K_{N_i}} f \phi_i \\
&+ \frac{1}{2} \int_{\Gamma_{N_i,1}} \phi_i (\mathbf{q}_h|_{K_{N_i}} - \mathbf{q}_h|_{K_1}) \cdot \mathbf{n}_{K_{N_i}} + \frac{1}{2} \int_{\Gamma_{N_i-1,N_i}} \phi_i (\mathbf{q}_h|_{K_{N_i-1}} - \mathbf{q}_h|_{K_{N_i}}) \cdot \mathbf{n}_{K_{N_i-1}}.
\end{aligned}$$

We introduce

$$j_{\alpha,\beta} = \frac{1}{2} (\mathbf{q}_h|_{K_\alpha} - \mathbf{q}_h|_{K_\beta}) \cdot \mathbf{n}_{K_\alpha}, \quad J_{\alpha,\beta}(i) = \int_{\Gamma_{\alpha,\beta}} \phi_i j_{\alpha,\beta}, \quad (96)$$

and remark that $j_{\beta,\alpha} = j_{\alpha,\beta}$ and $J_{\beta,\alpha}(i) = J_{\alpha,\beta}(i)$. Using these notations, we

write the local linear system as

$$\begin{aligned}
\widehat{d}_{1,2}(i) - \widehat{d}_{N_i,1}(i) &= - \int_{K_1} f\phi_i + J_{1,2}(i) + J_{N_i,1}(i), \\
\widehat{d}_{2,3}(i) - \widehat{d}_{1,2}(i) &= - \int_{K_2} f\phi_i + J_{2,3}(i) + J_{1,2}(i), \\
&\vdots \\
\widehat{d}_{N_i,1}(i) - \widehat{d}_{N_{i-1},N_i}(i) &= - \int_{K_{N_i}} f\phi_i + J_{N_i,1}(i) + J_{N_{i-1},N_i}(i).
\end{aligned} \tag{97}$$

Just like the system (53), the system (97) has an infinity of solutions. As explained in Remark 14, the one minimizing $\sum_{\alpha,\beta} \frac{(\widehat{d}_{\alpha,\beta}(i))^2}{|\Gamma_{\alpha,\beta}|^2}$ is chosen in practice.

The constrained minimization leads to an explicit solution of the form (see Remark 14 and [150])

$$\widehat{d}_{N_i,1}(i) = s, \quad \widehat{d}_{1,2}(i) = s + \overline{Q}_i^{K_1}, \quad \widehat{d}_{2,3}(i) = s + \overline{Q}_i^{K_1} + \overline{Q}_i^{K_2}, \quad \dots$$

with $\overline{Q}_i^{K_\alpha} = - \int_{K_\alpha} f\phi_i + J_{\alpha,\alpha+1}(i) + J_{\alpha-1,\alpha}(i)$ and $s = - \frac{\sum_{\alpha,\beta} |\Gamma_{\alpha,\beta}|^{-2} \overline{Q}_i^{K_\beta}}{\sum_{\alpha,\beta} |\Gamma_{\alpha,\beta}|^{-2}}$.

Using the regularity of the mesh, we deduce that there exists C independent of h and i such that $|s| \leq C \sum_{n \in \Omega_i} |\overline{Q}_i^{K_n}|$, which implies that

$$|\widehat{d}_{\alpha,\beta}(i)| \leq C \sum_{n \in \Omega_i} |\overline{Q}_i^{K_n}|.$$

We thus get that there exists a constant C independent of h , i , α and β such that

$$|\widehat{d}_{\alpha,\beta}(i)| \leq C \left[\sum_{n \in \Omega_i} \left| \int_{K_n} f\phi_i \right| + \sum_{n,m \in \Omega_i} |J_{n,m}(i)| \right]. \tag{98}$$

Step 2. On the edge linking vertices i_1 and i_2 (at the interface between triangles K_α and K_β), we wish to find c_{i_1} and c_{i_2} such that the function

$$\sigma_{\Gamma_{\alpha,\beta}, K_\alpha} \widehat{g}_{\Gamma_{\alpha,\beta}} = c_{i_1} \phi_{i_1} + c_{i_2} \phi_{i_2}$$

satisfies

$$\int_{\Gamma_{\alpha,\beta}} \phi_{i_1} \sigma_{\Gamma_{\alpha,\beta}, K_\alpha} \widehat{g}_{\Gamma_{\alpha,\beta}} = \widehat{b}_{\alpha,\beta}(i_1), \quad \int_{\Gamma_{\alpha,\beta}} \phi_{i_2} \sigma_{\Gamma_{\alpha,\beta}, K_\alpha} \widehat{g}_{\Gamma_{\alpha,\beta}} = \widehat{b}_{\alpha,\beta}(i_2). \tag{99}$$

Introduce

$$\begin{aligned}
\widehat{G}_{i_1, i_2} &= \sigma_{\Gamma_{\alpha,\beta}, K_\alpha} \widehat{g}_{\Gamma_{\alpha,\beta}} - \frac{1}{2} \left(\mathbf{q}_{h|K_\alpha} + \mathbf{q}_{h|K_\beta} \right) \cdot \mathbf{n}_{K_\alpha} \\
&= \left(c_{i_1} - q_h^{\alpha\beta} \right) \phi_{i_1} + \left(c_{i_2} - q_h^{\alpha\beta} \right) \phi_{i_2}
\end{aligned} \tag{100}$$

where $q_h^{\alpha\beta} = \frac{1}{2} \left(\mathbf{q}_{h|K_\alpha} + \mathbf{q}_{h|K_\beta} \right) \cdot \mathbf{n}_{K_\alpha}$ is a constant (Assumption (H2)) and we recall that $\phi_{i_1} + \phi_{i_2} = 1$ on the edge. It is straightforward to observe that (99) is equivalent to

$$\begin{cases} \int_{\Gamma_{\alpha,\beta}} \phi_{i_1} \widehat{G}_{i_1,i_2} = \widehat{b}_{\alpha,\beta}(i_1) - b_{\alpha,\beta}^m(i_1) = \widehat{d}_{\alpha,\beta}(i_1), \\ \int_{\Gamma_{\alpha,\beta}} \phi_{i_2} \widehat{G}_{i_1,i_2} = \widehat{b}_{\alpha,\beta}(i_2) - b_{\alpha,\beta}^m(i_2) = \widehat{d}_{\alpha,\beta}(i_2). \end{cases} \quad (101)$$

Collecting (100) and (101), we obtain

$$\begin{pmatrix} \int_{\Gamma_{\alpha,\beta}} \phi_{i_1}^2 & \int_{\Gamma_{\alpha,\beta}} \phi_{i_1} \phi_{i_2} \\ \int_{\Gamma_{\alpha,\beta}} \phi_{i_1} \phi_{i_2} & \int_{\Gamma_{\alpha,\beta}} \phi_{i_2}^2 \end{pmatrix} \begin{pmatrix} c_{i_1} - q_h^{\alpha\beta} \\ c_{i_2} - q_h^{\alpha\beta} \end{pmatrix} = \begin{pmatrix} \widehat{d}_{\alpha,\beta}(i_1) \\ \widehat{d}_{\alpha,\beta}(i_2) \end{pmatrix}, \quad (102)$$

a system the explicit solution of which is

$$\begin{pmatrix} c_{i_1} - q_h^{\alpha\beta} \\ c_{i_2} - q_h^{\alpha\beta} \end{pmatrix} = \frac{1}{D} \begin{pmatrix} \int_{\Gamma_{\alpha,\beta}} \phi_{i_2}^2 & - \int_{\Gamma_{\alpha,\beta}} \phi_{i_1} \phi_{i_2} \\ - \int_{\Gamma_{\alpha,\beta}} \phi_{i_1} \phi_{i_2} & \int_{\Gamma_{\alpha,\beta}} \phi_{i_1}^2 \end{pmatrix} \begin{pmatrix} \widehat{d}_{\alpha,\beta}(i_1) \\ \widehat{d}_{\alpha,\beta}(i_2) \end{pmatrix}, \quad (103)$$

with D the determinant of the 2×2 matrix in (102). In dimension $d = 2$, the terms of the matrix in (102) are of the order of $O(h)$, hence D is of the order of $O(h^2)$ (in dimension d , the matrix appearing in (102) is of size $d \times d$, and each of its term is of the order of $O(h^{d-1})$; its determinant is thus of the order of $O(h^{d(d-1)})$, and its cofactors, appearing in (103), are of the order of $O(h^{d(d-1)^2})$). Introducing these scalings, we get from (103) that

$$\left| c_{i_1} - q_h^{\alpha\beta} \right| + \left| c_{i_2} - q_h^{\alpha\beta} \right| \leq \frac{C}{h^{d-1}} \left(\left| \widehat{d}_{\alpha,\beta}(i_1) \right| + \left| \widehat{d}_{\alpha,\beta}(i_2) \right| \right),$$

and therefore

$$\int_{\Gamma_{\alpha,\beta}} \left| \widehat{G}_{i_1,i_2} \right|^2 \leq \frac{C}{h^{d-1}} \left(\left| \widehat{d}_{\alpha,\beta}(i_1) \right| + \left| \widehat{d}_{\alpha,\beta}(i_2) \right| \right)^2. \quad (104)$$

Step 3. We introduce $\Sigma_h = \widehat{\mathbf{q}}_h - \mathbf{q}_h$, where $\widehat{\mathbf{q}}_h$ is the equilibrated field constructed in Section 5.3.1 and $\mathbf{q}_h = \mathbb{A} \nabla u_h$. We recall that, for any triangle K_α ,

$$-\operatorname{div} \widehat{\mathbf{q}}_h = f \text{ in } K_\alpha, \quad \widehat{\mathbf{q}}_h \cdot \mathbf{n}_{K_\alpha} = \sigma_{\Gamma_{\alpha,\beta}, K_\alpha} \widehat{g}_{\Gamma_{\alpha,\beta}} \text{ on the edges } \Gamma_{\alpha,\beta} \subset \partial K_\alpha$$

where \mathbf{n}_{K_α} is the outgoing normal vector to K_α . Among all equilibrated flux fields which verify the previous condition, we select the one that minimizes the complementary energy (or CRE functional) over K_α so that, by duality,

it derives from a primal field \widehat{u}_h . We thus choose $\widehat{\mathbf{q}}_h = \mathbb{A}\nabla\widehat{u}_h$ where \widehat{u}_h is a solution to

$$-\operatorname{div}\mathbb{A}\nabla\widehat{u}_h = f \text{ in } K_\alpha, \quad \mathbb{A}\nabla\widehat{u}_h \cdot \mathbf{n}_{K_\alpha} = \sigma_{\Gamma_{\alpha,\beta},K_\alpha} \widehat{g}_{\Gamma_{\alpha,\beta}} \text{ on the edges } \Gamma_{\alpha,\beta} \subset \partial K_\alpha,$$

and is of course uniquely defined up to an additive constant. We choose it such that

$$\int_{K_\alpha} \widehat{u}_h = \int_{K_\alpha} u_h. \quad (105)$$

Using Assumption (H1), we see that Σ_h verifies

$$-\operatorname{div}\Sigma_h = f \quad \text{in } K_\alpha. \quad (106)$$

Furthermore, on the edge $\Gamma_{\alpha,\beta} \subset \partial K_\alpha$ linking vertices i_1 and i_2 , we have

$$\Sigma_h \cdot \mathbf{n}_{K_\alpha} = \sigma_{\Gamma_{\alpha,\beta},K_\alpha} \widehat{g}_{\Gamma_{\alpha,\beta}} - \mathbf{q}_{h|K_\alpha} \cdot \mathbf{n}_{K_\alpha} = \widehat{G}_{i_1,i_2} - j_{\alpha,\beta}, \quad (107)$$

where \widehat{G}_{i_1,i_2} and $j_{\alpha,\beta}$ are defined in (100) and (96), respectively.

Using (106), we get

$$\begin{aligned} \int_{K_\alpha} \Sigma_h^T \mathbb{A}^{-1} \Sigma_h &= \int_{K_\alpha} \Sigma_h \cdot \nabla(\widehat{u}_h - u_h) \\ &= \int_{\partial K_\alpha} \Sigma_h \cdot \mathbf{n}_{K_\alpha} (\widehat{u}_h - u_h) - \int_{K_\alpha} (\widehat{u}_h - u_h) \operatorname{div} \Sigma_h \\ &\leq \|\Sigma_h \cdot \mathbf{n}_{K_\alpha}\|_{0,\partial K_\alpha} \|\widehat{u}_h - u_h\|_{0,\partial K_\alpha} + \|f\|_{0,K_\alpha} \|\widehat{u}_h - u_h\|_{0,K_\alpha}. \end{aligned}$$

Using (105) and scaling arguments similar to those employed in [157, Sec. 4.2, eqs. (4.5) and (4.3)], we deduce from the previous inequality that

$$\begin{aligned} &\int_{K_\alpha} \Sigma_h \mathbb{A}^{-1} \Sigma_h \\ &\leq C\sqrt{h} \|\nabla(\widehat{u}_h - u_h)\|_{0,K_\alpha} \|\Sigma_h \cdot \mathbf{n}_{K_\alpha}\|_{0,\partial K_\alpha} + Ch \|\nabla(\widehat{u}_h - u_h)\|_{0,K_\alpha} \|f\|_{0,K_\alpha} \\ &\leq C\sqrt{h} \|\mathbb{A}^{-1/2} \Sigma_h\|_{0,K_\alpha} \|\Sigma_h \cdot \mathbf{n}_{K_\alpha}\|_{0,\partial K_\alpha} + Ch \|\mathbb{A}^{-1/2} \Sigma_h\|_{0,K_\alpha} \|f\|_{0,K_\alpha}. \end{aligned}$$

It should be noticed that the previous scalings are independent of the dimension d . We infer from the above bound that

$$\int_{K_\alpha} \Sigma_h \mathbb{A}^{-1} \Sigma_h \leq Ch \|\Sigma_h \cdot \mathbf{n}_{K_\alpha}\|_{0,\partial K_\alpha}^2 + Ch^2 \|f\|_{0,K_\alpha}^2.$$

We now use (107) and obtain

$$\int_{K_\alpha} \Sigma_h \mathbb{A}^{-1} \Sigma_h \leq Ch \sum_{\Gamma_{\alpha,\beta} \subset \partial K_\alpha} \int_{\Gamma_{\alpha,\beta}} \left(|\widehat{G}_{i_1,i_2}|^2 + |j_{\alpha,\beta}|^2 \right) + Ch^2 \|f\|_{0,K_\alpha}^2.$$

Using (104), we deduce

$$\begin{aligned} \int_{K_\alpha} \boldsymbol{\Sigma}_h \mathbb{A}^{-1} \boldsymbol{\Sigma}_h \leq Ch^{2-d} \sum_{\Gamma_{\alpha,\beta} \subset \partial K_\alpha} \left(\left| \widehat{d}_{\alpha,\beta}(i_1) \right| + \left| \widehat{d}_{\alpha,\beta}(i_2) \right| \right)^2 \\ + Ch \sum_{\Gamma_{\alpha,\beta} \subset \partial K_\alpha} \int_{\Gamma_{\alpha,\beta}} |j_{\alpha,\beta}|^2 + Ch^2 \|f\|_{0,K_\alpha}^2. \end{aligned} \quad (108)$$

In order to bound the first term above, we are going to use (98). We recast that estimate as follows: for any vertex i and any triangles K_α and K_β in Ω_i , we have

$$\begin{aligned} & \left| \widehat{d}_{\alpha,\beta}(i) \right| \\ & \leq C \left[\sum_{n \in \Omega_i} \left| \int_{K_n} f \phi_i \right| + \sum_{n,m \in \Omega_i} |J_{n,m}(i)| \right] \\ & \leq C \sum_{n \in \Omega_i} \|f\|_{0,K_n} \|\phi_i\|_{0,K_n} + C \sum_{n,m \in \Omega_i} \|j_{n,m}\|_{0,\Gamma_{n,m}} \|\phi_i\|_{0,\Gamma_{n,m}} \\ & \leq C \sqrt{\sum_{n \in \Omega_i} \|f\|_{0,K_n}^2} \sqrt{\sum_{n \in \Omega_i} \|\phi_i\|_{0,K_n}^2} + C \sqrt{\sum_{n,m \in \Omega_i} \|j_{n,m}\|_{0,\Gamma_{n,m}}^2} \sqrt{\sum_{n,m \in \Omega_i} \|\phi_i\|_{0,\Gamma_{n,m}}^2} \\ & \leq Ch^{d/2} \|f\|_{0,\Omega_i} + Ch^{(d-1)/2} \sqrt{\sum_{n,m \in \Omega_i} \|j_{n,m}\|_{0,\Gamma_{n,m}}^2}. \end{aligned}$$

Inserting this estimate in (108) yields

$$\int_{K_\alpha} \boldsymbol{\Sigma}_h \mathbb{A}^{-1} \boldsymbol{\Sigma}_h \leq Ch^2 \sum_{i \in K_\alpha} \|f\|_{0,\Omega_i}^2 + Ch \sum_{i \in K_\alpha} \sum_{n,m \in \Omega_i} \|j_{n,m}\|_{0,\Gamma_{n,m}}^2. \quad (109)$$

Step 4. In this step, we bound $\|f\|_{0,K}$ from above by the error $u - u_h$. Let K be a triangle element with vertices i, j and k . We consider the test function $\tilde{v} \in V$ defined as $\tilde{v}(\mathbf{x}) = \phi_i(\mathbf{x}) \phi_j(\mathbf{x}) \phi_k(\mathbf{x})$ over K and $\tilde{v}(\mathbf{x}) = 0$ elsewhere (bubble function). Inserting this test function in (3), we get

$$\int_K \mathbb{A} \nabla u \cdot \nabla \tilde{v} = f_K \int_K \phi_i \phi_j \phi_k$$

with f_K the constant value of f in K (see Assumption (H4)). Using an integration by parts, we get

$$\int_K \mathbb{A} \nabla u_h \cdot \nabla \tilde{v} = \int_{\partial K} \tilde{v} \mathbb{A} \nabla u_h \cdot \mathbf{n}_K - \int_K \tilde{v} \operatorname{div}(\mathbb{A} \nabla u_h) = 0$$

where we have used that $\tilde{v}|_{\partial K} = 0$ (to cancel the first term) and Assumption (H1) (to cancel the second term). We deduce that

$$f_K \int_K \phi_i \phi_j \phi_k = \int_K \mathbb{A} \nabla(u - u_h) \cdot \nabla \tilde{v},$$

which implies that there is a constant $C > 0$ independent of h such that

$$Ch^d |f_K| \leq \|\mathbb{A}^{1/2} \nabla \tilde{v}\|_{0,K} \|\mathbb{A}^{1/2} \nabla(u - u_h)\|_{0,K}. \quad (110)$$

Since the three terms in $\nabla \tilde{v}$ are of the same order of magnitude and $\nabla \phi_i$ is constant in K , we get

$$\|\mathbb{A}^{1/2} \nabla \tilde{v}\|_{0,K}^2 \leq C \int_K |\nabla \phi_i|^2 \phi_j^2 \phi_k^2 \leq Ch^{-2} \int_K \phi_j^2 \phi_k^2 \leq Ch^{d-2}.$$

We deduce from (110) that

$$|f_K| \leq Ch^{-d/2-1} \|\mathbb{A}^{1/2} \nabla(u - u_h)\|_{0,K}$$

and thus

$$\|f\|_{0,K}^2 \leq Ch^d f_K^2 \leq Ch^{-2} \|\mathbb{A}^{1/2} \nabla(u - u_h)\|_{0,K}^2. \quad (111)$$

Step 5. In this step, we bound $\|j_{\alpha,\beta}\|_{0,\Gamma_{\alpha,\beta}}$ from above by the error $u - u_h$. We consider the edge $\Gamma_{\alpha,\beta}$, separating the triangles K_α and K_β , and denote i_1 and i_2 its vertices. We choose the test function \tilde{v} defined as $\tilde{v}(\mathbf{x}) = \phi_{i_1}(\mathbf{x}) \phi_{i_2}(\mathbf{x})$ over $K_\alpha \cup K_\beta$ and $\tilde{v}(\mathbf{x}) = 0$ elsewhere. Inserting this test function in (3), we get

$$\int_{K_\alpha \cup K_\beta} \mathbb{A} \nabla u \cdot \nabla \tilde{v} = \int_{K_\alpha \cup K_\beta} f \phi_{i_1} \phi_{i_2}.$$

Considering now the approximate solution u_h , we compute, using Assumption (H1), that

$$\begin{aligned} \int_{K_\alpha \cup K_\beta} \mathbb{A} \nabla u_h \cdot \nabla \tilde{v} &= \int_{K_\alpha} \mathbb{A} \nabla u_h \cdot \nabla \tilde{v} + \int_{K_\beta} \mathbb{A} \nabla u_h \cdot \nabla \tilde{v} \\ &= \int_{\partial K_\alpha} \mathbb{A} \nabla u_h|_{K_\alpha} \cdot \mathbf{n}_{K_\alpha} \tilde{v} - \int_{K_\alpha} \tilde{v} \operatorname{div}(\mathbb{A} \nabla u_h) \\ &\quad + \int_{\partial K_\beta} \mathbb{A} \nabla u_h|_{K_\beta} \cdot \mathbf{n}_{K_\beta} \tilde{v} - \int_{K_\beta} \tilde{v} \operatorname{div}(\mathbb{A} \nabla u_h) \\ &= \int_{\Gamma_{\alpha,\beta}} \mathbf{q}_h|_{K_\alpha} \cdot \mathbf{n}_{K_\alpha} \tilde{v} + \int_{\Gamma_{\alpha,\beta}} \mathbf{q}_h|_{K_\beta} \cdot \mathbf{n}_{K_\beta} \tilde{v} \\ &= 2 \int_{\Gamma_{\alpha,\beta}} j_{\alpha,\beta} \tilde{v}. \end{aligned}$$

Consequently,

$$\int_{K_\alpha \cup K_\beta} f \phi_{i_1} \phi_{i_2} - 2 \int_{\Gamma_{\alpha,\beta}} j_{\alpha,\beta} \tilde{v} = \int_{K_\alpha \cup K_\beta} \mathbb{A} \nabla(u - u_h) \cdot \nabla \tilde{v}.$$

The term $j_{\alpha,\beta}$ being constant on the edge $\Gamma_{\alpha,\beta}$ (see Assumption (H3)), there is a constant $C > 0$ independent of h such that

$$\begin{aligned} Ch^{d-1} |j_{\alpha,\beta}| &\leq \|\mathbb{A}^{1/2} \nabla \tilde{v}\|_{0,K_\alpha \cup K_\beta} \|\mathbb{A}^{1/2} \nabla(u - u_h)\|_{0,K_\alpha \cup K_\beta} \\ &\quad + \|f\|_{0,K_\alpha \cup K_\beta} \|\phi_{i_1} \phi_{i_2}\|_{0,K_\alpha \cup K_\beta}. \quad (112) \end{aligned}$$

Since the two terms in $\nabla\tilde{v}$ are of the same order of magnitude and $\nabla\phi_{i_1}$ is constant over each triangle, we get

$$\|\mathbb{A}^{1/2}\nabla\tilde{v}\|_{0,K_\alpha\cup K_\beta}^2 \leq C \int_{K_\alpha\cup K_\beta} |\nabla\phi_{i_1}|^2 \phi_{i_2}^2 \leq Ch^{-2} \int_{K_\alpha\cup K_\beta} \phi_{i_2}^2 \leq Ch^{d-2}.$$

Besides, we have $\|\phi_{i_1}\phi_{i_2}\|_{0,K_\alpha\cup K_\beta}^2 \leq Ch^d$. We hence deduce from (112) that

$$h^{d-1}|j_{\alpha,\beta}| \leq Ch^{d/2-1}\|\mathbb{A}^{1/2}\nabla(u-u_h)\|_{0,K_\alpha\cup K_\beta} + Ch^{d/2}\|f\|_{0,K_\alpha\cup K_\beta}, \quad (113)$$

and hence, using (111),

$$\begin{aligned} |j_{\alpha,\beta}| &\leq Ch^{-d/2}\|\mathbb{A}^{1/2}\nabla(u-u_h)\|_{0,K_\alpha\cup K_\beta} + Ch^{1-d/2}\|f\|_{0,K_\alpha\cup K_\beta} \\ &\leq Ch^{-d/2}\|\mathbb{A}^{1/2}\nabla(u-u_h)\|_{0,K_\alpha\cup K_\beta}. \end{aligned}$$

We therefore obtain

$$\|j_{\alpha,\beta}\|_{0,\Gamma_{\alpha,\beta}}^2 \leq Ch^{d-1}|j_{\alpha,\beta}|^2 \leq Ch^{-1}\|\mathbb{A}^{1/2}\nabla(u-u_h)\|_{0,K_\alpha\cup K_\beta}^2. \quad (114)$$

Step 6. Collecting (109), (111) and (114), we obtain

$$\begin{aligned} &\int_{K_\alpha} \Sigma_h \mathbb{A}^{-1} \Sigma_h \\ &\leq C \sum_{i \in K_\alpha} \|\mathbb{A}^{1/2}\nabla(u-u_h)\|_{0,\Omega_i}^2 + C \sum_{i \in K_\alpha} \sum_{n,m \in \Omega_i} \|\mathbb{A}^{1/2}\nabla(u-u_h)\|_{0,K_n \cup K_m}^2 \\ &\leq C \sum_{i \in K_\alpha} \|\mathbb{A}^{1/2}\nabla(u-u_h)\|_{0,\Omega_i}^2. \end{aligned}$$

Using the regularity of the mesh, we deduce that

$$E_{\text{CRE}}^2(u_h, \hat{\mathbf{q}}_h) = \int_{\Omega} \Sigma_h \mathbb{A}^{-1} \Sigma_h \leq C \|\mathbb{A}^{1/2}\nabla(u-u_h)\|_{0,\Omega}^2.$$

This concludes the proof of Theorem 35. \square

Corollary 36. *We work under the assumptions of Theorem 35, except Assumption (H4) (i.e. f constant in each triangle) which is replaced by $f \in H^1(\Omega)$. We then have*

$$E_{\text{CRE}}^2(u_h, \hat{\mathbf{q}}_h) \leq C \|\mathbb{A}^{1/2}\nabla(u-u_h)\|_{0,\Omega}^2 + Ch^4 \|\nabla f\|_{0,\Omega}^2. \quad (115)$$

Since we use P1 elements, we note that the first term in the right-hand side of (115) is of the order of $O(h^2)$. The second term, of the order of $O(h^4)$, is hence expected to be much smaller than the first term.

Proof. The first three steps of the proof of Theorem 35 again hold, and we thus have (see (109))

$$\int_{K_\alpha} \mathbf{\Sigma}_h \mathbb{A}^{-1} \mathbf{\Sigma}_h \leq Ch^2 \sum_{i \in K_\alpha} \|f\|_{0,\Omega_i}^2 + Ch \sum_{i \in K_\alpha} \sum_{n,m \in \Omega_i} \|j_{n,m}\|_{0,\Gamma_{n,m}}^2. \quad (116)$$

We now follow Step 4 of the proof of Theorem 35. Let K be a triangle element with vertices i, j and k . We consider the test function $\tilde{v} \in V$ defined as $\tilde{v}(\mathbf{x}) = f(\mathbf{x}) \phi_i(\mathbf{x}) \phi_j(\mathbf{x}) \phi_k(\mathbf{x})$ over K and $\tilde{v}(\mathbf{x}) = 0$ elsewhere. We have

$$\int_K f^2 \phi_i \phi_j \phi_k = \int_K \mathbb{A} \nabla(u - u_h) \cdot \nabla \tilde{v},$$

hence

$$\int_K f^2 \phi_i \phi_j \phi_k \leq \|\mathbb{A}^{1/2} \nabla \tilde{v}\|_{0,K} \|\mathbb{A}^{1/2} \nabla(u - u_h)\|_{0,K}.$$

Since we have

$$\|\mathbb{A}^{1/2} \nabla \tilde{v}\|_{0,K}^2 \leq C \int_K |\nabla \tilde{v}|^2 \leq C \left(h^{-2} \int_K f^2 + \int_K |\nabla f|^2 \right),$$

we obtain

$$\int_K f^2 \phi_i \phi_j \phi_k \leq C (h^{-1} \|f\|_{0,K} + \|\nabla f\|_{0,K}) \|\mathbb{A}^{1/2} \nabla(u - u_h)\|_{0,K}. \quad (117)$$

We now claim that there exists a constant C , independent of h and f , such that

$$\int_K f^2 \leq C \left(\int_K f^2 \phi_i \phi_j \phi_k + h^2 \int_K |\nabla f|^2 \right). \quad (118)$$

To prove (118), we first argue on the unit triangle \bar{K} . Consider a function $\bar{\theta} \in L^1(\bar{K})$ such that $\bar{\theta} \geq 0$ on \bar{K} and $\int_{\bar{K}} \bar{\theta} > 0$. Then there exists C such that, for any $g \in H^1(\bar{K})$, we have

$$\int_{\bar{K}} g^2 \leq C \left(\int_{\bar{K}} g^2 \bar{\theta} + \int_{\bar{K}} |\nabla g|^2 \right). \quad (119)$$

This can be shown using a contradiction argument. Then, by scaling, we deduce (118) from (119).

Collecting (118) and (117), we obtain

$$\|f\|_{0,K}^2 \leq Ch^2 \|\nabla f\|_{0,K}^2 + C (h^{-1} \|f\|_{0,K} + \|\nabla f\|_{0,K}) \|\mathbb{A}^{1/2} \nabla(u - u_h)\|_{0,K},$$

from which we infer that

$$\begin{aligned} \|f\|_{0,K}^2 &\leq Ch^{-2} \|\mathbb{A}^{1/2} \nabla(u - u_h)\|_{0,K}^2 + C \|\nabla f\|_{0,K} \|\mathbb{A}^{1/2} \nabla(u - u_h)\|_{0,K} \\ &\quad + Ch^2 \|\nabla f\|_{0,K}^2, \end{aligned}$$

and hence (compare with (111))

$$\|f\|_{0,K}^2 \leq Ch^{-2} \|\mathbb{A}^{1/2} \nabla(u - u_h)\|_{0,K}^2 + Ch^2 \|\nabla f\|_{0,K}^2. \quad (120)$$

Following Step 5 of the proof of Theorem 35, we obtain (113), which we write as

$$|j_{\alpha,\beta}| \leq Ch^{-d/2} \|\mathbb{A}^{1/2} \nabla(u - u_h)\|_{0,K_\alpha \cup K_\beta} + Ch^{1-d/2} \|f\|_{0,K_\alpha \cup K_\beta}.$$

Using (120), we get

$$|j_{\alpha,\beta}| \leq Ch^{-d/2} \|\mathbb{A}^{1/2} \nabla(u - u_h)\|_{0,K_\alpha \cup K_\beta} + Ch^{2-d/2} \|\nabla f\|_{0,K_\alpha \cup K_\beta},$$

and thus (compare with (114))

$$\begin{aligned} \|j_{\alpha,\beta}\|_{0,\Gamma_{\alpha,\beta}}^2 &\leq Ch^{d-1} |j_{\alpha,\beta}|^2 \\ &\leq Ch^{-1} \|\mathbb{A}^{1/2} \nabla(u - u_h)\|_{0,K_\alpha \cup K_\beta}^2 + Ch^3 \|\nabla f\|_{0,K_\alpha \cup K_\beta}^2. \end{aligned} \quad (121)$$

Collecting (116), (120) and (121), we obtain, as in Step 6 of the proof of Theorem 35, that

$$\int_{K_\alpha} \Sigma_h \mathbb{A}^{-1} \Sigma_h \leq C \sum_{i \in K_\alpha} \|\mathbb{A}^{1/2} \nabla(u - u_h)\|_{0,\Omega_i}^2 + Ch^4 \sum_{i \in K_\alpha} \|\nabla f\|_{0,\Omega_i}^2.$$

Using the regularity of the mesh, we deduce that

$$E_{\text{CRE}}^2(u_h, \hat{\mathbf{q}}_h) = \int_{\Omega} \Sigma_h \mathbb{A}^{-1} \Sigma_h \leq C \|\mathbb{A}^{1/2} \nabla(u - u_h)\|_{0,\Omega}^2 + Ch^4 \|\nabla f\|_{0,\Omega}^2.$$

This concludes the proof of Corollary 36. \square

Acknowledgments. The first author thanks Inria for enabling his two-year leave (2014–2016) in the MATERIALS project team. The work of the second author is partially supported by ONR under grant N00014-20-1-2691 and by EOARD under grant FA8655-20-1-7043. The second author acknowledges the continuous support from these two agencies. The authors would also like to thank Claude Le Bris for the fruitful discussions we had on the topics covered by this article.

References

- [1] Abdulle A., Bai Y. Adaptive reduced basis finite element heterogeneous multiscale method. *Computer Methods in Applied Mechanics and Engineering* 2013; **257**:203–220.
- [2] Abdulle A., Nonnenmacher A. A posteriori error analysis of the heterogeneous multiscale method for homogenization problems. *C.R. Acad. Sci. Paris, Série I* 2009; **347**:1081–1086.

- [3] Aggestam E., Larsson F., Runesson K., Ekre F. Numerical model reduction with error control in computational homogenization of transient heat flow. *Computer Methods in Applied Mechanics and Engineering* 2017; **326**:193–222.
- [4] Ainsworth M. A synthesis of a posteriori error estimation techniques for conforming, non-conforming and discontinuous Galerkin finite element methods. In *Recent Advances in Adaptive Computation*, Contemporary Mathematics, vol. 383, Z.-C. Shi, Z. Chen, T. Tang and D. Yu eds., AMS 2005, pp. 1–14.
- [5] Ainsworth M. Robust a posteriori error estimation for nonconforming finite element approximation. *SIAM Journal on Numerical Analysis* 2006; **42**(6):2320–2341.
- [6] Ainsworth M. A posteriori error estimation for discontinuous Galerkin finite element approximation. *SIAM Journal on Numerical Analysis* 2007; **45**(4):1777–1798.
- [7] Ainsworth M., Fu G. Fully computable a posteriori error bounds for hybridizable discontinuous Galerkin finite element approximations. *J. Sci. Comput.* 2018; **77**(1):443–466.
- [8] Ainsworth M., Oden J.T. A unified approach to a posteriori error estimation using element residual methods. *Numerische Mathematik* 1993; **65**:23–50.
- [9] Ainsworth M., Oden J.T. *A posteriori error estimation in finite element analysis*. John Wiley & Sons, 2000.
- [10] Ainsworth M., Rankin R. Guaranteed computable bounds on quantities of interest in finite element computations. *International Journal for Numerical Methods in Engineering* 2012; **89**(13):1605–1634.
- [11] Ainsworth M., Zhu J.Z., Craig A.W., Zienkiewicz O.C. Analysis of the Zienkiewicz-Zhu a posteriori error estimator in the finite element method. *International Journal for Numerical Methods in Engineering* 1989; **28**(9):2161–2174.
- [12] Allier P.-E., Chamoin L., Ladevèze P. Towards simplified and optimized a posteriori error estimation using PGD reduced models. *International Journal for Numerical Methods in Engineering* 2018; **113**(6):967–998.
- [13] Ammar A., Chinesta F., Díez P., Huerta A. An error estimator for separated representations of highly multidimensional models. *Computer Methods in Applied Mechanics and Engineering* 2010; **199**(25):1872–1880.
- [14] Arnold D.N., Brezzi F., Cockburn B., Marini L.D. Unified analysis of discontinuous Galerkin methods for elliptic problems. *SIAM Journal on Numerical Analysis* 2002; **39**(5):1749–1779.

- [15] Arnold D.N., Douglas J., Gupta C.P. A family of higher order mixed finite element methods for plane elasticity. *Numerische Mathematik* 1984; **45**(1):1–22.
- [16] Aubry D., Lucas D., Tie B. Adaptive strategy for transient/coupled problems – applications to thermoelasticity and elastodynamics. *Computer Methods in Applied Mechanics and Engineering* 1999; **176**:41–50.
- [17] Azziz K., Babuška I. *The mathematical foundations of the finite element method with applications to partial differential equations*. Academic Press, New-York, 1972.
- [18] Babuška I., Miller A. The post-processing approach in the finite element method – Part 1: Calculation of displacements, stresses and other higher derivatives of the displacements. *International Journal for Numerical Methods in Engineering* 1984; **20**:1085–1109.
- [19] Babuška I., Miller A. A feedback finite element method with a posteriori error estimation. Part 1: The finite element method and some basic properties of the a posteriori error estimator. *Computer Methods in Applied Mechanics and Engineering* 1987; **61**:1–40.
- [20] Babuška I., Oden J.T. The reliability of computer predictions: can they be trusted? *International Journal of Numerical Analysis and Modeling* 2005; **1**:1–18.
- [21] Babuška I., Rheinboldt W.C. Error estimates for adaptive finite element computations. *SIAM Journal on Numerical Analysis* 1978; **15**:736–754.
- [22] Babuška I., Rheinboldt W.C. Computational error estimates and adaptive processes for some nonlinear structural problems. *Computer Methods in Applied Mechanics and Engineering* 1982; **34**:895–937.
- [23] Babuška I., Schwab C. A posteriori error estimation for hierarchic models of elliptic boundary value problems on thin domains. *SIAM Journal on Numerical Analysis* 1996; **33**(1):221–246.
- [24] Babuška I., Strouboulis T. *The finite element method and its reliability*. Oxford University Press, 2001.
- [25] Babuška I., Strouboulis T., Upadhyay C.S., Gangaraj S.K. Computer-based proof of the existence of superconvergent points in the finite element method; superconvergence of the derivatives in finite element solutions of Laplace’s, Poisson’s and the elasticity equations. *Numerical Methods for Partial Differential Equations* 1996; **12**(3):347–392.
- [26] Babuška I., Strouboulis T., Upadhyay C.S., Gangaraj S.K., Copps K. Validation of a posteriori error estimators by numerical approach. *International Journal for Numerical Methods in Engineering* 1994; **37**(7):1073–1123.

- [27] Bank R.E., Smith K. A posteriori error estimates based on hierarchical bases. *SIAM Journal on Numerical Analysis* 1993; **30**:921–935.
- [28] Bank R.E., Weiser A. Some a posteriori error estimators for elliptic partial differential equations. *Mathematics of Computation* 1985; **44**:283–301.
- [29] Bathe K.J. *Finite element procedures*. Englewood Cliffs, NJ, Prentice Hall, 1996.
- [30] Bazilevs Y., Beirao da Veiga L., Cottrell J.A., Hughes T.J.R., Sangalli G. Isogeometric analysis: approximation, stability and error estimates for h-refined meshes. *Mathematical Models and Methods in Applied Sciences* 2006; **16**(7):1031–1090.
- [31] Becker R., Capatina D., Luce R. Local flux reconstruction for standard finite element method on triangular meshes. *SIAM Journal on Numerical Analysis* 2016; **54**(4):2684–2706.
- [32] Becker R., Hansbo P., Larson M.G. Energy norm a posteriori error estimation for discontinuous Galerkin methods. *Computer Methods in Applied Mechanics and Engineering* 2003; **192**(5-6):723–733.
- [33] Becker R., Rannacher R. A feed-back approach to error control in finite element methods: basic analysis and examples. *East-West Journal of Numerical Mathematics* 1996; **4**:237–264.
- [34] Becker R., Rannacher R. An optimal control approach to a posteriori error estimation in finite element methods. *Acta Numerica* 2001; **10**:1–102.
- [35] Beirao da Veiga L., Manzini G. Residual a posteriori error estimation for the virtual element method for elliptic problems. *ESAIM Mathematical Modelling and Numerical Analysis* 2015; **49**(2):577–599.
- [36] Ben Belgacem F., Bernardi C., Blouza A., Vohralik M. On the unilateral contact between membranes. Part 2: a posteriori analysis and numerical experiments. *IMA Journal of Numerical Analysis* 2012; **32**(3):1147–1172.
- [37] Bergam A., Bernardi C., Mghazli Z. A posteriori analysis of the finite element discretization of some parabolic equations. *Mathematics of Computation* 2005; **74**:1117–1138.
- [38] Bernardi C., Hecht F. Error indicators for the mortar finite element discretization of the Laplace equation. *Mathematics of Computation* 2002; **71**:1371–1402.
- [39] Bernardi C., Maday Y., Rapetti F. *Discrétisations variationnelles de problèmes aux limites elliptiques*. Mathématiques et Applications, vol. 45, Springer, 2004.

- [40] Bernardi C., Verfürth R. Adaptive finite element methods for elliptic equations with non-smooth coefficients. *Numerische Mathematik* 2000; **85**(4):579–608.
- [41] Berrone S., Borio A. A residual a posteriori error estimate for the virtual element method. *Mathematical Models and Methods in Applied Sciences* 2017; **27**(8):1423–1458.
- [42] Binev P., Dahmen W., Devore R. Adaptive finite element methods with convergence rates. *Numerische Mathematik* 2004; **97**(2):219–268.
- [43] Blacker T., Belytschko T. Superconvergent patch recovery with equilibrium and conjoint interpolant enhancements. *International Journal for Numerical Methods in Engineering* 1994; **37**(3):517–536.
- [44] Boffi D., Brezzi F., Fortin M. *Mixed Finite Element Methods and Applications*. Springer, Heidelberg, 2013.
- [45] Bonnet M., Frangi A., Rey C. *The finite element method in solid mechanics*. McGraw-Hill Education, 2014.
- [46] Boroomand B., Zienkiewicz O.C. Recovery by equilibrium in patches (REP). *International Journal for Numerical Methods in Engineering* 1997; **40**:137–164.
- [47] Braess D., Klaas O., Niekamp R., Stein E., Wobschal F. Error indicators for mixed finite elements in 2-dimensional linear elasticity. *Computer Methods in Applied Mechanics and Engineering* 1995; **127**:345–356.
- [48] Braess D., Schöberl J. Equilibrated residual error estimator for edge elements. *Mathematics of Computation* 2008; **77**:651–672.
- [49] Brenner S., Scott R. *The Mathematical Theory of Finite Element Methods*. Springer, New-York, 2008.
- [50] Brezzi F., Bristeau M.O., Franca L.P., Mallet M., Rogé G. A relationship between stabilized finite element methods and the Galerkin method with bubble functions. *Computer Methods in Applied Mechanics and Engineering* 1992; **96**(1):117–129.
- [51] Brink U., Stein E. A posteriori error estimation in large strain elasticity using equilibrated local Neumann problems. *Computer Methods in Applied Mechanics and Engineering* 1998; **161**(1-2):77–101.
- [52] Buffa A., Giannelli C. Adaptive isogeometric methods with hierarchical splines: error estimator and convergence. *Mathematical Models and Methods in Applied Sciences* 2016; **26**(1):1–25.
- [53] Butler T., Dawson C., Wildey T. A posteriori error analysis of stochastic differential equations using polynomial chaos expansions. *SIAM Journal on Scientific Computing* 2011; **33**(3):1267–1291.

- [54] Cai Z., He C., Zhang S. Improved ZZ a posteriori error estimators for diffusion problems: conforming linear elements. *Computer Methods in Applied Mechanics and Engineering* 2017; **313**:433–449.
- [55] Cai Z., Zhang S. Recovery-based error estimator for interface problems: conforming linear elements. *SIAM Journal on Numerical Analysis* 2009; **47**(3):2132–2156.
- [56] Cangiani A., Georgoulis E.H., Pryer T., Sutton O.J. A posteriori error estimates for the virtual element method. *Numerische Mathematik* 2017; **137**:857–893.
- [57] Canuto C., Hussaini M.Y., Quarteroni A., Zang, T.A. *Spectral methods*. Springer, 2006.
- [58] Cao T., Kelly D.W. Pointwise and local error estimates for the quantities of interest in two-dimensional elasticity. *Computers and Mathematics with Applications* 2003; **46**(1):69–79.
- [59] Carstensen C., Bartels S., Jansche S. A posteriori error estimates for nonconforming finite element methods. *Numerische Mathematik* 2002; **92**(2):233–256.
- [60] Carstensen C., Eigel M., Hoppe R.W.H., Lobhard C. A review of unified a posteriori finite element error control. *Numerical Mathematics: Theory, Methods and Applications* 2012; **5**:509–558.
- [61] Carstensen C., Funken S.A. Constants in Clément-interpolation error and residual based a posteriori error estimates in finite element methods. *East-West Journal of Numerical Mathematics* 2000; **8**(3):153–175.
- [62] Carstensen C., Funken S.A. Fully reliable localized error control in the FEM. *SIAM Journal on Scientific Computing* 2000; **4**(21):1465–1484.
- [63] Cascon J., Kreuzer C., Nochetto R.H., Siebert K.G. Quasi-optimal convergence rate for an adaptive finite element method. *SIAM Journal on Numerical Analysis* 2008; **46**:2524–2550.
- [64] Chamoin L., Allier P.-E., Marchand B. Synergies between the Constitutive Relation Error concept and PGD model reduction for simplified V&V procedures. *Advanced Modeling and Simulation in Engineering Sciences* 2016; **3**:18.
- [65] Chamoin L., Diez P. *Verification and validation for and with reduced order modeling*. Special issue of Advanced Modeling and Simulation in Engineering Sciences, 2015 (available at <https://www.springeropen.com/collections/vvrom>).
- [66] Chamoin L., Florentin E., Pavot S., Visseq V. Robust goal-oriented error estimation based on the constitutive relation error for stochastic problems. *Computers & Structures* 2012; **106-107**:189–195.

- [67] Chamoin L., Ladevèze P. A non-intrusive approach of goal-oriented error estimation for evolution problems solved by the finite element method. *Computer Methods in Applied Mechanics and Engineering* 2008; **197**(9-12):994–1014.
- [68] Chamoin L., Legoll F. A posteriori error estimation and adaptive strategy for the control of MsFEM computations. *Computer Methods in Applied Mechanics and Engineering* 2018; **336**:1–38.
- [69] Chamoin L., Legoll F. Goal-oriented error estimation and adaptivity in MsFEM computations. *Computational Mechanics* 2021; **67**(4):1201–1228.
- [70] Chamoin L., Pled F., Allier P.-E., Ladevèze P. A posteriori error estimation and adaptive strategy for PGD model reduction applied to parametrized linear parabolic problems. *Computer Methods in Applied Mechanics and Engineering* 2017; **327**:118–146.
- [71] Chamoin L., Thai H.P. Certified real-time shape optimization using isogeometric analysis, PGD model reduction, and a posteriori error estimation. *International Journal for Numerical Methods in Engineering* 2019; **119**:151–176.
- [72] Cheney E.W. *Introduction to approximation theory*. New York McGraw-Hill, 1966.
- [73] Choi H.-W., Paraschivoiu M. Adaptive computations of a posteriori finite element output bounds: a comparison of the “hybrid-flux” approach and the “flux-free” approach. *Computer Methods in Applied Mechanics and Engineering* 2004; **193**:4001–4033.
- [74] Chung E.T., Leung W.T., Pollock S. Goal-oriented adaptivity for GMS-FEM. *Journal of Computational and Applied Mathematics* 2016; **296**:625–637.
- [75] Ciarlet P.G. *The finite element method for elliptic problems*. North Holland, 1978.
- [76] Cirak F., Ramm E. A posteriori error estimation and adaptivity for linear elasticity using the reciprocal theorem. *Computer Methods in Applied Mechanics and Engineering* 1998; **156**:351–362.
- [77] Cirak F., Ramm E. A posteriori error estimation and adaptivity for elastoplasticity using the reciprocal theorem. *International Journal for Numerical Methods in Engineering* 2000; **47**:379–393.
- [78] Clément P. Approximation by finite element functions using local regularization. *RAIRO – Analyse Numérique* 1975; **9**(R2):77–84.
- [79] Combe J.-P., Ladevèze P., Pelle J.-P. Constitutive relation error estimator for transient finite element analysis. *Computer Methods in Applied Mechanics and Engineering* 1999; **176**:165–185.

- [80] Coorevits P., Hild P., Pelle J.-P. A posteriori error estimation for unilateral contact with matching and non-matching meshes. *Computer Methods in Applied Mechanics and Engineering* 2000; **186**:65–83.
- [81] Cottreau R., Díez P., Huerta A. Strict error bounds for linear solid mechanics problems using a subdomain-based flux-free method. *Computational Mechanics* 2009; **44**(4):533–547.
- [82] Dabaghi J., Martin V., Vohralik M. A posteriori estimates distinguishing the error components and adaptive stopping criteria for numerical approximations of parabolic variational inequalities. *Computer Methods in Applied Mechanics and Engineering* 2020; **367**:113105.
- [83] Dari E., Duran R., Padra C., Vampa V. A posteriori error estimators for nonconforming finite element methods. *ESAIM Mathematical Modelling and Numerical Analysis* 1996; **30**(4):385–400.
- [84] Debongnie J.F., Zhong H.G., Beckers P. Dual analysis with general boundary conditions. *Computer Methods in Applied Mechanics and Engineering* 1995; **122**:183–192.
- [85] Demkowicz L., Oden J.T., Strouboulis T. Adaptive finite elements for flow problems with moving boundaries. Part 1: Variational principles and a posteriori error estimates. *Computer Methods in Applied Mechanics and Engineering* 1984; **46**(2):217–251.
- [86] Destuynder P. A new strategy for improving a finite element method based on explicit error estimates. *Computer Methods in Applied Mechanics and Engineering* 1999; **176**:203–213.
- [87] Destuynder P., Métivet B. Explicit error bounds for a nonconforming finite element method. *SIAM Journal of Numerical Analysis* 1998; **35**(5):2099–2115.
- [88] Destuynder P., Métivet B. Explicit error bounds in a conforming finite element method. *Mathematics of Computation* 1999; **68**(288):1379–1396.
- [89] Díez P., Huerta A. A unified approach to remeshing strategies for finite element h -adaptivity. *Computer Methods in Applied Mechanics and Engineering* 1999; **176**(1-4):215–229.
- [90] Díez P., Parés N., Huerta A. Recovering lower bounds of the error by postprocessing implicit residual a posteriori error estimates. *International Journal for Numerical Methods in Engineering* 2003; **56**:1465–1488.
- [91] Díez P., Ródenas J.J., Zienkiewicz O.C. Equilibrated patch recovery error estimates: simple and accurate upper bounds of the error. *International Journal for Numerical Methods in Engineering* 2007; **69**(10):2075–2098.

- [92] Dorfel M., Juttler B., Simeon B. Adaptive isogeometric analysis by local h-refinement with T-splines. *Computer Methods in Applied Mechanics and Engineering* 2010; **199**(5-8):264–275.
- [93] Dorfler W. A convergent adaptive algorithm for Poisson’s equation. *SIAM Journal on Numerical Analysis* 1996; **33**:1106–1124.
- [94] Ekre F., Larsson F., Runesson K., Janicke R. A posteriori error estimation for numerical model reduction in computational homogenization of porous media. *International Journal for Numerical Methods in Engineering* 2020; **121**(23):5350–5380.
- [95] El Alaoui L., Ern A., Vohralik M. Guaranteed and robust a posteriori error estimates and balancing discretization and linearization errors for monotone nonlinear problems. *Computer Methods in Applied Mechanics and Engineering* 2011; **200**(37):2782–2795.
- [96] El Boustani C., Bleyer J., Arquier M., Ferradi M.K., Sab K. Dual finite-element analysis using second-order cone programming for structures including contact. *Engineering Structures* 2020; **208**:109892.
- [97] Eriksson K., Estep D., Hansbo P., Johnson C. Introduction to adaptive methods for differential equations. *Acta Numerica* 1995; **4**:105–158.
- [98] Ern A., Guermond J.-L. *Theory and practice of finite elements*. Applied Mathematical Sciences, Springer, vol. 159, 2004.
- [99] Ern A., Nicaise S., Vohralik M. An accurate H(div) flux reconstruction for discontinuous Galerkin approximations of elliptic problems. *C.R. Acad. Sci. Paris, Série I* 2007; **345**(12):709–712.
- [100] Ern A., Stephansen A.F., Vohralik M. Guaranteed and robust discontinuous Galerkin a posteriori error estimates for convection-diffusion-reaction problems. *Journal of Computational and Applied Mathematics* 2010; **234**(1):114–130.
- [101] Ern A., Vohralik M. A posteriori error estimation based on potential and flux reconstruction for the heat equation. *SIAM Journal on Numerical Analysis* 2010; **345**(48):198–223.
- [102] Ern A., Vohralik M. Adaptive inexact Newton methods with a posteriori stopping criteria for nonlinear diffusion PDEs. *SIAM Journal on Scientific Computing* 2013; **35**(4):1761–1791.
- [103] Ern A., Vohralik M. Polynomial-degree-robust a posteriori estimates in a unified setting for conforming, nonconforming, discontinuous Galerkin, and mixed discretizations. *SIAM Journal on Numerical Analysis* 2015; **53**(2):1058–1081.

- [104] Estep D., Holst M., Larson M. Generalized Green's functions and the effective domain of influence. *SIAM Journal on Scientific Computing* 2005; **26**:1314–1339.
- [105] Florentin E., Gallimard L., Pelle J.-P. Evaluation of the local quality of stresses in 3d finite element analysis. *Computer Methods in Applied Mechanics and Engineering* 2002; **191**:4441–4457.
- [106] Fourment L., Chenot J.-L. Error estimators for viscoplastic materials: application to forming processes. *International Journal for Numerical Methods in Engineering* 1995; **12**(5):469–490.
- [107] Fraeijns de Veubeke B. Displacement and equilibrium models in the finite element method. *International Journal for Numerical Methods in Engineering, Classical Reprint Series* 2001; **52**(3):287–342.
- [108] Franca L.P., Frey S.L., Hughes T.J.R. Stabilized finite element methods. I. Application to the advective-diffusive model. *Computer Methods in Applied Mechanics and Engineering* 1992; **95**(2):253–276.
- [109] Fuenmayor F.J., Oliver J.L. Criteria to achieve nearly optimal meshes in the h -adaptive finite element method. *International Journal for Numerical Methods in Engineering* 1996; **39**(23):4039–4061.
- [110] Gallimard L. A constitutive relation error estimator based on traction-free recovery of the equilibrated stress. *International Journal for Numerical Methods in Engineering* 2009; **78**(4):460–482.
- [111] Gallimard L., Ladevèze P., Pelle J.-P. Error estimation and adaptivity in elastoplasticity. *International Journal for Numerical Methods in Engineering* 1996; **39**:189–217.
- [112] Gallimard L., Panetier J. Error estimation of stress intensity factors for mixed-mode cracks. *International Journal for Numerical Methods in Engineering* 2006; **68**(3):299–316.
- [113] Gerasimov T., Rüter M., Stein E. An explicit residual-type error estimator for Q1-quadrilateral extended finite element method in two-dimensional linear elastic fracture mechanics. *International Journal for Numerical Methods in Engineering* 2012; **90**:1118–1155.
- [114] Ghorashi S.S., Rabczuk T. Goal-oriented error estimation and mesh adaptivity in 3D elastoplasticity problems. *International Journal of Fracture* 2017; **203**:3–19.
- [115] Giles M.B., Süli E. Adjoint methods for PDEs: a posteriori error analysis and postprocessing by duality. *Acta Numerica* 2002; **11**:145–236.
- [116] Grätsch T., Bathe K.-J. A posteriori error estimation techniques in practical finite element analysis. *Computers and Structures* 2005; **83**:235–265.

- [117] Grätsch T., Hartmann F. Finite element recovery techniques for local quantities of linear problems using fundamental solutions. *Computational Mechanics* 2003; **33**:15–21.
- [118] Grepl M.A., Patera A.T. A posteriori error bounds for reduced-basis approximation of parametrized parabolic partial differential equations. *ESAIM Mathematical Modelling and Numerical Analysis* 2005; **39**(1):157–181.
- [119] Haberl A., Praetorius D., Schimanko S., Vohralik M. Convergence and quasi-optimal cost of adaptive algorithms for nonlinear operators including iterative linearization and algebraic solver. *Numerische Mathematik* 2021; **147**(3):679–725.
- [120] Henning P., Ohlberger M., Schweizer B. An adaptive multiscale finite element method. *SIAM Multiscale Modeling & Simulation* 2014; **12**(3):1078–1107.
- [121] Hoang K.C., Kim T.Y., Song J.H. Fast and accurate two-field reduced basis approximation for parametrized thermoelasticity problems. *Finite Elements in Analysis and Design* 2018; **141**:96–118.
- [122] Huerta A., Diez P. Error estimation including pollution assessment for nonlinear finite element analysis. *Computer Methods in Applied Mechanics and Engineering* 2000; **181**:21–41.
- [123] Hughes T.J.R. Multiscale phenomena: Green’s functions, the Dirichlet-to-Neumann formulation, subgrid scale models, bubbles and the origins of stabilized methods. *Computer Methods in Applied Mechanics and Engineering* 1995; **127**(1):387–401.
- [124] Jhurani C., Demkowicz L. Multiscale modeling using goal-oriented adaptivity and numerical homogenization. Part 1: Mathematical formulation and numerical results *Computer Methods in Applied Mechanics and Engineering* 2012; **213-216**:399–417.
- [125] Jiranek P., Strakos Z., Vohralik M. A posteriori error estimates including algebraic error and stopping criteria for iterative solvers. *SIAM Journal on Scientific Computing* 2010; **32**(3):1567–1590.
- [126] John V. A numerical study of a posteriori error estimators for convection-diffusion equations. *Computer Methods in Applied Mechanics and Engineering* 2000; **190**:757–781.
- [127] Johnson C., Hansbo P. Adaptive finite element methods in computational mechanics. *Computer Methods in Applied Mechanics and Engineering* 1992; **101**(1-3):143–181.
- [128] Joly, P. *Mise en oeuvre de la méthode des éléments finis*. SMAI, Mathématiques et Applications, Ellipses, Paris, 1990.

- [129] Kanschat G., Suttmeier F.T. A posteriori error estimates for nonconforming finite element schemes. *Calcolo* 1999; **36**(3):129–141.
- [130] Kelly D.W., Gago O.C., Zienkiewicz O.C., Babuška I. A posteriori error analysis and adaptive processes in the finite element method: Part I: error analysis. *International Journal for Numerical Methods in Engineering* 1983; **19**:1593–1619.
- [131] Kempeneers M., Debongnie J.F., Beckers P. Pure equilibrium tetrahedral finite elements for global error estimation by dual analysis. *International Journal for Numerical Methods in Engineering* 2009; **81**(4):513–536.
- [132] Kerfriden P., Rodenas J.J., Bordas S.P.A. Certification of projection-based reduced order modelling in computational homogenization by the constitutive relation error. *International Journal for Numerical Methods in Engineering* 2014; **97**:395–422.
- [133] Kleiss S.K., Tomar S.K. Guaranteed and sharp a posteriori error estimates in isogeometric analysis. *Computers and Mathematics with Applications* 2015; **70**(3):167–190.
- [134] Kumar M., Kvamsdal T., Johannessen K.A., Superconvergent patch recovery and a posteriori error estimation technique in adaptive isogeometric analysis. *Computer Methods in Applied Mechanics and Engineering* 2017; **316**:1086–1156.
- [135] Kuru G., Verhoosel C.V., Van der Zee K., Van Brummelen E.H. Goal-adaptive isogeometric analysis with hierarchical splines. *Computer Methods in Applied Mechanics and Engineering* 2014; **270**:270–292.
- [136] Kvamsdal T., Okstad K.M. Error estimation based on superconvergent patch recovery using statically admissible stress fields. *International Journal for Numerical Methods in Engineering* 1998; **42**(3):443–472.
- [137] Ladevèze P. Constitutive error estimators for time-dependent non-linear FE analysis. *Computer Methods in Applied Mechanics and Engineering* 2000; **188**(4):775–788.
- [138] Ladevèze P. Constitutive relation error estimations for finite element analyses considering (visco)-plasticity and damage. *International Journal for Numerical Methods in Engineering* 2001; **52**(5-6):527–542.
- [139] Ladevèze P. Strict upper error bounds for computed outputs of interest in computational structural mechanics. *Computational Mechanics* 2008; **42**(2):271–286.
- [140] Ladevèze P., Blaysat B., Florentin E. Strict upper bounds of the error in calculated outputs of interest for plasticity problems. *Computer Methods in Applied Mechanics and Engineering* 2012; **245-246**:194–205.

- [141] Ladevèze P., Chamoin L. Calculation of strict error bounds for finite element approximations of nonlinear pointwise quantities of interest. *International Journal for Numerical Methods in Engineering* 2010; **84**:1638–1664.
- [142] Ladevèze P., Chamoin L. On the verification of model reduction methods based on the Proper Generalized Decomposition. *Computer Methods in Applied Mechanics and Engineering* 2011; **200**:2032–2047.
- [143] Ladevèze P., Chamoin L., Florentin E. A new non-intrusive technique for the construction of admissible stress fields in model verification. *Computer Methods in Applied Mechanics and Engineering* 2010; **199**(9-12):766–777.
- [144] Ladevèze P., Florentin E. Verification of stochastic models in uncertain environments using the constitutive relation error method. *Computer Methods in Applied Mechanics and Engineering* 2006; **196**:225–234.
- [145] Ladevèze P., Leguillon D. Error estimate procedure in the finite element method and application. *SIAM Journal of Numerical Analysis* 1983; **20**(3):485–509.
- [146] Ladevèze P., Maunder E.A.W. A general method for recovering equilibrating element tractions. *Computer Methods in Applied Mechanics and Engineering* 1996; **137**:111–151.
- [147] Ladevèze P., Moës N. A new a posteriori error estimation for nonlinear time-dependent finite element analysis. *Computer Methods in Applied Mechanics and Engineering* 1998; **157**:45–68.
- [148] Ladevèze P., Moës N., Douchin B. Constitutive relation error estimators for (visco)plastic finite element analysis with softening. *Computer Methods in Applied Mechanics and Engineering* 1999; **176**:247–264.
- [149] Ladevèze P., Pelle J.-P. Accuracy in finite element computation for eigenfrequencies. *International Journal for Numerical Methods in Engineering* 1989; **28**:1929–1949.
- [150] Ladevèze P., Pelle J.-P. *Mastering calculations in linear and nonlinear mechanics*. Springer NY, 2004.
- [151] Ladevèze P., Pled F., Chamoin L. New bounding techniques for goal-oriented error estimation applied to linear problems. *International Journal for Numerical Methods in Engineering* 2013; **93**(13):1345–1380.
- [152] Ladevèze P., Rougeot P. New advances on a posteriori error on constitutive relation in finite element analysis. *Computer Methods in Applied Mechanics and Engineering* 1997; **150**:239–249.
- [153] Ladevèze P., Rougeot P., Blanchard P., Moreau J.P. Local error estimators for finite element linear analysis. *Computer Methods in Applied Mechanics and Engineering* 1999; **176**:231–246.

- [154] Larson M.G., Malqvist A. Adaptive variational multiscale methods based on a posteriori error estimation: energy norm estimates for elliptic problems *Computer Methods in Applied Mechanics and Engineering* 2007; **196**(21-24):2313–2314.
- [155] Larsson F., Hansbo P., Runesson K. Strategies for computing goal-oriented a posteriori error measures in nonlinear elasticity. *International Journal for Numerical Methods in Engineering* 2002; **55**:879–894.
- [156] Larsson F., Runesson K., Hansbo P. Time finite elements and error computation for (visco) plasticity with hardening or softening. *International Journal for Numerical Methods in Engineering* 2003; **56**:2213–2231.
- [157] Le Bris C., Legoll F., Lozinski A. MsFEM à la Crouzeix-Raviart for highly oscillatory elliptic problems. *Chinese Annals of Mathematics, Series B* 2013; **34**(1):113–138.
- [158] Lee T., Park H.C., Lee S.W. A superconvergent stress recovery technique with equilibrium constraint. *International Journal for Numerical Methods in Engineering* 1997; **40**(6):1139–1160.
- [159] Louf F., Combe J.-P., Pelle J.-P. Constitutive error estimator for the control of contact problems involving friction. *Computers and Structures* 2003; **81**(18-19):1759–1772.
- [160] Luce R., Wohlmuth B.I. A local a posteriori error estimator based on equilibrated fluxes. *SIAM Journal on Numerical Analysis* 2005; **42**(4):1394–1414.
- [161] Lucquin B., Pironneau O. *Introduction au calcul scientifique*. Masson, Paris, 1997.
- [162] Mac D.H., Tang Z., Clénet S., Creusé E. Residual-based a posteriori error estimation for stochastic magnetostatic problems. *Journal of Computational and Applied Mathematics* 2015; **289**:51–67.
- [163] Machiels L., Maday Y., Patera A.T. A “flux-free” nodal Neumann sub-problem approach to output bounds for partial differential equations. *C.R. Acad. Sci. Paris, Série I* 2000; **300**(1):249–254.
- [164] Machiels L., Maday Y., Patera A.T. Output bounds for reduced-order approximations of elliptic partial differential equations. *Computer Methods in Applied Mechanics and Engineering* 2001; **190**(9-12):3413–3426.
- [165] Maday Y., Patera A.T., Peraire J. A general formulation for a posteriori bounds for output functional of partial differential equations. *C.R. Acad. Sci. Paris, Série I* 1999; **328**:823–828.

- [166] Mallik G., Vohralik M., Yousef S. Goal-oriented a posteriori error estimation for conforming and nonconforming approximations with inexact solvers. *Journal of Computational and Applied Mathematics* 2020; **366**:112367.
- [167] Moitinho de Almeida J.P., Maunder E.A.W. Recovery of equilibrium on star patches using a partition of unity technique. *International Journal for Numerical Methods in Engineering* 2009; **79**:1493–1516.
- [168] Moitinho de Almeida J.P., Maunder E.A.W. *Equilibrium finite element formulations*. Wiley, 2017.
- [169] Mommer M., Stevenson R. A goal-oriented adaptive finite element method with convergence rates. *SIAM Journal on Numerical Analysis* 2009; **47**(2):861–886.
- [170] Morin P., Nochetto R.H., Siebert K.G. Convergence of adaptive finite element methods. *SIAM Review* 2002; **44**(4):631–658.
- [171] Morin P., Nochetto R.H., Siebert K.G. Local problems on stars: a posteriori error estimators, convergence, and performance. *Mathematics of Computation* 2003; **72**:1067–1097.
- [172] Mozolevski I., Prudhomme S. Goal-oriented error estimation based on equilibrated-flux reconstruction for finite element approximations of elliptic problems. *Computer Methods in Applied Mechanics and Engineering* 2015; **288**:127–145.
- [173] Nicaise S., Witowski K., Wohlmuth B.I. An a posteriori error estimator for the Lamé equation based on equilibrated fluxes. *IMA Journal of Numerical Analysis* 2008; **28**(2):331–353.
- [174] Oden J.T., Babuška I., Nobile F., Feng Y., Tempone R. Theory and methodology for estimation and control of error due to modeling, approximation, and uncertainty. *Computer Methods in Applied Mechanics and Engineering* 2005; **194**:195–204.
- [175] Oden J.T., Prudhomme S. Goal-oriented error estimation and adaptivity for the finite element method. *Computers and Mathematics with Applications* 2001; **41**:735–756.
- [176] Oden J.T., Prudhomme S. Estimation of Modeling Error in Computational Mechanics. *Journal of Computational Physics* 2002; **182**:496–515.
- [177] Oden J.T., Prudhomme S., Westermann T., Bass J., Botkin M. Error estimation of eigenfrequencies for elasticity and shell problems. *Mathematical Models and Methods in Applied Sciences* 2003; **13**:323–344.

- [178] Ohnibus S., Stein E., Walhorn E. Local error estimates of FEM for displacements and stresses in linear elasticity by solving local Neumann problems. *International Journal for Numerical Methods in Engineering* 2001; **52**:727–746.
- [179] Onate E., Bugeda G. A study of mesh optimality criteria in adaptive finite element analysis. *Engineering Computations* 1993; **10**:307–321.
- [180] Panetier J., Ladevèze P., Chamoin L. Strict and effective bounds in goal-oriented error estimation applied to fracture mechanics problems solved with the XFEM. *International Journal for Numerical Methods in Engineering* 2010; **81**(6):671–700.
- [181] Paraschivoiu M., Peraire J., Patera A.T. A posteriori finite element bounds for linear functional outputs of elliptic partial differential equations. *Computer Methods in Applied Mechanics and Engineering* 1997; **150**:289–312.
- [182] Parés N., Bonet J., Huerta A., Peraire J. The computation of bounds for linear-functional outputs of weak solutions to the two-dimensional elasticity equations. *Computer Methods in Applied Mechanics and Engineering* 2006; **195**(4-6):406–429.
- [183] Parés N., Díez P. A new equilibrated residual method improving accuracy and efficiency of flux-free error estimates. *Computer Methods in Applied Mechanics and Engineering* 2017; **313**:785–816.
- [184] Parés N., Díez P., Huerta A. Subdomain-based flux-free a posteriori error estimators. *Computer Methods in Applied Mechanics and Engineering* 2006; **195**:297–323.
- [185] Parés N., Díez P., Huerta A. Exact bounds for linear outputs of the advection-diffusion-reaction equation using flux-free error estimates. *SIAM Journal on Scientific Computing* 2009; **31**(4):3064–3089.
- [186] Parés N., Díez P., Huerta A. Computable exact bounds for linear outputs from stabilized solutions of the advection-diffusion-reaction equation. *International Journal for Numerical Methods in Engineering* 2013; **93**(5):483–509.
- [187] Parés N., Santos H., Díez P. Guaranteed energy error bounds for the Poisson equation using a flux-free approach: solving the local problems in subdomains. *International Journal for Numerical Methods in Engineering* 2009; **79**:1203–1244.
- [188] Parret-Fréaud A., Rey C., Gosselet P., Feyel F. Fast estimation of discretization error for FE problems solved by domain decomposition. *Computer Methods in Applied Mechanics and Engineering* 2010; **199**(49-52):3315–3323.

- [189] Pelle J.-P., Ryckelynck D. An efficient adaptive strategy to master the global quality of viscoplastic analysis. *Computers & Structures* 2000; **78**(1-3):169–184.
- [190] Peraire J., Patera A.T. Bounds for linear-functional outputs of coercive partial differential equations; local indicators and adaptive refinements. *Advances in Adaptive Computational Methods in Mechanics*, P. Ladevèze and J.T. Oden eds., Elsevier 1998, pp. 199–216.
- [191] Peric D., Yu J., Owen D.R.J. On error estimates and adaptivity in elastoplastic solids: Application to the numerical simulation of strain localization in classical and Cosserat continua. *International Journal for Numerical Methods in Engineering* 1994; **37**:1351–1379.
- [192] Pijaudier-Cabot G., Bode L., Huerta A. Arbitrary Lagrangian-Eulerian finite element analysis of strain localization in transient problems. *International Journal for Numerical Methods in Engineering* 1995; **38**(24):4171–4191.
- [193] Pled F., Chamoin L., Ladevèze P. On the techniques for constructing admissible stress fields in model verification: performances on engineering examples. *International Journal for Numerical Methods in Engineering* 2011; **88**(5):409–441.
- [194] Pled F., Chamoin L., Ladevèze P. An enhanced method with local energy minimization for the robust a posteriori construction of equilibrated stress fields in finite element analyses. *Computational Mechanics* 2012; **49**:357–378.
- [195] Porsching T.A. Estimation of the error in the reduced basis method solution of nonlinear equations. *Mathematics of Computation* 1985; **45**:487–496.
- [196] Prudhomme S., Nobile F., Chamoin L., Oden J.T. Analysis of a subdomain-based error estimator for finite element approximations of elliptic problems. *Numerical Methods for Partial Differential Equations* 2004; **20**(2):165–192.
- [197] Prudhomme S., Oden J.T. On goal-oriented error estimation for elliptic problems: application to the control of pointwise errors. *Computer Methods in Applied Mechanics and Engineering* 1999; **176**:313–331.
- [198] Prud’homme C., Rovas D., Veroy K., Maday Y., Patera A.T., Turinici G. Reliable real-time solution of parametrized partial differential equations: reduced-basis output bound methods. *Journal of Fluids Engineering* 2002; **124**(1):70–80.
- [199] Quarteroni A., Rozza G., Manzoni A. Certified reduced basis approximation for parametrized partial differential equations and applications. *Journal of Mathematics in Industry* 2011; **1-3**:1–44.

- [200] Quarteroni A., Valli A. *Numerical Approximation of Partial Differential Equations*. Springer, Berlin, 1994.
- [201] Radovitzky R., Ortiz M. Error estimation and adaptive meshing in strongly nonlinear dynamics problems. *Computer Methods in Applied Mechanics and Engineering* 1999; **172**:203–240.
- [202] Rannacher R., Suttmeier F.T. A feedback approach to error control in finite element methods: application to linear elasticity. *Computational Mechanics* 1997; **19**:434–446.
- [203] Rannacher R., Suttmeier F.T. A posteriori error estimation and mesh adaptation for finite element models in elasto-plasticity. *Computer Methods in Applied Mechanics and Engineering* 1999; **176**:333–361.
- [204] Rappaz M., Bellet M., Deville M. *Modélisation numérique en science et génie des matériaux*. Traité des matériaux, vol. 10, Presses Polytechniques et Universitaires Romandes, 1999.
- [205] Raviart P.-A., Thomas J.-M. *Introduction à l'analyse numérique des équations aux dérivées partielles*. Masson, Paris, 1983.
- [206] Reis J., Moitinho de Almeida J.P., Diez P., Zlotnik S. Error estimation for PGD solutions: a dual approach. *International Journal for Numerical Methods in Engineering* 2020; **121**(23):5275–5294.
- [207] Repin S.I. A posteriori error estimates for approximate solutions to variational problems with strongly convex functionals. *Journal of Mathematical Sciences* 1999; **97**:4311–4328.
- [208] Rey V., Rey C., Gosselet P. A strict error bound with separated contributions of the discretization and of the iterative solver in non-overlapping domain decomposition methods. *Computer Methods in Applied Mechanics and Engineering* 2014; **270**:293–303.
- [209] Rivière B., Wheeler M.F. A posteriori error estimates for a discontinuous Galerkin method applied to elliptic problems. *Computers and Mathematics with Applications* 2003; **46**(1):141–163.
- [210] Ródenas J.J., Gonzales-Estrada O.A., Tarancon J.E., Fuenmayor F.J. A recovery-type error estimator for the extended finite element method based on singular+smooth stress field splitting. *International Journal for Numerical Methods in Engineering* 2008; **76**(4):545–571.
- [211] Ródenas J.J., Tur M., Fuenmayor F.J., Vercher A. Improvement of the superconvergent patch recovery technique by the use of constraint equations: the SPR-C technique. *International Journal for Numerical Methods in Engineering* 2007; **70**(6):705–727.

- [212] Rovas D.V., Machiels L., Maday Y. Reduced-basis output bound methods for parabolic problems. *IMA Journal of Numerical Analysis* 2006; **26**(3):423–445.
- [213] Rozza G., Huynh D.B.P., Patera A.T. Reduced basis approximation and a posteriori error estimation for affinely parametrized elliptic coercive partial differential equations. *Archives of Computational Methods in Engineering* 2008; **15**:229–275.
- [214] Ruter M., Stein E. Goal-oriented a posteriori error estimates in linear elastic fracture mechanics. *Computer Methods in Applied Mechanics and Engineering* 2006; **195**:251–278.
- [215] Sauer-Budge A.M., Bonet J., Huerta A., Peraire J. Computing bounds for linear functionals of exact weak solutions to Poisson’s equation. *SIAM Journal of Numerical Analysis* 2004; **42**(4):1610–1630.
- [216] Sauer-Budge A.M., Peraire J. Computing bounds for linear functionals of exact weak solutions to the advection-diffusion-reaction equation. *SIAM Journal of Scientific Computing* 2006; **26**(2):636–652.
- [217] Scarabosio L., Wohlmuth B., Oden J.T., Faghihi D. Goal-Oriented Adaptive Modeling of Random Heterogeneous Media and Model-Based Multi-level Monte Carlo Methods. *Computers & Mathematics with Applications* 2019; **78**(8):2700–2718.
- [218] Scott L.R., Zhang S. Finite element interpolation of non-smooth functions satisfying boundary conditions. *Mathematics of Computation* 1990; **54**:483–493.
- [219] Segeth K. A review of some a posteriori error estimates for adaptive finite element methods. *Mathematics and Computers in Simulation* 2010; **80**:1589–600.
- [220] Stein E. *Error controlled adaptive finite elements in solid mechanics*. J. Wiley, 2003.
- [221] Stevenson R. Optimality of a standard adaptive finite element method. *Foundations of Computational Mathematics* 2007; **7**:245–269.
- [222] Stewart J.R., Hughes T.J.R. A tutorial in elementary finite element error analysis: a systematic presentation of a priori and a posteriori error estimates. *Computer Methods in Applied Mechanics and Engineering* 1998; **158**:1–22.
- [223] Stone T.J., Babuska I. A numerical method with a posteriori error estimation for determining the path taken by a propagating crack. *Computer Methods in Applied Mechanics and Engineering* 1998; **160**:245–271.

- [224] Strang W.G., Fix G.J. *An analysis of the finite element method*. Wellesley Cambridge Press, 1973.
- [225] Strouboulis T., Babuška I., Datta D., Copps K., Gangaraj S. A posteriori estimation and adaptive control of the error in the quantity of interest – part I: a posteriori estimation of the error in the von Mises stress and the stress intensity factor. *Computer Methods in Applied Mechanics and Engineering* 2000; **181**(1-3):261–294.
- [226] Strouboulis T., Haque K.A. Recent experiences with error estimation and adaptivity, Part I: review of error estimators for scalar elliptic problems. *Computer Methods in Applied Mechanics and Engineering* 1992; **97**(3):399–436.
- [227] Strouboulis T., Zhang L., Wang D., Babuška I. A posteriori error estimation for generalized finite element methods. *Computer Methods in Applied Mechanics and Engineering* 2006; **195**:852–879.
- [228] Stynes M. Steady-state convection-diffusion problems. *Acta Numerica* 2005; **14**(1):445–508.
- [229] Thai H.P., Chamoin L., Ha Minh C. A posteriori error estimation for isogeometric analysis using the concept of constitutive relation error. *Computer Methods in Applied Mechanics and Engineering* 2019; **355**:1062–1096.
- [230] Tirvaudey M., Chamoin L., Bouclier R., Passieux J.C. A posteriori error estimation and adaptivity in non-intrusive couplings between concurrent models. *Computer Methods in Applied Mechanics and Engineering* 2020; **367**:113104.
- [231] Ubertini F. Patch recovery based on complementary energy. *International Journal for Numerical Methods in Engineering* 2004; **59**(11):1501–1538.
- [232] Verdugo F., Diez P. Computable bounds of functional outputs in linear visco-elastodynamics. *Computer Methods in Applied Mechanics and Engineering* 2012; **245-246**:313–330.
- [233] Verfürth R. A posteriori error estimation and adaptive mesh-refinement techniques. *Journal of Computational and Applied Mathematics* 1994; **50**:67–83.
- [234] Verfürth R. *A review of a posteriori error estimates and adaptive mesh-refinement techniques*. Wiley-Teubner, 1996.
- [235] Verfürth R. *A posteriori error estimation techniques for finite element methods*. Numerical Mathematics and Scientific Computation, Oxford University Press, Oxford, 2013.
- [236] Vohralik M. A posteriori error estimates for lowest-order mixed finite element discretizations of convection-diffusion-reaction equations. *SIAM Journal on Numerical Analysis* 2007; **45**:1570–1599.

- [237] Vohralik M. A posteriori error estimation in the conforming finite element method based on its local conservativity and using local minimization. *Comptes Rendus Mathématique* 2008; **346**(11-12):687–690.
- [238] Vohralik M. Guaranteed and fully robust a posteriori error estimates for conforming discretizations of diffusion problems with discontinuous coefficients. *Journal of Scientific Computing* 2011; **46**:397–438.
- [239] Vohralik M., Wheeler M.F. A posteriori error estimates, stopping criteria, and adaptivity for two-phase flows. *Computers & Geosciences* 2013; **17**:789–812.
- [240] Waeytens J., Chamoin L., Ladevèze P. Guaranteed error bounds on pointwise quantities of interest for transient viscodynamics problems. *Computational Mechanics* 2012; **49**:291–307.
- [241] Wang L., Chamoin L., Ladevèze P., Zhong H. Computable guaranteed bounds of eigenfrequencies. *Computer Methods in Applied Mechanics and Engineering* 2016; **302**:27–43.
- [242] Weiss A., Wohlmuth B.I. A posteriori error estimator and error control for contact problems. *Mathematica of Computation* 2009; **78**(267):1237–1267.
- [243] Wheeler M.F., Whiteman J.R. Superconvergent recovery of gradients on subdomains from piecewise linear finite element approximations. *Numerical Methods for Partial Differential Equations* 1987; **3**:357–374.
- [244] Wiberg N.E., Abdulwahab F. Error estimation with postprocessed finite element solutions. *Computers & Structures* 1997; **64**(1-4):113–137.
- [245] Wiberg N.E., Abdulwahab F., Ziukas S. Enhanced superconvergent patch recovery incorporating equilibrium and boundary conditions. *International Journal for Numerical Methods in Engineering* 1994; **37**:3417–3440.
- [246] Wiberg N.E., Zeng L., Li X. Error estimation and adaptivity in elastodynamics. *Computer Methods in Applied Mechanics and Engineering* 1992; **101**(1-3):369–395.
- [247] Xuan Z.C., Parés N., Peraire J. Computing upper and lower bounds of the J-integral in two-dimensional linear elasticity. *Computer Methods in Applied Mechanics and Engineering* 2006; **195**(4-6):430–443.
- [248] Zhang Z., Naga A. A new finite element gradient recovery method: superconvergence property. *SIAM Journal on Scientific Computing* 2005; **26**(4):1192–1213.
- [249] Zhang Z., Zhu J.Z. Analysis of the superconvergent patch recovery technique and a posteriori error estimator in the finite element method. *Computer Methods in Applied Mechanics and Engineering* 1995; **163**(1-4):159–170.

- [250] Zienkiewicz O.C., Zhu J.Z. A simple error estimator and adaptive procedure for practical engineering analysis. *International Journal for Numerical Methods in Engineering* 1987; **24**:337–357.
- [251] Zienkiewicz O.C., Zhu J.Z. The superconvergent patch recovery and a posteriori error estimates. Part 1: the recovery technique. *International Journal for Numerical Methods in Engineering* 1992; **33**(7):1331–1364.
- [252] Zienkiewicz O.C., Zhu J.Z. The superconvergent patch recovery and a posteriori error estimates. Part 2: error estimates and adaptivity. *International Journal for Numerical Methods in Engineering* 1992; **33**(7):1365–1382.